2016

Analysis of Envelope Glycoprotein Complex of Arenaviruses

SUNDARESH SHANKAR
The University of Montana

ANALYSIS OF ENVELOPE GLYCOPROTEIN COMPLEX OF ARENAVIRUSES

By

SUNDARESH SHANKAR

M.Sc. (Biotechnology), Bangalore University, Bangalore, India, 2006

Dissertation

presented in partial fulfillment of the requirements
for the degree of

Doctor of Philosophy
Cellular, Molecular and Microbial Biology

The University of Montana
Missoula, MT

June, 2016

Approved by:

Scott Whittenburg, Dean of The Graduate School
Graduate School

Jack H. Nunberg, Chair
Division of Biological Sciences

J. Stephen Lodmell
Division of Biological Sciences

Brent J. Ryckman
Division of Biological Sciences

Stephen R. Sprang
Center for Biomolecular Structure and Dynamics

Mark A. Pershouse
Department of Biomedical and Pharmaceutical Sciences

Shankar, Sundaresh, PhD, Summer 2016 Cellular, Molecular and Microbial Biology

Analysis of Envelope Glycoprotein Complex of Arenaviruses

Chairperson: Jack H. Nunberg, Ph.D.

Arenaviruses, the causative agents of severe hemorrhagic fevers, are endemic in rodent populations and can be transmitted to humans by contact. Without effective treatment or licensed vaccines, these viruses pose serious public health and biodefense concern. The sole treatment option is the off-label use of the nucleoside analog ribavirin, which is effective only when given at an early stage of infection and shows significant toxicity in humans. Hence, there exists a clear need for developing better therapies. Arenavirus entry into the cell is initiated by the virus envelope glycoprotein complex (GPC), primed to undergo conformational changes triggered by the acidic pH of the maturing endosome, leading to virus and endosomal membrane fusion. Thus, GPC represents as an important molecular target for therapeutic intervention. Recently, several chemically diverse small-molecule fusion inhibitors were identified that block virus entry by stabilizing the prefusion form of GPC against pH-activation. Improved structural and mechanistic understanding of pH-dependent membrane fusion will advance the design and development of potent inhibitors. Here we report that recombinant native-like GPC can be expressed and purified from insect cells, and mediate pH-dependent membrane fusion when reconstituted into proteoliposomes. This fusion reaction is inhibited by small-molecule fusion inhibitors. Further, I show the first physical evidence of binding of small-molecule inhibitors to the pH-sensitive SSP-GP2 interface using photoreactive inhibitors. In addition, I explored mechanism of pH-induced activation of membrane fusion in Old World Lassa virus (LASV). Although the pH-induced activation mechanism is similar to the well-studied New World Junín virus (JUNV), the differences lie in the usage of an additional secondary (LAMP1) receptor for LASV entry. Another antiviral strategy is to block the packaging and release of virus particles from an infected host cell. Studies have shown that the viral matrix protein Z plays a critical role in virus assembly and budding. Additionally, accumulation of Z at the plasma membrane and interaction with GPC and nucleoprotein (NP) is thought to orchestrate the assembly and budding events. The assembly process involving interaction of GPC with Z has not been clearly understood. I explored the use of confocal microscopy approach to study the association of GPC and Z at the plasma membrane during assembly of the virus.

Acknowledgements

First and foremost, I sincerely thank my mentor, Jack Nunberg for his support, guidance and patience. I am indebted to him for helping me become a better scientist and improving my writing skills. I am thankful to my committee members, Steve Lodmell, Steve Sprang, Brent Ryckman, and Mark Pershouse for their time, advice, insightful comments and encouragement. I am grateful to all current and previous lab members particularly, Joanne York, Hedi Casquilho-Gray, Emily Messina, Nick Baird and Donna Twedt for their friendship, support and for creating a wonderful environment to work in. I would also like to extend my thanks to Hedi for helping me with insect cell culture. I am grateful to all members of Sprang lab for their generosity and technical support, particularly Celestine Thomas for his excellent guidance and for finding time in his busy schedule.

I would like to express my deepest gratitude to my family and friends especially, my parents, sisters, parent-in-laws for their love and belief in my abilities. I am grateful to Emily and Paul Messina for their friendship and support. Finally, I would like to thank my wife, Indu Warrier for cheering me on and standing by me through good and bad times.

Table of Contents **Page**

Abstract i

Acknowledgements ii

List of figures and tables v

Chapter 1: Introduction 1

A. Overview 1
   i. Lassa virus (LASV) 2
   ii. Junín virus (JUNV) 2
B. Arenavirus genome and life cycle 4
C. Arenavirus treatment 7
D. The unique tripartite arenavirus envelope glycoprotein 8
   i. Arenavirus GPC: a class I fusion protein 10
   ii. Role of GPC in pH-dependent fusion 12
E. Arenavirus assembly and egress 13
F. Significance 15

Chapter 2: Biochemical reconstitution of hemorrhagic fever arenavirus envelope glycoprotein- mediated membrane fusion 18

A. Introduction 20
B. Materials and methods 22
C. Results 27
D. Discussion 43

Chapter 3: Small-molecule fusion inhibitors bind the pH-sensing SSP-GP2 subunit interface of the Lassa virus envelope glycoprotein 46

A. Introduction 48
B. Materials and methods 51
C. Results 56

D. Discussion 74

Chapter 4: Characterization of pH-dependent fusion of Old World Lassa virus GPC 80

A. Introduction 80
B. Materials and methods 81
C. Results 82
D. Discussion 88

Chapter 5: Role of envelope glycoprotein complex in arenavirus assembly and egress 89

A. Introduction 89
B. Materials and methods 93
C. Results 97
D. Discussion 102

Chapter 6: Conclusion 103

References 108

LIST OF FIGURES AND TABLES

Chapter 1 **Page**

Figure 1-1: Geographical distribution of human pathogenic New World and Old World arenaviruses 3

Figure 1-2: Arenavirus virion structure and genome 4

Figure 1-3: Arenavirus life cycle 6

Figure 1-4: Schematic model of GPC monomer 9

Figure 1-5: Stages in membrane fusion of class I fusion proteins 11

Chapter 2

Figure 2-1: The GPC^{fur} mutant is fusogenic in mammalian cell culture 28

Figure 2-2: Purification and proteolytic cleavage of $rGPC^{fur}$ 30

Figure 2-3: SPR studies of interactions with lipid-reconstituted $rGPC^{fur}$ 33

Figure 2-4: SPR analysis of pH-induced GP1 shedding 36

Figure 2-5: SPR studies of ST-294 binding to $rGPC^{fur}$ following cleavage and exposure to acidic pH 37

Figure 2-6: pH-induced membrane fusion by $rGPC^{fur}$ proteoliposomes: lipid mixing 39

Figure 2-7: pH-induced membrane fusion by $rGPC^{fur}$ proteoliposomes: content mixing 42

Table 2-1: Summary of $rGPC^{fur}$ interaction parameters from SPR studies 31

Table 2-2: Summary of inhibitor-$rGPC^{fur}$ interaction parameters from SPR studies 31

Chapter 3

Figure 3-1: Model for the subunit organization of the tripartite GPC complex 50

Figure 3-2: Chemical structures of fusion inhibitors and photoaffinity derivatives 57

Figure 3-3: Photoaffinity derivatives 3 – 5 potently inhibit LASV GPC-mediated cell-cell fusion 58

Figure 3-4: Characterization of purified LASV GPC from insect cells 60

Figure 3-5: Photoaffinity labeling of LASV GPC 62

Figure 3-6: Cleavage-defective LASV GPC is not susceptible to photoaffinity labeling 65

Figure 3-7: pH-triggered fusion activation abrogates photoaffinity labeling 67

Figure 3-8: Sequence coverage map of unmodified LASV GPC 69

Figure 3-9: Streptavidin enriched LASV GPC photo-adduct 71

Figure 3-10: Size-exclusion chromatography profile of peptide-adducts after clean-up 73

Figure 3-11: MALDI-TOF analysis of pooled size-exclusion chromatography fractions (6-8) of Folch extracted sample 73

Figure S1: Synthesis of photoaffinity probes 76

Chapter 4

Figure 4-1: Membrane fusion activity of LASV SSP K33 mutants 83

Figure 4-2: pH-threshold of cell-cell fusion 85

Figure 4-3: K33Q mutant resistant to inhibition by 17D1 and ST-193 87

Chapter 5

Figure 5-1: Graphical representation of dimerization-dependent fluorescent proteins 92

Figure 5-2: Analysis of GPC and Z expression 98

Figure 5-3: GPC interacts with Z 100

Figure 5-4: Z G2A mutant do not associate with GPC 100

Figure 5-5: Z associates with human CD4 (control) protein 101

Table 5-1: Primers for generating PCR product/mega primers for In-fusion reaction 96

Table 5-2: Primers for generating linear plasmid for In-fusion reaction 96

Table 5-3: Primers for generating G2A mutant using Quikchange mutagenesis 96

Table 5-4: Primers used for generating BiFC constructs using In-Fusion reaction 96

Chapter 1

Introduction

A. Overview

The *Arenaviridae* family comprises of a group of negative-sense single-stranded RNA viruses. A majority of arenavirus species are non-pathogenic to humans, but some can be transmitted to humans to cause severe acute hemorrhagic fever [1]. These viruses are endemic in rodent population and occasionally transmit to humans through zoonosis [2]. Primary hosts of these viruses are from rodent family, *Muridae* with the exception of Tacaribe virus (TCRV) that was isolated from fruit-eating bats [3]. Each year new pathogenic species continue to emerge [4, 5]. New species of arenavirus has been recently identified in boid species of constrictor snakes [6, 7]. In the light of this observation, arenaviruses were reclassified into genera mammarenaviruses and reptarenaviruses for mammalian and snake hosts respectively. Based on their genetic and geographical distribution, mammarenaviruses are broadly classified into Old World (OW) and New World (NW) serotypes [8, 9] (Fig. 1-1). OW viruses include Lassa fever virus (LASV), Lymphocytic choriomenengitis virus (LCMV) and Lujo virus. LCMV infections are generally asymptomatic or mild, but LASV and Lujo virus are known to cause hemorrhagic fever [4, 10]. In the case of NW viruses, they are further divided into three clades (A, B and C) [9, 11]. Several species of NW arenaviruses that belong to clade B, including Junín virus (JUNV), Machupo (MACV) and Guanarito (GTOV), are responsible for sporadic outbreaks among agricultural workers in South America [12, 13]. My work mainly focuses on studying OW LASV and NW JUNV.

i. Lassa fever Virus (LASV)

Among the OW viruses, LASV is endemic in western Africa and infects 300,000 people causing 5000-10,000 deaths annually [14, 15]. The natural reservoir of LASV is the ubiquitous rodent, *Mastomy natalensis*, mostly found in sub-Saharan Africa [16]. LASV was first discovered in 1969, during outbreaks seen in Nigeria, Sierra Leone and Liberia. About 20-50% of the adult populations are seropositive in these regions of western Africa, thus making LASV a major public health concern [17]. Disease ranges from being asymptomatic to flu-like symptoms to hemorrhagic fever and ultimately death, with incubation period of upto 20 days. Although the overall mortality rate is relatively low, but can be as high as 15-20% in hospitalized patients. The fatality rate in pregnant women in their third trimester can be more than 30%, with neonatal mortality of ~90% [18]. A recent outbreak of Lassa fever in Nigeria has caused over 100 deaths since August 2015 [19].

ii. Junín Virus (JUNV)

JUNV is a causative agent of Argentina hemorrhagic fever (AHF), which is endemic in pampas regions of Argentina. The natural host of JUNV is a vesper mouse (*Calomys musculinus*) found in the vast drylands, which causes disease among the agricultural workers. JUNV was first isolated in 1958 [20] and periodic outbreaks with a total of over 1000 cases are reported each year, with fatality rate of 15-30% in untreated cases. The infection is primarily spread through aerosolization of rodent excreta and urine, and through small abrasion in the skin. Due to the aerosolization of infectious virus particles, primary site of infection is lung alveolar macrophage [21]. Further it migrates to lymph nodes, where the virus replicates, disseminating through the vascular system and spreading to different organs

[22]. NW arenaviruses of clade B use murine transferrin receptor 1 (TfR1) in their respective rodent host and pathogenic viruses are distinguished by their ability to use human transferrin receptor 1 (hTfR1) for attachment to the cell-surface, mediated by viral envelope glycoprotein complex (GPC) [23, 24].

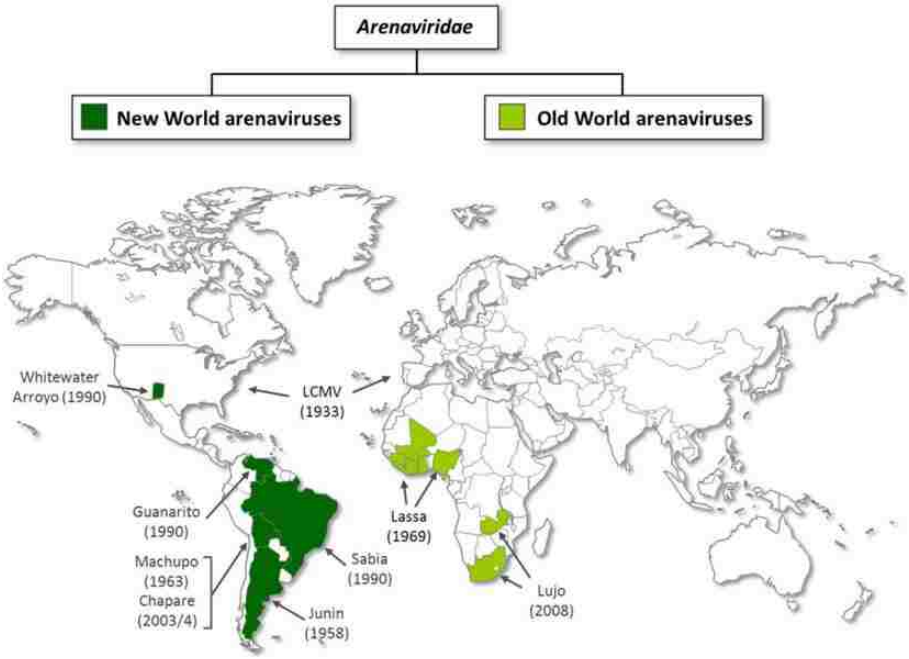

Figure 1-1. Geographical distribution of human pathogenic New World and Old World arenaviruses [25]

B. Arenavirus genome and life cycle

Arenaviruses acquired their name from a Latin word *Arena* meaning "sandy", owing to its sand-like appearance under the electron microscope due to the presence of host ribosomes. Virions are spherical or pleomorphic with a diameter of 50-300 nm (Fig. 1-2). They are enveloped viruses with the envelope glycoprotein embedded in the lipid bilayer to form viral spikes that recognize and attach to cell-surface receptor. The genome of arenaviruses consists of two negative-sense single-stranded RNAs, Large (L) and Small (S) RNA. The L RNA is ~7.3 kb in length and encodes RNA-dependent RNA polymerase (RdRp) and the matrix Z protein. The S RNA is ~3.4 kb in length and encodes envelope glycoprotein (GPC) and nucleoprotein (NP) [26]. On both RNAs, the two open-reading frames are in opposite directions and separated by an intergenic region. Thus, arenaviruses use an ambisense coding strategy for protein expression (Fig. 1-2).

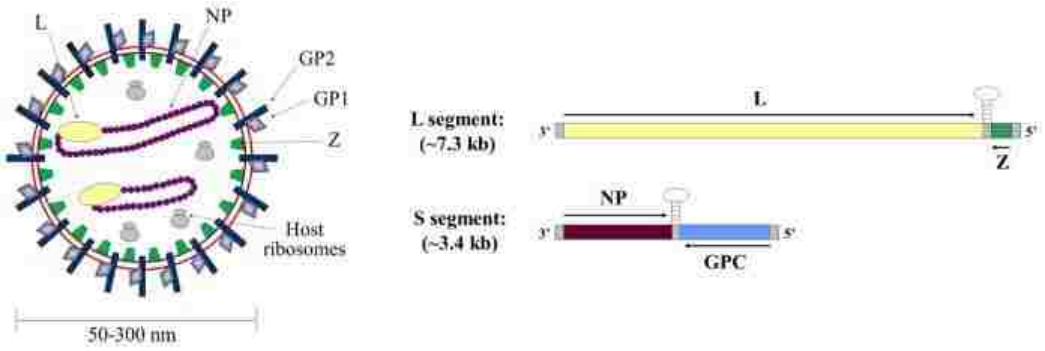

Figure 1-2: Arenavirus virion structure and genome. General structure of arenavirus particle is shown in the left with GPC embedded in the membrane, matrix protein Z (green) and nucleocapsid inside with RNA-dependent RNA polymerase (yellow) and host ribosome. Genome is shown in the right with L and S fragment drawn in 3' to 5' direction. Intergenic region is shown as a stem and loop structure on the genome [9].

The Arenavirus life cycle starts with attachment of the virus to its host cell. For entry into the host cell, the OW viruses and some of the NW viruses that belong to clade A use α-dystroglycan as the cell-surface receptor, whereas the pathogenic NW clade B viruses use human transferrin receptor 1 (hTfR1). Recently, a secondary receptor, LAMP1 in the late endosome, has been proposed to also be required for OW LASV entry [27]. Virus attachment to the cell-surface receptor is mediated by GPC. NW viruses enter the host cell via clathrin-mediated endocytosis, while the OW viruses enter through a novel endocytic pathway that is independent of clathrin, dymanin, actin and caveolin [28, 29]. Irrespective of the mode of entry, both OW and NW viruses are delivered into the late endosome where they fuse with the endosomal membrane in a pH-dependent manner to release the viral ribonucleoprotein (vRNP) into the cytoplasm [30]. Once released into the cytosol, NP and RdRp carry out viral genome replication and transcription by forming discrete structures known as the replication-transcription complexes (RTCs) [31]. Virus is then assembled on the cell-surface and the progeny viruses are released from the infected cell through a budding process (Fig. 1-3).

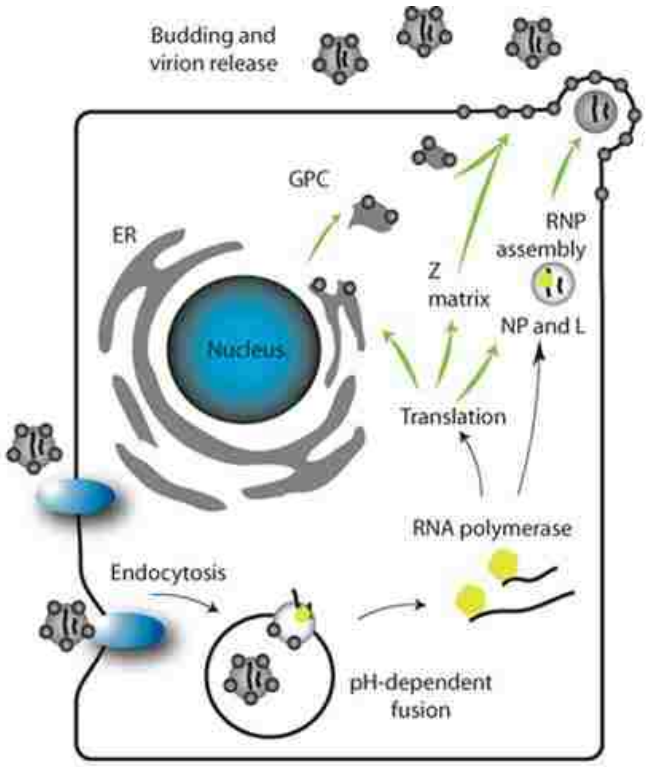

Figure 1-3: Arenavirus life cycle. Cellular entry is achieved by binding to the cell-surface receptor, followed by endocytosis and release of the virion core into the cytosol. The virus then undergoes transcription, replication, and is finally assembled and released from the cell through a budding process.

C. Arenavirus treatment

Among OW and NW viruses, some are known to cause severe hemorrhagic fever with high mortality [12]. In the absence of licensed vaccines and effective treatment measures, they pose significant threat to public health and biodefense [32]. Accordingly, they are classified as category A priority pathogens [33]. The current treatment given for JUNV infection includes convalescent serum/neutralizing antibodies for JUNV, although the analogous treatment has had little success in LASV. Ribavirin, a nucleoside analog with non-specific viral activity has shown mixed results in treatment of arenavirus infection [34]. The only available vaccine Candid #1, a live attenuated strain of JUNV, is licensed in Argentina to treat Argentina hemorrhagic fever (AHF) [32].

Ribavirin (1-beta-D-ribofuranosyl-1, 2, 4-triazole-3-carboxamide) is a purine analog that has been used for the treatment of a number of viral infections, albeit with significant toxicity. In the case of arenaviruses, ribavirin is effective only when given early in infection [34]. The mechanism of action of ribavirin is not entirely clear and may vary among different viruses. Distinct mode of actions have been proposed, including inhibition of the host cell inosine monophosphate dehydrogenase (IMPDH) involved in guanosine triphosphate biosynthesis, inhibition of the viral polymerase, interference in RNA capping and lethal mutagenesis [35]. T-705 or Favipiravir, also a purine analog, is thought to act by inhibiting arenavirus replication by blocking viral transcription without appreciable inhibition of IMPDH [36]. Currently, favipiravir (AVIGAN) is approved as an anti-influenza virus drug in Japan.

Virus entry is mediated by the envelope glycoprotein that attaches to the cell-surface receptor and promotes membrane fusion. Thus envelope glycoproteins act as robust targets for therapeutic intervention. Newly discovered small-molecule compounds, identified by high-throughput screening, block the entry of arenavirus by preventing glycoprotein-mediated pH-dependent membrane fusion [37-40]. Inhibitors ST-294 and ST-193 (from SIGA Technologies) act by stabilizing the prefusion complex against acidic pH-induced activation [41]. ST-193 has also been tested in guinea pig model of LASV disease and shown to increase the survival rate of infected animal [42]. These inhibitors serve as promising leads that can be used to design and develop optimized compounds towards treatment of arenavirus infection.

D. The unique tripartite arenavirus envelope glycoprotein complex (GPC)

The mature GPC comprises 3 subunits: a receptor binding (GP1) subunit, a transmembrane fusion subunit (GP2) and stable signal peptide (SSP). GPC is synthesized as a precursor and co-translationally directed to endoplasmic reticulum (ER) by a 58 amino acid signal peptide, SSP. In the ER, SSP is cleaved by cellular signal peptidase (SPase) and stays non-covalently associated with the GPC complex, a feature unique to arenavirus GPC (Fig. 1-4) [43, 44]. SSP associates with the GP1-GP2 precursor in part by the interaction of its penultimate cysteine 57 (C57) with the zinc-binding domain (ZBD) in the cytoplasmic tail of GP2 [45]. Precursor forms a trimer in the ER and is then translocated to the Golgi apparatus, where it undergoes maturation by the action of cellular proprotein convertase subtilisin/kexin isozyme-1 (SKI-1/S1P) to generate the GP1 and GP2 subunits [46, 47]. Upon proteolytic cleavage, the mature GPC complex adopts a kinetically trapped metastable state poised for activation by acidic pH and membrane fusion. Studies have shown that SSP association with

the GP1-GP2 precursor is required for its transit from the ER through the Golgi apparatus and to the cell-surface. Co-expression of SSP in *trans* with the GP1-GP2 precursor (containing human CD4 signal peptide for translocation to the ER) allows SSP association and maturation of GPC complex [48, 49].

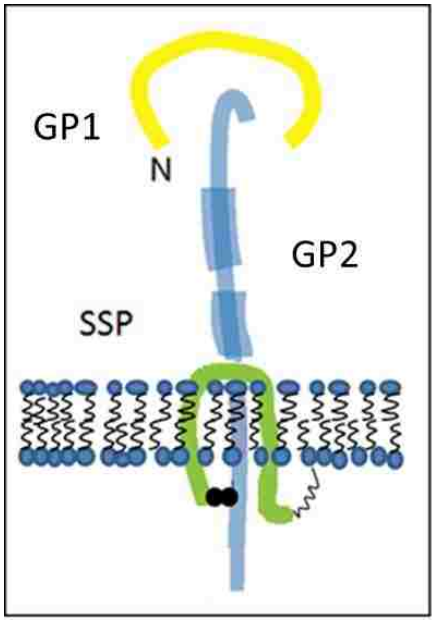

Figure 1-4: Schematic model of GPC monomer. GP1, GP2 and SSP subunits are not to scale. The myristoylated N terminus of SSP, the binuclear inter-subunit (SSP-GP2) zinc-binding domain (Zn spheres) and the two heptad-repeat regions in the ectodomain of GP2 (thickened) are indicated.

i. Arenavirus GPC: a class I fusion protein

Sequence analysis of arenavirus GPC reveals the presence of two heptad-repeat regions in the ectodomain of GP2, characteristic of class I fusion proteins (Fig. 1-4). The widely accepted model for membrane fusion by class I viral fusion protein comes from studies carried out mainly on human immunodeficiency virus (HIV) Env and influenza virus hemagglutinin (HA) (Fig. 1-5) [50, 51]. Other studied class I fusion proteins also include Parainfluenza virus 5 F [50, 51]. Class I fusion proteins are trimeric and undergo a series of conformational changes following an activation event. These structural changes lead to exposure and subsequent insertion of the hydrophobic N-terminal fusion peptide of the fusion subunit into the cellular membrane. This so-called prehairpin intermediate is unstable and collapses to form a stable six-helix bundle structure. Formation of the thermodynamically favored six-helix bundle brings the viral and cellular membranes together and is thought to drive membrane fusion (Fig. 1-5) [50, 52]. The detailed mechanism by which GPC is activated and promotes pH-dependent fusion still remains elusive. Our lab studies the structure and function of GPC and the role of SSP in driving the activation and fusion activity of GPC. We also focus on exploring the mechanism by which the small-molecule inhibitors block virus entry. In order to better understand the molecular mechanism of fusion and its inhibition by small-molecule entry inhibitors, in chapter 2 we carried out studies on recombinant GPC expressed in insect cells.

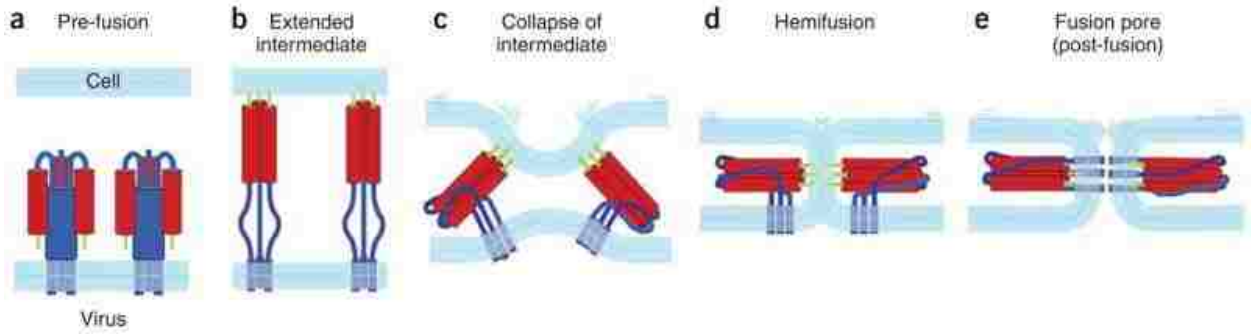

Figure 1-5: Stages in membrane fusion of a class I fusion protein. a to **b**: Activation of the prefusion trimer by acidic pH and/or receptor binding is followed by exposure of the fusion subunit and insertion of the fusion peptide into the cell membrane to form the extended prehairpin intermediate. **b** to **c** to **d**: Collapse of the intermediate to form the six-helix-bundle core of the postfusion trimer-of-hairpins structure, thereby bringing the membranes into apposition for hemifusion (merger of the outer membrane leaflets). **d** to **e:** Complete fusion of the membranes and formation of the fusion pore [Adapted from [50]].

ii. Role of GPC in pH-dependent fusion

In GPC, SSP interacts with GP2 subunit to stabilize the prefusion conformation, and thereby modulate the low-pH-induced triggering event. This pH-induced activation is targeted by independently identified classes of small-molecule inhibitors that act by antagonizing the fusion-activation by GPC [37, 38, 41]. Among these inhibitors, some are specific to OW or NW arenaviruses and some are broadly active. Despite differences in specificity against NW and/or OW arenavirus species, these compounds share a common binding site on GPC [41, 53]. Studies carried out with inhibitors from SIGA Technologies demonstrate that mutations in GPC engender resistance to inhibition by these compounds [37, 38, 41]. These mutants often show cross-resistance to other chemically distinct small-molecule inhibitors. In SSP, mutations at P12 and T13 in the cytosolic end of transmembrane domain 1 (TM1) and K33 and N37 in the ectodomain loop render the virus resistant to inhibition [41, 54, 55]. Some of the mutations lie in the ectodomain and transmembrane region of GP2 (D400A, T418N, L420T, F427A, A435I, and F438I), positioned to interact with SSP. Apart from these resistance mutants, N20 mutant of SSP show dependence on inhibitor for WT level of fusion [55]. Taken together, this led us to hypothesize that these inhibitors act by targeting the pH-sensitive SSP-GP2 interface. In chapter 3, we provide direct biochemical evidence for binding at the interface of mature LASV GPC, using photoreactive inhibitors designed by our collaborators at The Scripps Research Institute (TSRI).

A conserved residue K33 in SSP is important for pH-induced activation of GPC. Amino acid substitutions that decrease the positive charge of K33 residue in SSP of JUNV were shown to alter the pH of fusion [54]. Since the charge of the lysine is not altered at acidic pH,

we hypothesized that the lysine side chain interacts with a titratable pocket in the ectodomain of GP2. In addition, interaction between TM1 of SSP and the transmembrane domain (TMD) of GP2 is important for fusion [55]. Studies carried out on chimeric LASV and JUNV GPCs identify a requirement of a specific homotypic match in the TM1 of SSP as a determinant for pH-dependent membrane fusion [55]. In chapter 4, we investigate the pH-induced fusion in LASV GPC to compare the underlying mechanism with that described for the well-studied NW JUNV GPC.

E. Arenavirus assembly and egress

Enveloped viruses use host-derived membranes to form their external envelope, which then buds to form progeny virus. Among enveloped viruses, there are several ways by which viral components associate and assemble to form a budding virus particle. Budding in several viruses occurs at the plasma membrane, although some of the viruses bud from various intracellular compartments such as of ER and Golgi (e.g. Foamy virus, murine hepatitis virus and Hepatitis B virus) or nucleus (e.g. Herpesvirus) [56]. Other viruses, including members of *Poxviridae* family, have much more complicated process involving multiple budding and fusion events [56, 57]. In different viruses, either the matrix protein, capsid or the envelope protein can determine the site of assembly and budding. The assembly process involved in bringing envelope glycoprotein and matrix protein together or bringing the virus nucleocapsid and envelope glycoprotein together at the virus budding site is still unclear. In case of negative stranded RNA viruses like orthomyxoviruses, paramyxoviruses and arenaviruses, viral matrix protein mediate the interaction between nucleocapsid and envelope glycoprotein. The general steps involved in assembly of negative stranded RNA viruses are: (a) the envelope glycoprotein and the matrix protein is arranged on the plasma membrane (b)

encapsidation of viral RNA with nucleoprotein to form nucleocapsid (c) recruitment of nucleocapsid to the budding site and (d) virus release from the host membrane through scission [58]. However in positive-strand RNA viruses, like alphaviruses which lack matrix protein, the capsid protein directly interacts with envelope glycoprotein resulting in budding [59]. In the case of arenaviruses, it is not clear if the nucleocapsid can interact directly with envelope glycoprotein during assembly or through matrix Z protein, a 11kDa RING zinc-finger protein which plays an important role in the budding of virus particle.

Z alone is able to mediate budding of Z containing virus-like particles (VLPs) [60]. Myristoylation at glycine 2 of Z is required for association of Z to the cytoplasmic side of the plasma membrane [61]. Evidence suggests that Z interacts with GPC at the plasma membrane by associating with the SSP subunit and this interaction does not require the RING domain or late domain of Z [62]. In many viruses, the envelope glycoprotein is believed to assemble in membrane microdomains called "lipid rafts" that are resistant to solubilization by triton X-100 detergent [58]. For example, Influenza virus HA is targeted to detergent-resistant membrane microdomains (DRMs) and then recruits the matrix protein and other viral components for virus assembly [63, 64]. However in certain other viruses e.g., vesicular stomatitis virus (VSV) there is evidence of viral glycoproteins (G) that are non-raft associated. Immunoelectron microscopy show that VSV G protein cluster in membrane microdomains of plasma membrane forming discrete regions of 100-150 nm in size, similar in size to lipid-rafts [65]. A similar assembly process is seen in JUNV where the GPC is excluded from the DRMs, yet assembles on the cell-surface into non-raft microdomains [66]. Although interaction of GPC with Z in these microdomains was not apparent in the Electron Microscopy studies, perhaps the interaction is transient. Alternatively, other viral

components may also be required for the interaction [66]. My work in chapter 5 focuses on developing new methodology to investigate the interaction between GPC and Z at the plasma membrane and examine the role of GPC in assembly and egress.

F. Significance

Arenaviruses are responsible for severe hemorrhagic fever with high morbidity and mortality [12]. LASV is endemic in western Africa and can be imported to other parts of the world by infected travelers [67, 68]. Several species of NW arenaviruses, including JUNV, cause fatal disease in the Americas [12, 13]. Each year, new species continue to emerge from their respective rodent species [4, 5]. In the absence of vaccine prophylaxis or effective treatment, arenaviruses remain an urgent public health concern and are considered as a potential bioterrorism agent [32]. One promising intervention strategy is to block virus entry into the host cell. Arenavirus entry is initiated by GPC binding to its cell-surface receptor, followed by endocytosis. The fusion of viral and endosomal membrane is mediated by GPC, which undergoes a series of structural rearrangements upon exposure to acidic pH in the maturing endosome. Upon fusion the virion core is subsequently released into the cytosol [69]. Thus, GPC may serve as a robust target for therapeutic intervention.

Our current understanding of class I fusion protein comes from the structural studies based on the soluble ectodomain fragment of influenza HA, HIV Env etc. [50, 51]. These studies do not include information regarding the important role membrane anchorage plays in envelope glycoprotein assembly, maintenance of prefusion state and the resulting fusogenic conformational change. In an effort to enhance our structural and mechanistic understanding of pH-dependent membrane-fusion and activation of GPC, we carried out studies on recombinant JUNV GPC expressed in insect cells [70]. We screened different conditions for

crystallizing intact cleavage-defective JUNV GPC [53] in collaboration with Dr. Stephen R. Sprang's laboratory. We also collaborated with New York Consortium on Membrane Protein Structure (NYCOMPS) consortium and carried out extensive screening for identifying suitable detergents for crystallizing GPC. Despite our efforts, we were unsuccessful in generating crystals. Our current strategy is to use cryo-Electron Microscopy to obtain structural details of GPC in collaboration with Dr. Thomas A. Bowden at Oxford University, United Kingdom. In chapter 2, we examine the role of recombinant JUNV GPC by studying the mechanism involved in activation of membrane fusion. This work provides a platform for better understanding of GPC-mediated pH-induced membrane fusion and its inhibition.

Newly identified small-molecule fusion inhibitors specifically target the pH-induced activation process of GPC, thereby blocking the virus entry. Several of these compounds have shown efficacy against lethal arenavirus infection in animal models [37, 42]. Even though the different classes of inhibitors differ in specificity for OW and NW species, they seem to share a common binding site on GPC [53]. Further, studies with JUNV GPC suggest that these inhibitors bind to the pH-sensitive interface between SSP and GP2 subunits [41]. Characterization of the inhibitor-binding site will provide insights into the molecular basis of fusion activation and its inhibition. In chapter 3, we describe the use of photoaffinity-labeling to identify the inhibitor-binding site on GPC. This work contributes towards a mechanistic understanding of pH-dependent fusion and may guide the development of potent and broadly active inhibitors.

Our initial studies with JUNV GPC have shown that K33 residue in SSP is required for low-pH-induced activation of GPC [54]. K33 interacts with a titratable pocket in GP2 to sense and respond to the acidic pH of the late endosome. The small-molecule fusion

inhibitors target this interaction between SSP and GP2. In chapter 4, we investigate the mechanism of pH-induced activation of LASV GPC, and compare and contrast it to that observed in JUNV GPC. Although the mechanism of activation may be similar, the difference in specificity of fusion-inhibitors can be due to the amino acid difference at the SSP-GP2 interface. Studies with LASV and JUNV GPC chimeras show a requirement of homotypic match for WT-level of fusion. This work will enhance our understanding of molecular details of species specificity of these small-molecule fusion inhibitors that is essential for structure-activity relationships and optimization of compounds.

In some of the enveloped viruses, assembly occurs at the plasma membrane involving interaction between viral proteins, ultimately leading to budding of progeny virus. Arenavirus budding is mediated by matrix Z protein, which can form Z-containing virus-like particles [60]. The assembly process whereby GPC and Z are together at the budding site is less clear. Studies report biochemical evidence of GPC and Z interaction [62]. Our studies, however, indicate the possibility of requirement of additional signals for association of GPC and Z, and recruitment of viral components to the site of budding [66]. To that end, we aim to develop a technique to study the interaction of GPC and Z at the cell-surface, which may be transient. We are also interested in exploring the role of other viral or host proteins that may promote GPC and Z association. To study the interactions at plasma membrane, we chose newly developed biosensors, which are engineered to fluoresce when brought into close proximity by interaction of their fused GPC and Z partners. This approach and our results are reviewed in chapter 5.

Chapter 2

Biochemical Reconstitution of Hemorrhagic-Fever Arenavirus Envelope Glycoprotein-Mediated Membrane Fusion

Abstract

The membrane-anchored proteins of enveloped viruses form labile spikes on the virion surface, primed to undergo largescale conformational changes culminating in virus-cell membrane fusion and viral entry. The prefusion form of these envelope glycoproteins thus represents an important molecular target for antiviral intervention. A critical roadblock to this endeavor has been our inability to produce the prefusion envelope glycoprotein trimer for biochemical and structural analysis. Through our studies of the GPC envelope glycoprotein of the hemorrhagic fever arenaviruses, we have shown that GPC is unique among class I viral fusion proteins in that the mature complex retains a stable signal peptide (SSP) in addition to the conventional receptor-binding and transmembrane fusion subunits. In this report we show that the recombinant GPC precursor can be produced as a discrete native-like trimer and that its proteolytic cleavage generates the mature glycoprotein. Proteoliposomes containing the cleaved GPC mediate pH-dependent membrane fusion, a characteristic feature of arenavirus entry. This reaction is inhibited by arenavirus-specific monoclonal antibodies and small-molecule fusion inhibitors. The *in vitro* reconstitution of GPC-mediated membrane-fusion activity offers unprecedented opportunities for biochemical and structural studies of arenavirus entry and its inhibition. To our knowledge, this report is the first to demonstrate functional reconstitution of membrane fusion by a viral envelope glycoprotein.

This study was carried out in collaboration with Dr. Stephen R. Sprang's laboratory from the Center for Biomolecular Structure and Dynamics (CBSD) at the University of Montana, where all the protein work was carried out. I contributed in purification of GPC and furin enzyme from insect cells and worked together with Celestine J. Thomas in all other experiments. Celestine J Thomas carried out Biacore experiments at Rocky Mountain Center of Excellence for Biodefense and Emerging Infectious Diseases Research (RMRCE). This study is published in PLoS One and the citation is given below.

Thomas, C., S. Shankar, H. E. Casquilho-Gray, J. York, S. R. Sprang and J. H. Nunberg (2012). "Biochemical reconstitution of arenavirus envelope glycoprotein-mediated membrane fusion." PLOS One **7**: e51114

A. Introduction

Entry of enveloped viruses into their host cells requires fusion of the viral and cellular membranes, a process that is mediated by the viral envelope glycoprotein. Class I viral fusion proteins, including those of influenza and human immunodeficiency virus type 1 (HIV-1), are synthesized as inactive precursor glycoproteins that assemble as trimers and are subsequently primed by proteolytic cleavage to generate the mature fusogenic spikes. The membrane anchored spike is thought to exist in a kinetically trapped metastable state that can be triggered, by engagement with cell-surface receptor or exposure to acidic pH in the endosome, to undergo a series of structural transitions leading to a thermodynamically favored postfusion state and concomitant virus-cell membrane fusion (reviewed in references [50, 51]). Intervention strategies that prevent membrane fusion and virus entry thus provide a sound basis for vaccine and drug development. A detailed mechanistic understanding of viral membrane fusion and its inhibition has been hindered by the inherent instability of the prefusion envelope glycoprotein trimer. Solubilization from its membrane-anchored environment invariably causes disassembly and/or refolding to the postfusion conformation. X-ray crystallographic analyses of the most extensively characterized class I envelope glycoproteins – influenza virus hemagglutinin (HA), HIV-1 envelope glycoprotein (Env) and parainfluenza virus 5 F (PIV5 F) - are based on soluble ectodomain fragments. These studies necessarily exclude information regarding the important role of membrane anchorage in envelope glycoprotein assembly, maintenance of the prefusion state and activation of fusogenic conformational changes. The failure of current HIV-1 vaccines to elicit broadly neutralizing antibodies is largely attributed to our inability to produce the trimeric native Env immunogen in a prefusion conformation [71].

Arenaviruses are responsible for severe hemorrhagic fevers worldwide, and Junín (JUNV) and Lassa (LASV) viruses are recognized to pose significant threats to public health and biodefense [12-14, 33, 72]. Arenavirus entry into the host cell is mediated by the viral envelope glycoprotein GPC, a member of the class I viral fusion proteins. The GPC precursor trimerizes and is proteolytically cleaved by the cellular site-1-protease/subtilisin-like kexin isozyme-1 (S1P/SKI-1) [46, 47, 73] in the Golgi to generate the receptor-binding (GP1) and transmembrane fusion (GP2) subunits. Upon engaging a cell-surface receptor–transferrin receptor 1 (TfR1) for JUNV[23] or alpha-dystroglycan for LASV [74] - the virion is endocytosed and GPC-mediated fusion is triggered by acidic pH in the maturing endosome [75]. The ensuing conformational changes are driven by formation of the stable postfusion trimer-of-hairpins in GP2 [76-78]. Unlike other class I fusion proteins, the mature GPC retains its signal peptide as an essential subunit [48, 79]. The unusually long (58 amino-acid residues) stable signal peptide (SSP) traverses the membrane twice [80] and binds the cytoplasmic domain of GP2 via an intersubunit zinc finger [45, 81]. Evidence suggests that SSP interacts with the ectodomain of GP2 to maintain the prefusion GPC complex at neutral pH and facilitate its fusogenic response to acidic pH [54]. Importantly, small-molecule fusion inhibitors [37, 38, 41] target the pH-sensitive SSP-GP2 interface to prevent fusion of the viral and endosomal membranes, and thereby viral entry [54].

Our previous studies showed that the JUNV GPC precursor purified from insect cells exists as a stable trimer and efficiently binds the TfR1 receptor and arenavirus-specific small-molecule fusion inhibitors [53]. The unusual structural integrity of the precursor likely reflects its unique tripartite organization, and suggested the feasibility of generating the mature GPC complex for biochemical analysis. To this end, we have produced the prefusion

GPC trimer through *in vitro* proteolytic cleavage, and demonstrated that proteoliposomes containing this complex are able to mediate pH-dependent membrane fusion that is specifically inhibited by small-molecule fusion inhibitors. Biochemical reconstitution of the fusogenic activity of GPC provides a platform for understanding pH-induced membrane fusion and its inhibition.

B. Materials and Methods

Monoclonal Antibodies (MAbs) and Small-molecule fusion inhibitors. MAbs directed to JUNV GP1 (BF11, BF09, BE08 and AG02) and N (BG12) were obtained from the CDC [82] through the NIAID Biodefense and Emerging Infectious Diseases Research Resources Repository. MAb F100G5 recognizes the fusion peptide of JUNV GP2 [77] and was provided by the Public Health Agency of Canada. Plasma-derived human soluble TfR (sTfR) was obtained from American Research Products, and the M2 anti- FLAG MAb from Sigma. The small-molecule fusion inhibitors discovered by SIGA Technologies - ST-193 [38], ST-161 [41], ST-761 [53], ST-294 [37] and its dansyl analog ST-375 [53]-were obtained from the company. Compounds discovered at The Scripps Research Institute (TSRI) - 17C8 and 8C1 [39]- were provided by Stefan Kunz, Andrew M. Lee and Michael B. A. Oldstone. ST-294 and ST-761 are specific to NW arenaviruses and ST-161 and TSRI 8C1 are specific to the OW LASV. ST-193 and TSRI 17C8 are broadly active against NW and OW viruses.

Expression and Purification of rGPC^{fur}. Recombinant baculoviruses were constructed as previously described [53] using a pFastBac Dual expression vector (Life Technologies) and separate SSP and GP1-GP2 precursor open reading frames from GPC of the pathogenic MC2 strain of JUNV [79]. These two polypeptides associate in *trans* to reconstitute the native

GPC complex [48, 53, 79]. The signal peptide of human CD4 was fused to the N-terminus of the GP1-GP2 precursor, to which a C-terminal extension bearing a TEV-protease site and FLAG-tag sequence was added [53]. The furin recognition motif was introduced using QuikChange mutagenesis (Stratagene). Baculovirus expressing $rGPC^{fur}$ was used to infect Trichoplusia ni High- Five^{TM} cells and washed cell membranes were solubilized in 1.5% dodecyl beta-D-maltoside (DDM) as previously described [53]. $rGPC^{fur}$ was bound to immobilized M2 anti-FLAG MAb beads (Sigma), and eluted in buffer containing 0.1% DDM and 5 mM 3xFLAG peptide (Sigma). This material was dialyzed to remove the 3xFLAG peptide and subjected to size-exclusion chromatography using a Superdex-200/G-75 tandem column (GE Healthcare) in buffer containing 0.05% DDM. All buffers contained 100 µM Zn^{++} to prevent dissociation from the intersubunit zinc binding domain of GPC. Proteins were analyzed by sodium dodecylsulfate-polyacrylamide gel electrophoresis (SDS-PAGE) using NuPAGE 4–12% bis-Tris gels (Life Technologies). For mass spectrometry, proteins were eluted from gels in 0.15 M NaOH and subsequently neutralized and deglycosylated using PNGase F (New England Biolabs). Molecular weights were determined using a MALDI (Voyager DE) mass spectrometer.

Soluble Human Furin (sFurin). A plasmid for baculovirus expression of the recombinant soluble prodomain of human furin [83] was kindly provided by Dr. Alex Strongin (Burnham Institute for Medical Research) and the open reading frame, including the baculovirus gp67 signal peptide and C-terminal hexa-histidine tag, was transferred to pFastBac1 (Life Technologies) for generating baculovirus. The soluble furin enzyme was purified from the supernatant of infected Spodoptera frugiperda (Sf9) cells using Ni^{++}-affinity chromatography as described [83]. The purified sFurin (~33,000 units/mg [84] contained no detectable

nonspecific protease activity. Cleavage of $rGPC^{fur}$ in solution (0.6 mg/ml) was performed using a 3:1 molar ratio of $rGPC^{fur}$: sFurin at 20^0C for 4 hr in buffer containing 50 mM Tris (pH 7.2), 150 mM NaCl, 5 mM MgCl2, 1 mM CaCl2, 100 µM ZnSO4 and 0.05% DDM. Zn^{++} was present to stabilize the intersubunit zinc-binding domain in GPC and did not appear to reduce the extent of furin cleavage [85]. In preliminary studies, soluble human furin was purchased from New England Biolabs.

Surface Plasmon Resonance (SPR) Studies. SPR analyses of binding to $rGPC^{CD}$ and $rGPC^{fur}$ were performed using a Biacore T100 instrument (GE Healthcare) as previously described [53]. The proteins are immobilized to the biosensor chip via covalently coupled M2 anti-FLAG MAb. In most experiments, $rGPC^{fur}$ was reconstituted into a lipid bilayer on the chip as previously described [53]. Briefly, a Biacore L1 chip bearing immobilized $rGPC^{fur}$ in DDM-containing running buffer was rinsed with 20 mM 3-[(3 cholamidopropyl) dimethylammonio]- 1-propanesulfonate (CHAPS) (Sigma) and the detergent- containing buffer was replaced by liposomes containing a 3:1 mixture of dimyristoylphosphatidylcholine and phosphatidylcholine (DMPC:PC; Avanti Polar Lipids) in running buffer without DDM (non-detergent running buffer). By this procedure, protein-bound detergent is displaced by a lipid bilayer that forms on the hydrophobic chip [86]. At the completion of the SPR experiment, the L1 chip was regenerated with isopropanol/40 mM NaOH (2:3 v/v) to remove lipids and associated proteins, and the M2 MAb was reconditioned using glycine-HCl, pH 3.0.

For proteolytic cleavage of $rGPC^{fur}$, the L1 chip was incubated with 20,000 units/ml sFurin for 1 hr at 25^0 C in non-detergent running buffer (containing 1 µM Zn^{++}). The bolus of sFurin was then washed off to achieve a stable baseline. In all binding studies, multiple

concentrations of MAb (0.1–2.5 μM), sTfR (0.5–5.0 μM) and small-molecule fusion inhibitors (5–250 μM) were used to calculate the interaction parameters listed in Tables 1 and 2, respectively. pH-induced shedding of the GP1 subunit was determined by subjecting the cleaved $rGPC^{fur}$ to a 1 min pulse of non-detergent running buffer that had been adjusted to pH 5.0 using PIPES or sodium acetate. A new baseline was subsequently determined to assess the loss of protein from the chip. In studies using ST-294 to inhibit GP1 shedding, 10–20 μM of the compound was included at all stages of the experiment. The addition of ST-294 did not affect sFurin cleavage.

Preparation of liposomes and proteoliposomes. DMPC:PC liposomes used to form lipid bilayers in SPR studies were prepared as previously described [53]. For liposomal fusion assays, large unilamellar vesicles (LUVs) were prepared using a 7:3 mixture of POPG (1-palmitoyl, 2-oleoyl-snglycero-3-phosphoglycerol) and POPC (1-palmitoyl,2-oleoyl-snglycero- 3-phosphocholine) (Avanti Polar Lipids). Dried lipids were hydrated in 10 mM Tris (pH 7.2), 100 mM NaCl, 50 μM ZnSO4 and multilamellar liposomes were formed by repeated cycles of freeze/thaw. LUVs were produced by extrusion through 100-nm pore size polycarbonate membranes (Avestin). To generate target liposomes bearing a self-quenching concentration of the fluorescent lipid rhodamine-PE (1, 2-dioleoyl-snglycero- 3-phosphoethanolamine-N-(lissamine rhodamine B sulfonyl); Avanti Polar Lipids), the lipid mix was doped with 1% of the compound. For studies of content mixing (below), liposomes included 10% cholesterol hemisuccinate and contained either 50 μM Zn^{++} (proteoliposomes) or 1 μM of the soluble zinc sensitive fluorophore FluoZin-1 (Life Technologies) and no Zn^{++} (target liposomes). Free Zn^{++} or unincorporated FluoZin-1 was removed by dialysis or separation on a small Sepharose CL4B (Sigma) column. Proteoliposomes bearing $rGPC^{fur}$

were prepared by mixing $rGPC^{fur}$ (in buffer containing 50 µM Zn^{++} and 0.05% DDM) with the appropriate LUVs at a protein:lipid molar ratio of, 1:25. After 30 min of incubation at room temperature, the proteoliposomes were desalted by size-exclusion chromatography using Sepharose CL4B, and extruded through a polycarbonate membrane (100-nm pore). Protein incorporation was generally ~95%. Proteoliposomal $rGPC^{fur}$ (1.5–3.0 µM protein) was cleaved prior to use in fusion assays by incubation with 0.5 mM sFurin at 20^0C for 45 min in buffer containing 10 mM Tris (pH 7.2), 100 mM NaCl.

Liposome Fusion Assays. Lipid mixing: Target liposomes containing rhodamine-PE were added to furin-treated proteoliposomes (~1.5–3.0 µM $rGPC^{fur}$ in 50 µM lipid) at a ratio of 1:10, and lipid mixing was assessed intermittently by fluorescence (excitation 508 nm; emission 600 nm) using a Perkin Elmer LS55 spectrometer. pH was adjusted to 5.0 by the addition of 1 M sodium acetate, and complete dequenching of the fluorophore was determined upon solubilization in 2% Triton X-100. JUNV-specific MAbs and small-molecule fusion inhibitors were pre-incubated with proteoliposomes at a concentration of 5 and 15 µM, respectively.

Content mixing: Target liposomes containing 1 µM FluoZin-1 were added to Zn^{++} -containing furin-treated proteoliposomes (~1.5–3.0 µM protein in 50 µM lipid) at a 1:10 ratio, and content mixing was assessed as described above (excitation 370 nm; emission 485 nm). The fluorescence signal for complete mixing was determined by solubilizing the liposomes in buffer adjusted to 50 µM Zn^{++}.

Expression of GPC in Mammalian Cells. GPC was expressed in Vero cells, with SSP and the GP1-GP2 precursor in trans, using pcDNA-based plasmids and T7 polymerase provided

by the recombinant vaccinia virus rTF7-3 [87]. pH-induced cell-cell fusion activity was characterized as previously described [79].

C. Results

Expression of Recombinant GPC. In previous studies, we produced and characterized the recombinant cleavage-defective JUNV GPC precursor protein [53]. GPC^{CD} (previously referred to as icd-GPC) was purified from membranes of baculovirus-infected insect cells and found to retain its trimeric structure. We showed that the $rGPC^{CD}$ trimer binds the JUNV TfR1 receptor [23], JUNV-neutralizing MAbs [82], and small-molecule arenavirus-specific fusion inhibitors [53]. Because the $rGPC^{CD}$ mutant is unable to mediate membrane fusion [79], we expressed wild-type rGPC. As previously described [53], our expression strategy takes advantage of the unusual ability of SSP to associate in trans with the GP1-GP2 precursor to reconstitute the native tripartite complex [48, 49]. Thus, SSP and the wild-type GP1-GP2 precursor were co-expressed using a pFastBac-Dual dual-promoter baculovirus vector. The GP1-GP2 open-reading frame contains a conventional signal peptide and a FLAG tag is appended at the C-terminus to facilitate purification from solubilized insect-cell membranes.

Despite the existence of an insect S1P/SKI-1 orthologue [88], the wild-type rGPC was refractory to cleavage in insect cells. Serendipitously, several laboratories had previously reported functional GPC mutants in which the S1P/SKI-1 cleavage site (RRSLK|A) was replaced by that of furin [89, 90], a cellular protease used in the maturation of other viral envelope glycoproteins. We therefore introduced a furin recognition site (RRRKR|A) into the JUNV GP1-GP2 precursor (GPC^{fur}) and confirmed that the mutant protein was fusogenic when expressed in mammalian cells (Figure. 2-1). In insect cells, however, $rGPC^{fur}$ remained

refractory to cleavage (Figure. 2-2A), perhaps reflecting the differing specificity of the insect enzyme [91]. Based on these results, we purified the rGPC^{fur} precursor to investigate its susceptible to *in vitro* cleavage by human furin.

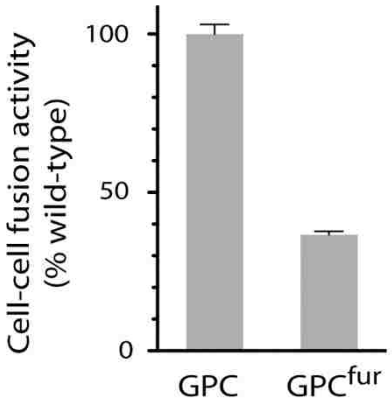

Figure 2-1: The GPC^{fur} mutant is fusogenic in mammalian cell culture. The furin cleavage-site mutation was introduced into the wild-type GP1-GP2 precursor, which was expressed in *trans* with SSP in Vero cells. pH-induced cell-cell fusion activity relative to the wild-type GPC was determined using a vaccinia virus-based beta-galactosidase fusion-reporter assay as previously described [79]. Error bars indicate the standard error of the mean. Background signals obtained in the absence of SSP are ≤2% of wild-type.

Purification of the rGPC^{fur} Precursor. The rGPC^{fur} precursor was solubilized from insect-cell membranes using 1.5% DDM and purified by affinity chromatography using the C-terminal FLAG tag [53]. SDS-PAGE analysis of the purified protein confirmed SSP association in the rGPC^{fur} complex as well as the lack of proteolytic cleavage in insect cells (Figure. 2-2A). Similarly to rGPC^{CD} [53], the rGPC^{fur} precursor formed a relatively homogenous oligomer on size-exclusion chromatography, with an apparent molecular size consistent with a trimer (~220 kDa) (Figure. 2-2A). The yield of purified rGPC^{fur} by this procedure was, 1 mg per liter of High- Five^{TM} cell culture.

The furin-site mutation in rGPC^{fur} did not appear to affect recognition of the trimer by virus-neutralizing MAbs or the TfR1 receptor in SPR studies. Briefly, rGPC^{fur} was captured onto a hydrophobic Biacore L1 sensor chip using immobilized FLAG MAb, and subsequently reconstituted into a lipid membrane [53, 86]. Using a panel of four well-characterized virus-neutralizing MAbs directed to JUNV GP1 [82], we found that the rGPC^{fur} precursor was antigenically indistinguishable from rGPC^{CD} and bound to soluble TfR1 with comparable affinity [53] (Figure. 2-3A and Table 2-1). Together, these results suggest that the purified rGPC^{fur} trimer retains important aspects of the native structure.

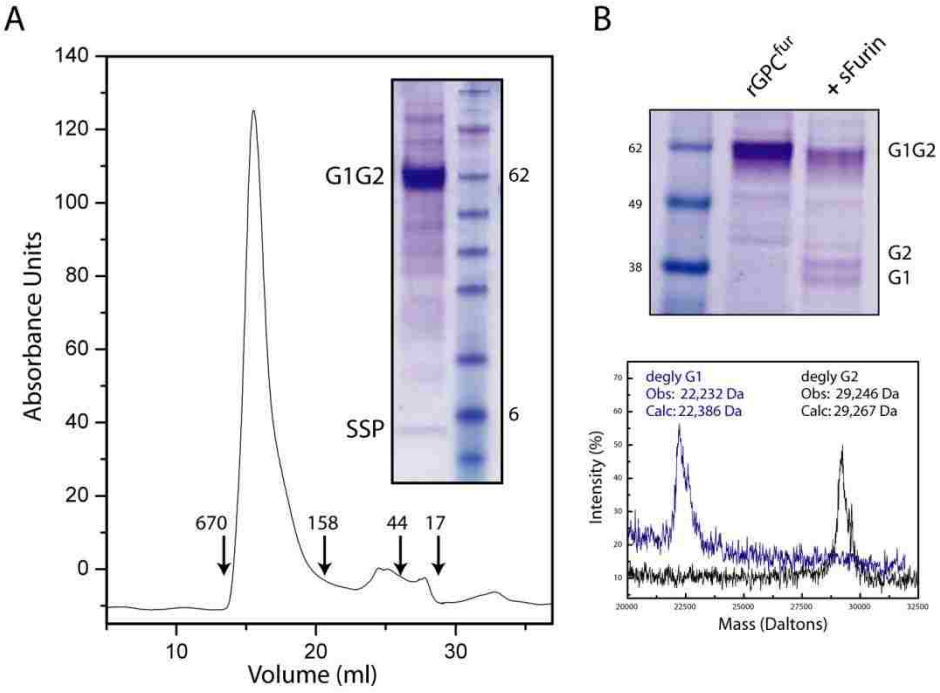

Figure 2-2. Purification and proteolytic cleavage of rGPC^{fur}. A. Affinity-purified rGPC^{fur} was subjected to size-exclusion chromatography (SEC) and the peak fraction was analyzed by SDS-PAGE. Molecular weight markers used in SEC and SDS-PAGE are shown (in kilodaltons) and GP1-GP2 precursor, GP1 and GP2 subunits and SSP are indicated. **B.** rGPC^{fur} precursor was incubated with sFurin (+sFurin) and examined by SDS-PAGE (top panel). MALDI mass spectrometry was used to determine the molecular weights of the deglycosylated (degly) GP1 and GP2 subunits. The calculated mass is based on the assumption that all potential glycosylation sites are used and subsequently deglycosylated

Table 2-1: Summary of rGPC^{fur} interaction parameters from SPR studies

	k_a ($M^{-1}s^{-1}$)	k_d (s^{-1})	K_d (nM)[a]	rGPC^{CD} K_d (nM)[b]
MAb BF11	4.2×10^5	0.007	16.66 (1.2)	10.1
MAb BF09	1.8×10^5	0.062	344.44 (14.5)	219
MAb BE08	1.2×10^5	0.081	675 (20.3)	125
MAb AG02	0.69×10^5	0.085	1,231 (93.2)	583
sTfR	0.29×10^5	0.078	2,689 (120.5)	1,296

[a]K_d values are the means derived by fitting two or three independent biosensor datasets. The number in parenthesis is the difference between the highest and lowest K_d values from individual datasets.
[b]K_d values for rGPC^{CD} binding are taken from Thomas *et al.*
doi:10.1371/journal.pone.0051114.t001

Table 2-2: Summary of inhibitor-rGPC^{fur} interaction parameters from SPR studies

Inhibitor	k_a ($M^{-1}s^{-1}$)	k_d (s^{-1})	K_d (μM)[a]	rGPC^{CD} K_d (μM)[b]
ST-294	7.9×10^3	0.015	1.89 (0.3)	1.08
17C8	1.8×10^3	0.031	17.22 (2.3)	9.50
ST-375	2.1×10^3	0.02	9.52 (0.8)	3.45
ST-193	1.2×10^3	0.02	16.66 (1.8)	10.52
ST-761	1.8×10^3	0.02	11.11 (0.9)	8.67

[a]K_d values are the means derived by fitting two or three independent biosensor datasets. The number in parenthesis is the difference between the highest and lowest K_d values from individual datasets.
[b]K_d values for rGPC^{CD} binding are taken from Thomas *et al.*
doi:10.1371/journal.pone.0051114.t002

Small-molecule arenavirus-specific fusion inhibitors. Six chemically distinct classes of small-molecule arenavirus-specific entry inhibitors have been identified through independent high-throughput screening exercises at SIGA Technologies (SIGA) and the Scripps Research Institute (TSRI) [37-39, 41]. These classes differ in their specificities for NW arenaviruses (JUNV) and/or OW viruses (LASV) (see Materials and Methods) yet appear to share a common binding site on GPC [41, 53]. The compounds are thought to act through the SSP-GP2 interface to stabilize prefusion GPC against activation at endosomal pH, thereby inhibiting membrane fusion [41, 53].

SPR studies were performed to determine the ability of these inhibitors to bind lipid-reconstituted $rGPC^{fur}$. Compounds active against NW viruses (ST-294, ST-761, ST-193, and TSRI 17C8) bound to JUNV $rGPC^{fur}$, whereas LASV-specific compounds (ST- 161 and TSRI 8C1) did not (Figure. 2-3B). Furthermore, the dissociation constants (K_ds) were similar to those determined for $rGPC^{CD}$ (Table 2-2), approaching concentrations required for 50% inhibition of cell-cell fusion (IC_{50}) by the wild-type GPC in mammalian cell culture [53]. Collectively, our binding studies suggest that the furin-site mutation is well tolerated, and that the $rGPC^{fur}$ precursor produced in insect cells adopts a native-like conformation.

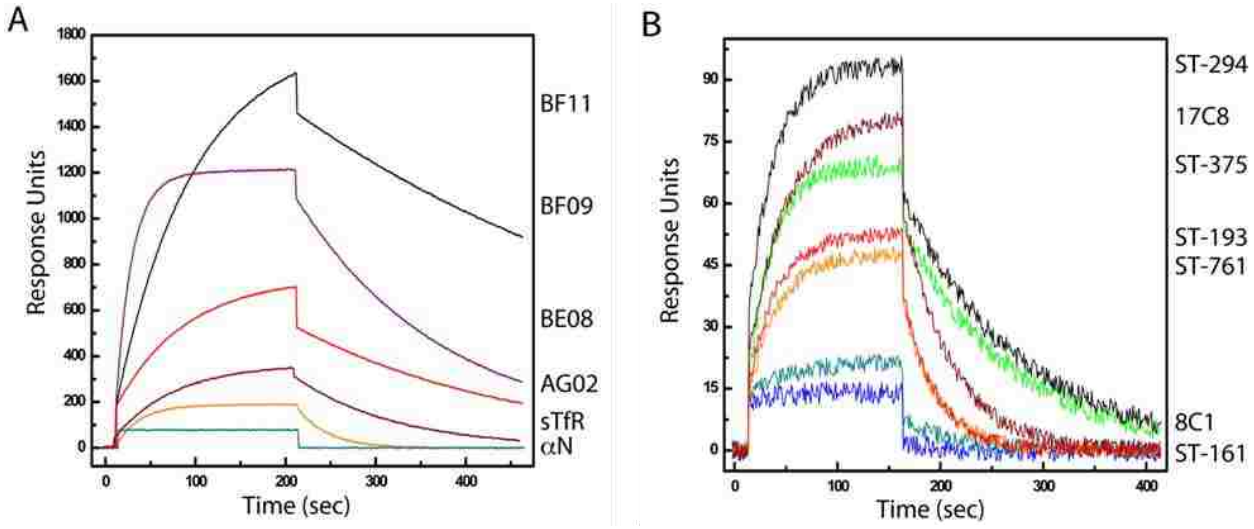

Figure 2-3: SPR studies of interactions with lipid-reconstituted rGPC^{fur}. The rGPC^{fur} precursor was immobilized onto a Biacore L1 chip and reconstituted in a lipid bilayer as described in Material and Methods. Two or three concentration-dependent data sets were analyzed and sensorgram figures were generated using a five-point smoothing procedure and ORIGIN graphing software. Labels to the right are drawn to coincide with the maximum RUs achieved by the respective ligand. **A.** Binding of GP1-directed MAbs (BF11, BF09, BE08, and AG02; 0.5 µM), sTfR (1.5 µM), and a nucleoprotein-directed MAb (α N; BG12). **B.** Binding of SIGA (ST-294, ST-375, ST-193, and ST-761; 150 µM) and TSRI (17C8; 100 µM) small-molecule fusion inhibitors. ST-161 and TSRI 8C1 are specific to the OW LASV and do not inhibit the NW arenavirus JUNV.

Proteolytic cleavage of purified rGPC^{fur}. For proteolytic cleavage of rGPC^{fur}, we expressed recombinant soluble human furin (sFurin) in insect cells and purified the enzyme by Ni^{++} - affinity chromatography [83]. sFurin digestion of the purified rGPC^{fur} precursor in nonionic detergent at 20^0 C resulted in only partial (~40%) cleavage (Figure. 2-2B). We were unable to identify conditions to drive the digestion to completion and speculate that the engineered furin recognition site may not be optimally presented for cleavage [92]. Nonetheless, MALDI mass spectrometric analysis of the GP1 and GP2 subunits generated by furin digestion at 20^0C confirmed cleavage at the predicted site (RRRKR|A) and the production of the wild-type GP2 subunit (Figure. 2-2B).

pH-induced conformational changes in furin-cleaved rGPC^{fur}. We reasoned that cleaved rGPC^{fur} should differ from the uncleaved protein in its response to acidic pH. Fusion activation in class I fusion proteins typically results in the dissociation of non-covalently associated receptor-binding and transmembrane subunits [93]. Indeed, mammalian cells expressing GPC have been shown to shed GP1 on exposure to acidic pH [41]. We therefore examined GP1 shedding from cleaved rGPC^{fur} as an indication of pH-induced fusion activation. In these experiments, lipid-reconstituted rGPC^{fur} was incubated on the biosensor chip with a bolus of sFurin (Figure. 2-4, middle trace, left). On washing, the SPR response units (RUs) returned to the pre-digestion baseline, indicating that no protein had been lost from the chip. Following transient exposure to pH 5.0, however, the baseline signal was reduced by ~800 RUs, consistent with pH-induced shedding of GP1 (Figure. 2-4, middle trace, center). By contrast, identical treatment of the rGPC^{CD} precursor resulted in no loss of protein (Figure. 2-4, top trace). Based on the magnitude of the pH-induced loss from furin-

treated rGPC^{fur}, we estimate that cleavage was ~70% complete under these conditions. Susceptibility of rGPC^{fur} to furin cleavage may be enhanced by membrane anchorage.

To confirm that the pH-induced reduction in baseline RUs reflects a loss of GP1, we probed the same chip surface with a GP1-specific MAb [82]. Binding of MAb BF11 to cleaved rGPC^{fur} was markedly reduced after exposure to pH 5.0 relative to the rGPC^{CD} control (Figure. 2-4, right), indicative of pH-induced GP1 shedding. Furthermore, the loss of GP1 from cleaved rGPC^{fur} was found to be inhibited by ST-294 (Figure. 2-4, lower trace), in agreement with results obtained using native GPC on the surface of mammalian cells [41]. We conclude rGPC^{fur} can be functionally matured *in vitro* and that the prefusion trimer is able to respond to acidic pH in a manner consistent with on-path conformational changes seen in the native GPC complex.

Proteolytic cleavage of the rGPC^{fur} precursor was found to have only a minimal effect on the extent and overall affinity of ST-294 binding (K_d=2 µM vs. 4 µM) (Figure. 2-5A). However, exposure to acidic pH markedly reduced the extent of subsequent ST-294 binding (Figure. 2-5A). The K_d of the residual binding was unaffected and is likely attributable to uncleaved rGPC^{fur} remaining on the SPR chip. This notion is supported by observations that the cleavage-defective rGPC^{CD} can be repeatedly cycled at low pH without loss of ST-294 binding activity (Figure. 2-5B). These latter observations suggest that the trimeric precursor does not undergo significant irreversible change in response to acidic pH. The covalent linkage of the GP1 and GP2 subunits in the precursor likely constrains pH-induced conformational excursions from the initial state.

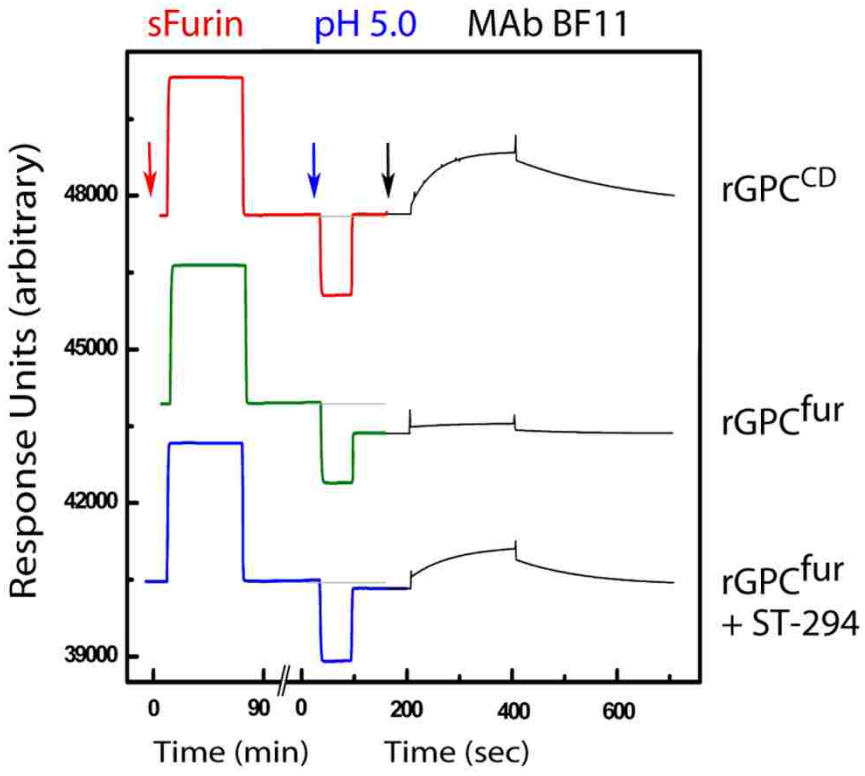

Figure 2-4. SPR analysis of pH-induced GP1 shedding. rGPC was immobilized onto a Biacore L1 chip and reconstituted in a lipid bilayer as described [53]. The figure includes a composite of SPR responses from single-chip experiments in which $rGPC^{CD}$ (top trace) or $rGPC^{fur}$ (bottom two traces) were sequentially incubated with sFurin (red arrow), exposed to pH 5.0 (blue arrow), and probed with the GP1-specific MAb BF11 (black arrow). In the lower trace, 20 μM of ST-294 was present throughout the experiment. The relative baseline before exposure to pH 5.0 is shown as a gray line and the absolute RU values on the y-axis are arbitrary.

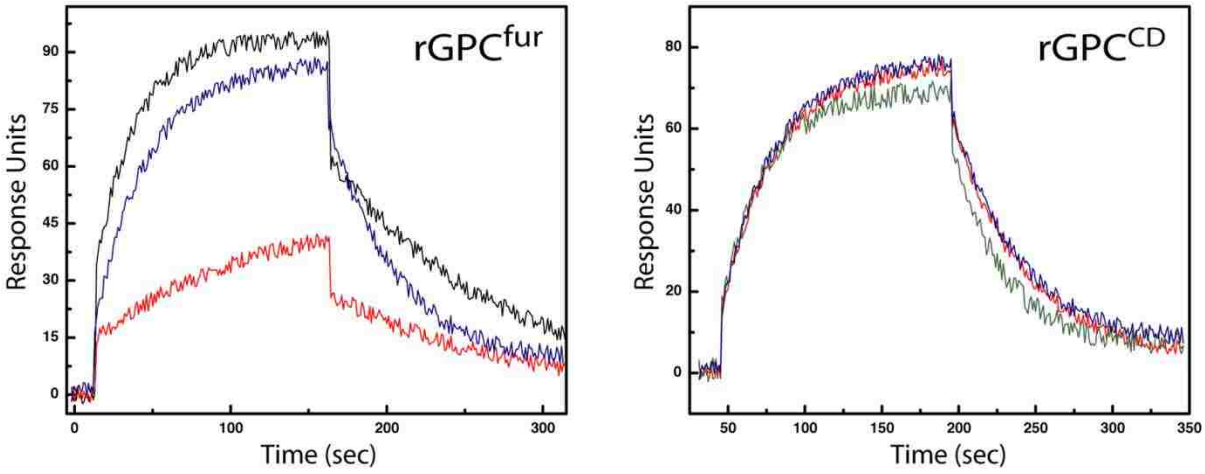

Figure 2-5. SPR studies of ST-294 binding to rGPC^{fur} following cleavage and exposure to acidic pH. A. ST-294 (100 µM) was bound to lipid-reconstituted rGPC^{fur} on a Biacore L1 chip prior to (black) and after (blue) sFurin cleavage, and following exposure of the latter to acidic pH (red). Bound ST-294 was allowed to dissociate from the complex between subsequent injections. **B.** In a similar study using immobilized cleavage-defective rGPC^{CD}, ST-294 was bound prior to (blue) and following one and two sequential exposures to acidic pH (red and green, respectively).

Furin-cleaved rGPC^{fur} mediates pH-dependent membrane fusion. In order to determine whether cleaved rGPC^{fur} is able to mediate membrane fusion, we incorporated the recombinant protein into LUVs and examined the ability of the proteoliposomes to fuse with target LUVs in a pH-dependent manner. The target liposomes were doped with a self-quenching concentration of rhodamine-PE, and fusion with the proteoliposome results in dilution of the rhodamine within the merged lipids and dequenching of the fluorophore [94]. At neutral pH, the liposome mixture was stable over the course of 15 min, regardless of whether proteoliposomes had previously been incubated with sFurin (Figure. 2-6). Proteoliposomes bearing uncleaved rGPC^{fur} were likewise stable when exposed to acidic pH. By contrast, acidification of sFurin-cleaved rGPC^{fur} resulted in a rapid increase in fluorescence over a period of 3 min (Figure. 2-6). After 5 min, rhodamine-PE fluorescence approached ~30% of the maximum obtained on complete dequenching in nonionic detergent. Importantly, pH-induced fusion was inhibited by the prior addition of ST-294, but not by the LASV-specific compound ST-161 (Figure. 2-6). Thus, reconstituted rGPC^{fur} is proteolytically primed and can be activated by acidic pH to mediate fusion.

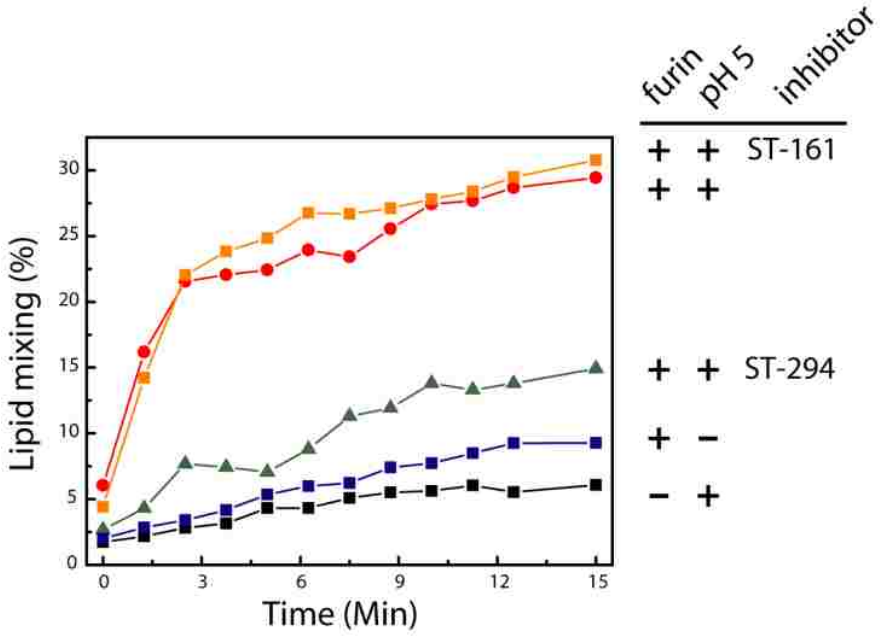

Figure 2-6: pH-induced membrane fusion by rGPC^{fur} proteoliposomes: lipid mixing. rGPC^{fur} was incorporated into POPG-POPC liposomes and mixed with target POPG-POPC liposomes doped with 1% Rhodamine-PE. In most cases, the rGPC^{fur} proteoliposomes were first treated with sFurin (as indicated by + in the first position of the labels, at right). Exposure to acidic pH at the start of the experiment (time=0) is indicated by + in the second position of the labels. 15 μM of ST-294 or ST-161 was present prior to and during exposure to acidic pH, where indicated. Lipid mixing and the resulting dequenching of the rhodamine fluorophore were measured at 600 nm (excitation 508 nm). Complete dequenching (100%) was determined by subsequent solubilization in Triton X-100 nonionic detergent.

Rhodamine dequenching upon pH-induced activation demonstrates mixing of the liposomal lipids. At a minimum, this result indicates that cleaved $rGPC^{fur}$ is capable of inducing hemifusion, an intermediate state in fusion where only the outer leaflets of the two membranes merge. Previous studies have shown that engineered envelope proteins linked to the cell membrane only via a lipid glycophosphatidylinositol (GPI) anchor, or in which the transmembrane domain is truncated, arrest at this hemifusion intermediate [95-98]. To determine whether $rGPC^{fur}$ proteoliposomes can proceed to complete fusion, with merger of both membrane leaflets and opening of a fusion pore, we monitored pH-induced mixing of liposome contents. In these studies, target liposomes containing the Zn^{++} -sensitive fluorophore FluoZin-1 were mixed with $rGPC^{fur}$ proteoliposomes containing 50 μM Zn^{++}. Complete fusion with content mixing results in an increase in FluoZin-1 fluorescence. Without sFurin-cleavage, only baseline fluorescence was detected over a 20 min period at acidic pH (Figure. 2-7A). Similarly, furin-treated proteoliposomes were stable at neutral pH. By contrast, acidification of the cleaved $rGPC^{fur}$ proteoliposomes led to a rapid increase in fluorescence that was preceded by a lag period of ~2 min (Figure. 2-7A). By 10 min, content mixing was ~40% of the maximum. The lag period in content mixing may indicate a kinetic barrier for resolution of the hemifusion intermediate [99]. Our results indicate that reconstituted $rGPC^{fur}$ mediates complete membrane fusion with content mixing. In addition, we found that $rGPC^{fur}$-mediated fusion was markedly inhibited by ST-294, but not by the LASV-specific inhibitor ST-161 (Figure. 2-7A). Taken together, our studies demonstrate that recombinant $rGPC^{fur}$ faithfully reproduces the pH-induced membrane-fusion activity of native GPC.

Distinct Modes of Antibody-mediated Neutralization. Reconstitution of the membrane-fusion reaction provides a platform to investigate the mechanisms of antibody-mediated virus neutralization. For example, MAb F100G5 has been shown to recognize the fusion peptide of JUNV GP2 [77] and, as this region is sequestered in prefusion GPC, does not bind virions and is therefore unable to inhibit entry following endocytic uptake of the particle. Liposomal fusion by $rGPC^{fur}$ proteoliposomes was, however, inhibited when F100G5 was present in the low-pH buffer (Figure. 2-7B). This result recapitulates previous observations from cell-cell fusion assays [77]. By contrast, the molecular basis for virus neutralization by the GP1-directed MAb BF11 [82] is unknown. Interestingly, MAb BF11 did not inhibit proteoliposomal fusion (Figure. 2-7B). We conclude that this MAb may block TfR binding or virion internalization. This *in vitro* model of membrane fusion offers unprecedented access for biochemical studies of GPC function and its inhibition.

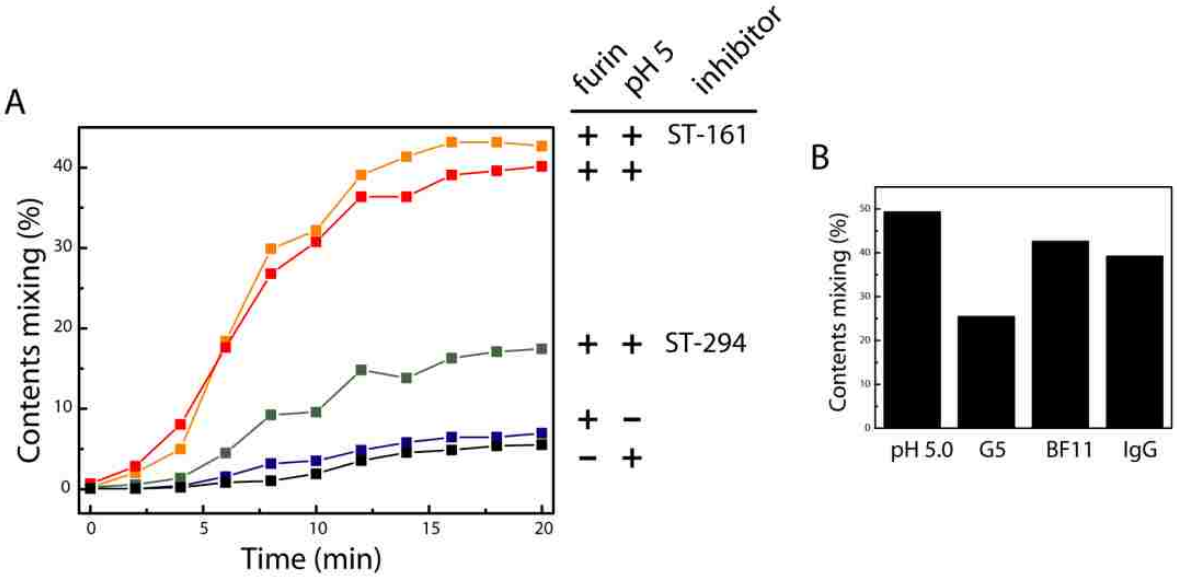

Figure 2-7. A. rGPC^{fur} was incorporated into POPG-POPC-CHS liposomes containing 50 µM $Zn^{++}$and these proteoliposomes were mixed with target POPG-POPC-CHS liposomes containing 1 µM FluoZin-1. The experimental treatments, labels and colors are as described in the legend of Figure 2-6. Content mixing was determined by Zn^{++}-induced FluoZin-1 fluorescence measured at 485 nm (excitation 370 nm). Complete mixing was determined by solubilization with Triton X-100 in buffer containing 50 µM Zn^{++}. **B.** pH-induced content mixing was determined in the continued presence of MAbs F100G5, BF11 or an irrelevant IgG (5 µM, 25 µM and 25 µM, respectively). In this experiment, content mixing in the absence of MAb (pH 5.0) was ~50%.

D. Discussion

Owing to the inherently labile nature of the prefusion envelope glycoprotein, solubilization of class I fusion proteins from the membrane typically destabilizes the trimeric structure sufficiently to cause disassembly and/or refolding to the stable postfusion state [100-102]. Indeed, this intrinsic instability has greatly hindered biochemical and biophysical studies on the viral fusion machinery, and frustrated efforts to design and develop native envelope glycoproteins as effective vaccine immunogens [103]. We hypothesize that the unique stability of GPC results from interaction among the nine transmembrane domains in the trimeric complex (vs. three in conventional class I fusion proteins), enforced by inter-subunit zinc-finger structures. The fortuitous resilience of GPC offers the possibility for investigating the molecular basis of membrane fusion mediated by a membrane-anchored envelope glycoprotein *in vitro*.

Our current mechanistic understanding of viral membrane fusion was developed in part from now-classical studies of influenza virus HA (reviewed in reference [104]). High-resolution crystallographic structures of the soluble HA ectodomain in its precursor [105], prefusion [106] and postfusion [52] states serve as reference points for the current model [105, 107]. Recent studies of PIV5 F [101, 102] have reinforced central tenets of the model. These crystallographic structures, as well as those of the stable postfusion core of other class I fusion proteins, have all been determined using soluble forms of the glycoprotein ectodomain and are therefore silent with respect to the transmembrane and cytoplasmic domains. To our knowledge, this report is the first to demonstrate full reconstitution of membrane-fusion activity by a complete virus envelope glycoprotein. Membrane anchorage is essential for membrane-fusion activity. Envelope glycoprotein ectodomains anchored in

the membrane by a GPI lipid or truncated transmembrane domains are unable to drive fusion to completion, arresting at the hemifusion state [95-98]. Anchorage may be required to transduce forces generated upon protein refolding towards complete fusion of the two bilayers. Lateral contacts within the membrane between several envelope glycoprotein spikes may also be important for formation of the stable fusion pore. Membrane interactions of the membrane-proximal ectodomain of HIV-1 Env are involved in the fusion process and contribute to important determinants for broadly neutralizing antibodies [108, 109]. Furthermore, envelope glycoprotein membrane-spanning domains also serve as conduits to transmit information between the internal and external domains for virion assembly and virus entry [110, 111]. In GPC, amino-acid changes in the membrane-proximal and transmembrane domains have been shown to affect GPC biosynthesis and intracellular trafficking of the complex [49, 80], its sensitivity to acidic pH and small-molecule fusion inhibitors [41, 55, 112] and, indeed, viral pathogenesis [113, 114]. Further analysis of GPC structure and function using this biochemically defined *in vitro* system will advance our understanding of the conformational transitions that promote viral membrane fusion. This knowledge will directly facilitate efforts to design novel entry inhibitors for the treatment of arenavirus hemorrhagic fevers.

Acknowledgments

We are grateful to Alex Strongin (Sanford-Burnham Medical Research Institute) and Martin Scott (Glaxo-SmithKline) for providing molecular clones and advice for expression of soluble furin. We are also grateful to Sean Amberg and Dongcheng Dai (SIGA Technologies) and Stefan Kunz, Andrew Lee and Michael Oldstone (The Scripps Research Institute) for providing small-molecule fusion inhibitors, and to Brian Crammer (Colorado State University) for assistance in biosensor studies. SPR studies were performed at the Proteomics Core of the Rocky Mountain Center of Excellence for Biodefense and Emerging Infectious Diseases Research at Colorado State University. We also thank the Baculovirus Expression Core of the CoBRE Center for Biomolecular Structure and Dynamics at The University of Montana for assistance with insect cell culture. GP1-directed JUNV MAbs were obtained from the CDC through the NIAID Biodefense and Emerging Infectious Diseases Research Resources Repository.

Chapter 3

Small-molecule fusion inhibitors bind the pH-sensing SSP-GP2 subunit interface of the Lassa virus envelope glycoprotein

Abstract

Arenavirus species are responsible for severe life-threatening hemorrhagic fevers in western Africa and South America. Without effective antiviral therapies or vaccines, these viruses pose serious public health and biodefense concerns. Chemically distinct small-molecule inhibitors of arenavirus entry have recently been identified and shown to act on the arenavirus envelope glycoprotein (GPC) to prevent membrane fusion. In the tripartite GPC complex, pH-dependent membrane fusion is triggered through a poorly understood interaction between the stable signal peptide (SSP) and the transmembrane fusion subunit GP2, and our genetic studies have suggested that these small-molecule inhibitors act at this interface to antagonize fusion activation. Here, we have designed and synthesized photoaffinity derivatives of the 4-acyl-1,6-dialkylpiperazin-2-one class of fusion inhibitors and demonstrate specific labeling of both the SSP and GP2 subunits in a native-like Lassa virus (LASV) GPC trimer expressed in insect cells. Photoaddition is competed by the parental inhibitor and other chemically distinct compounds active against LASV, but not those specific to New World arenaviruses. These studies provide direct physical evidence that these inhibitors bind at the SSP-GP2 interface. We also find that GPC containing the uncleaved GP1-GP2 precursor is not susceptible to photocrosslinking, suggesting that proteolytic maturation is accompanied by conformational changes at this site. Detailed mapping of residues modified by the photoaffinity adducts may provide insight to guide the

further development of these promising lead compounds as potential therapeutic agents to treat Lassa hemorrhagic fever.

Importance

Hemorrhagic fever arenaviruses cause lethal infections in humans and, in the absence of licensed vaccines or specific antiviral therapies, are recognized to pose significant threats to public health and biodefense. Lead small-molecule inhibitors that target the arenavirus envelope glycoprotein (GPC) have recently been identified and shown to block GPC-mediated fusion of the viral and cellular endosomal membranes, thereby preventing virus entry into the host cell. Genetic studies suggest that these inhibitors act through a unique pH-sensing intersubunit interface in GPC, but atomic-level structural information is unavailable. In this report, we utilize novel photoreactive fusion inhibitors and photoaffinity labeling to obtain direct physical evidence for inhibitor binding at this critical interface in LASV GPC. Future identification of modified residues at the inhibitor-binding site will help elucidate the molecular basis for fusion activation and its inhibition, and guide the development of effective therapies to treat arenaviral hemorrhagic fevers.

This chapter was taken from the paper cited below published in Journal of Virology, selected for the “Spotlight” section.

Shankar, S., L. R. Whitby, H. E. Casquilho-Gray, J. York, D. L. Boger and J. H. Nunberg (2016). "Small-molecule fusion inhibitors bind the pH-sensing SSP-GP2 subunit interface of the Lassa virus envelope glycoprotein." J Virol

A. Introduction

Arenaviruses are endemic in rodent populations worldwide, and some species can be transmitted to humans to cause severe hemorrhagic fevers with high morbidity and mortality [12, 15]. Lassa virus (LASV) is prevalent in western Africa [14] and can be exported to the US and Europe by infected travelers [67, 68, 115]. Five New World (NW) species cause fatal disease in the Americas, including the Argentine hemorrhagic fever virus Junín (JUNV) [12, 13]. New pathogenic species continue to emerge [4, 5] and novel arenaviruses have recently been identified in boid species of constrictor snakes [6, 7]. Absent effective vaccines or therapies, hemorrhagic fever arenaviruses pose significant threats to public health and biodefense [32]. Accordingly, these viruses are classified as Category A priority pathogens [33].

Antiviral strategies that interfere with virus entry into the host cell have in many instances proven effective in preventing infection and treating disease. Arenaviruses enter the host cell by pH-dependent fusion of the viral and endosomal membranes [75], a process mediated by the viral envelope glycoprotein GPC. GPC is synthesized as a precursor that trimerizes and is cleaved by the cellular S1P/SKI-1 protease [46, 47, 73] to generate the receptor-binding (GP1) [23, 74] and transmembrane fusion (GP2) subunits. Unlike other viral envelope glycoproteins, GPC retains a 58 amino-acid residue signal peptide as a third, noncovalently associated subunit in the mature complex (Fig. 3-1) [48, 116]. This stable signal peptide (SSP) contains two hydrophobic regions that span the membrane to form a hairpin structure [80], with a central ectodomain loop that interacts with GP2 to sense acidic pH and trigger membrane fusion [54, 112]. As a bona fide member of the Class I viral fusion proteins [76, 78, 117, 118], the mature GPC exists in a kinetically trapped metastable state, primed by

proteolytic cleavage and triggered by low pH to undergo a prescribed structural reorganization leading to formation of the thermodynamically favored trimer-of-hairpins structure and fusion of the viral and endosomal membrane (reviewed in [50, 51]). Small molecule compounds that inhibit in this orderly process can effectively inhibit virus entry.

High-throughput screening campaigns at SIGA Technologies [37, 38, 53, 119] and the Scripps Research Institute [39, 40] have recently identified six chemically distinct classes of small-molecule compounds that specifically target arenavirus GPC and inhibit arenavirus entry into its host cell. Several of these inhibitors have been shown to protect against lethal arenavirus infection in small-animal models [37, 42]. Despite differences in chemistries and activity profiles against NW and/or Old World (OW) arenavirus species, these compounds appear to share a common binding site on GPC [41]. Specifically, we have shown that all the inhibitors active against the NW JUNV compete for binding to recombinant JUNV GPC, but are not displaced by those specific to the OW LASV [53]. Yet, an SSP mutation in JUNV GPC that generates resistance to a NW-specific inhibitor renders the protein sensitive to inhibition by an OW-specific compound [41]. Amino-acid determinants of sensitivity to one or multiple classes of these inhibitors have been identified in both SSP and GP2 (Fig. 3-1) [37, 38, 55]. Interestingly, several resistance mutations also modulate the pH at which membrane fusion is triggered [54, 112]. Recognizing that these inhibitors antagonize fusion activation [41, 53], we infer that they target pH-sensing SSP-GP2 interface of GPC. However, atomic-level structural information on the intact GPC complex is not available. In this report, we describe the use of photoaffinity labeling to directly identify the inhibitor-binding site, as an initial step towards understanding the molecular basis for the pH-induced activation of GPC membrane fusion and its inhibition.

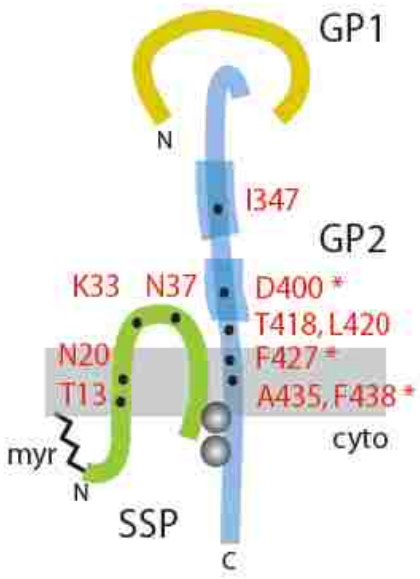

Figure 3-1. Model for the subunit organization of the tripartite GPC complex. The SSP, GP1 and GP2 subunits are drawn schematically and are not to scale. Features include: the myristate moiety at the N terminus of SSP (myr) [116], the binuclear zinc finger linking the penultimate cysteine-57 in SSP and the novel zinc-binding motif in the cytoplasmic tail of GP2 (gray balls) [45, 81], and the heptad-repeat regions in the ectodomain of GP2 that are diagnostic of Class I viral fusion proteins (thickened lines) [76, 78, 117, 118]. Residues in JUNV GPC associated with resistance to or dependence on small-molecule fusion inhibitors are indicated [37, 38, 41, 55]; asterisks denote mutations in GP2 that complement pH-dependent fusion defects engendered by mutations at K33 in SSP [112].

B. Materials and methods

Plasmids, cells and recombinant baculoviruses. The complete LASV GPC gene from the Josiah isolate (GenBank: J04324) was molecularly cloned into a pcDNA3.1 plasmid vector (Life Technologies) for expression in Vero cells [55]. For generating recombinant baculoviruses, the GPC open-reading frame was subdivided to express SSP and the GP1-GP2 precursor (using the conventional signal peptide of human CD4) in a pFastBac Dual plasmid vector (Life Technologies) as previously described [53, 70]. Expression in *trans* allows in reconstitution of the functional tripartite GPC complex in both mammalian [48, 79] and insect [53, 70] cells and obviates concerns regarding incomplete signal peptidase cleavage of SSP [48, 120, 121]. An innocuous FLAG tag appended to the C-terminus of the GP1-GP2 precursor facilitates detection and affinity purification using the M2 anti-FLAG monoclonal antibody (MAb; Sigma) [53, 70]. To generate a cleavage-defective (cd) LASV GPC mutant, the SKI-1/S1P cleavage site RRLL in the GP1-GP2 precursor was changed to AALL using QuikChange mutagenesis. Baculoviruses expressing wild-type and cd LASV GPC were generated using the Bac-to-Bac™ system (Life Technologies) [53, 70].

Expression of LASV GPC in insect cells: purification of insect-cell membranes and characterization of the purified protein. Recombinant baculoviruses were used to infect *Trichoplusia ni* High-Five™ cells and membranes were prepared after 24 hr of growth by rupturing the cells using nitrogen decompression (Parr bomb) as previously described [53, 70]. Typical yields are ~0.7 mg of LASV GPC per 3 x 10^9 cells per liter of culture. Washed membranes were resuspended at a concentration of ~160 mg wet-weight per ml (~1.4 x 10^8 cell equivalents per ml) in buffer containing 50 mM Tris, pH 7.5, 150 mM NaCl, 100 µM $ZnCl_2$ and 20% glycerol, and stored at minus 80°C.

LASV GPC was solubilized from insect-cell membranes by the addition of the nonionic detergent n-dodecyl β-D-maltoside (DDM, Anatrace) to 1.5% and immobilized onto agarose beads containing the anti-FLAG M2 monoclonal antibody (Sigma) as previously described [53, 70]. Beads were washed extensively in buffer containing 50 mM Tris (pH 7.5), 250 mM NaCl, 100 μM $ZnCl_2$ and 0.1% DDM (wash buffer) and LASV GPC was eluted with the addition of 5 μM 3X FLAG peptide (Sigma). Following dialysis to remove the small peptide, the sample was subjected to size-exclusion chromatography using a Superdex-200/G-75 tandem column (GE Healthcare) to determine the oligomeric state of the LASV GPC. Denaturing sodium dodecylsulfate polyacrylamide gel electrophoresis (SDS-PAGE) was performed using lithium dodecylsulfate (LDS) sample buffer with reducing agent (Life Technologies) and NuPAGE 4-12% bis-Tris gels (Life Technologies). Proteins were stained with Sypro Red (Life Technologies) or by western blot analysis using an anti-FLAG horseradish peroxidase-conjugated antibody (Cell Signaling) and ECL 2 substrate (Pierce), and visualized using a Fuji FLA-3000G fluorescence imager.

Small-molecule inhibitors and photoaffinity derivatives. Compounds **1** [lassamycin-1; (*S*)-16G8] and **2** [(*S*)-17D1] were synthesized as described previously [40]. Chemical synthesis of photoaffinity probes **3-5** (Fig. 3-2) is outlined in Fig. S1. Compounds were characterized by NMR and high-resolution mass spectrometry (HRMS). ST-193 [38], ST-161 [119] and ST-294 [37] were kindly provided by SIGA Technologies, Inc. (Corvallis, OR).

Inhibition of GPC-mediated cell-cell fusion. The inhibitory potency of the photoaffinity derivatives in Vero cells were determined in a vaccinia virus-based cell-cell fusion reporter assay as previously described [39, 54, 55]. In brief, cells infected with a recombinant

vaccinia virus encoding the bacteriophage T7 RNA polymerase (vTF7-3) and expressing LASV GPC from the minimal T7 promoter in the pcDNA3.1 vector are mixed with target cells infected with a recombinant vaccinia virus (vCB21R-LacZ) capable of expressing β-galactosidase under the control of the T7 promoter [122]. GPC-mediated cell-cell fusion is induced upon exposure to acidic medium (pH 5.0) and drives expression of the β-galactosidase reporter, which is quantitated using the chemiluminescent GalactoLite Plus β-Galactosidase Reporter Gene Assay System (Applied Biosystems) in a SpectraMax L microplate luminometer (Molecular Devises). The 50% inhibitory concentrations (IC_{50}s) were calculated using GraphPad Prism software by fitting data to single-slope dose-response curves constrained to 0% and 100% values.

Workflow for photoaffinity labeling. Volume of 500 µl of insect-cell membranes containing an estimated 16 µg of LASV GPC were incubated with photoreactive inhibitors (typically 10 µM final) for 45 min at room temperature, followed by exposure to long-wavelength UV irradiation (~366 nm) on ice for 30 min. Samples are positioned 5 cm from the Sylvania 100W Mercury Blacklight bulb (H44GS-100) and rocked intermittently. In some experiments, non-photoreactive fusion inhibitors were added at 50 µM with the photoaffinity probes to assess competition. Following photo-cross-linking, GPC was solubilized from the membranes by the addition of DDM to 2% and immobilized onto anti-FLAG agarose beads. Beads were washed extensively in wash buffer prior to using copper (I)-catalyzed azide-alkyne cycloaddition (click chemistry [123, 124]) to attach a tetramethylrhodamine (TAMRA) moiety to the pendant alkyne group of the photoaffinity adduct on LASV GPC. In this reaction, the beads are incubated in wash buffer containing 25 µM TAMRA-azide linker (Life Technologies, T10182), 1 mM tris(carboxyethyl) phosphine

(TCEP), 1 mM $CuSO_4$ and 100 µM tris[(1-benzyl-1*H*-1,2,3-triazol-4-yl)methyl]amine (TBTA) (Sigma) at room temperature for 1 hr. The reaction is stopped by extensive washing in wash buffer prior to elution of the bound LASV GPC in reducing LDS sample buffer (Life Technologies) and SDS-PAGE analysis using NuPAGE 4-12% bis-Tris gels (Life Technologies). TAMRA-containing protein bands were detected using a Fuji FLA-3000G imager. In some experiments, the LASV GPC was deglycosylated using peptide-N-glycosidase F (PNGase F; New England Biolabs) prior to SDS-PAGE analysis.

Protease digestion. FLAG elute was concentrated/dialysed to remove the 3X FLAG peptide using amicon (Millipore) 100 kDa filter. The concentrated pool was reduced by addition of 5 mM tris(2-carboxyethyl)phosphine (TCEP) for 30 min at room temperature followed by alkylation with 10 mM iodoacetamide for 30 min at room temperature in the dark. The reaction was quenched by adding 5 mM of dithiothreitol (DTT) for 10 min. The protein was then digested with 25 µg of chymotrypsin for 18 hr at 37^0 C in presence of 2 mM $CaCl_2$. The reaction was stopped by adding 1mM phenylmethanesulfonyl fluoride (PMSF).

Enrichment of photo-adduct using Streptavidin beads. Photoaffinity labeled intact LASV GPC or digested peptides were enriched on magnetic streptavidin bead (pierce). The FLAG-eluted protein was incubated with prewashed magnetic streptavidin beads for 1 hr at room temperature on a rotator. The tube was then placed on a magnetic stand to collect the beads against the side of the tube. The beads were initially washed with wash buffer containing 0.1% DDM. A stringent wash with 2% SDS at 60^0 C for 10 min was included to remove any non-specific binding [125]. The photoaffinity labeled biotin-adduct was eluted from the beads by incubating with SDS-biotin elution buffer (50 mM Tris pH 7.8, 150 mM $NaCl_2$, 2% SDS, 1 mM d-biotin) at 60^0 C for 30 min [125].

Folch extraction and gel filtration of the peptide-adducts. Peptide-adduct from the streptavidin elute was subjected to Folch extraction [126]. To the streptavidin elute, chloroform and methanol was added in 3:8:4 ratio respectively and allowed to stand for 1 hr at room temperature. The organic phase, the aqueous phase and interface were carefully separated into tubes and dried using speed vac. The contents in each tube were solubilized in 0.1% TFA water and 30% acetonitrile. Each phase was analyzed for recovery of peptides by monitoring TAMRA signal using dot blot. In a dot blot assay, samples were spotted on a nitrocellulose membrane and allowed to dry. The blots were then analyzed in Fuji FLA 3000 for TAMRA signal.

The organic phase containing photo-adducts were subjected to size-exclusion chromatography (SEC) using a Superdex Peptide 3.2/300 column (GE healthcare). 0.1% TFA water containing 25% acetonitrile was used as mobile phase. Absorbance at 214 nm for the peptide bond and 550 nm absorbance of TAMRA signal was monitored and fractions collected were subjected to dot blot assay. TAMRA positive fractions were further analyzed by Bruker microflex MALDI-TOF.

C. Results

Strategy for designing inhibitor derivatives for photoaffinity labeling. Lassamycin-1 (**1**; Fig. 3-2) [40] is the active enantiomer of 16G8, a member of a class of 4-acyl-1,6-dialkylpiperazin-2-one fusion inhibitors [39]. Compound **1** inhibits transduction by retroviral pseudotyped virions bearing LASV GPC with a 50% inhibitory concentration (IC_{50}) of ~200 nM [40]. Discovery of the (*S*)-configuration as the active enantiomer led to the design and synthesis of (*S*)-17D1 (**2**; Fig. 2) [39], which inhibits LASV GPC-mediated cell-cell fusion with an IC_{50} of 30 nM. Compounds **1** and **2** were subsequently used as starting scaffolds to design three alkynylated trifluoromethyldiazirine photoaffinity probes (**3**–**5;** Fig. 3-2 and Supplemental Fig. S1). The published synthesis of 4-(3-(trifluoromethyl)-3H-diazirin-3-yl)benzaldehyde (Fig. S1) provided a simple synthetic route to incorporate the diazirine [127]. The placement of the trifluoromethyldiazirine was guided by the known tolerance for functionality (4-OMe or 4-Me groups) at the 4-position of the N^1 benzyl group [39]. The optimal placement of the alkyne was then determined to be as a propargyl substituent on a heteroatom at the 4-position of the N^4 benzamide group for probes **3** and **5**. The insight for this alkyne placement was provided by **2** as well as a scanning library of derivatives of **2** that demonstrated that compounds with a variety of alkylated heteroatom substituents at the 4-position of the N^4 benzamide group showed potent activity. In order to study probes based upon compound **1**, we decided to incorporate the alkyne as an aryl propargyl ether at the 4-position of the C^6 benzyl group to generate **4**. This design was guided by our knowledge that a compound with an aryl methyl ether at this position retained potent activity (unpublished data).

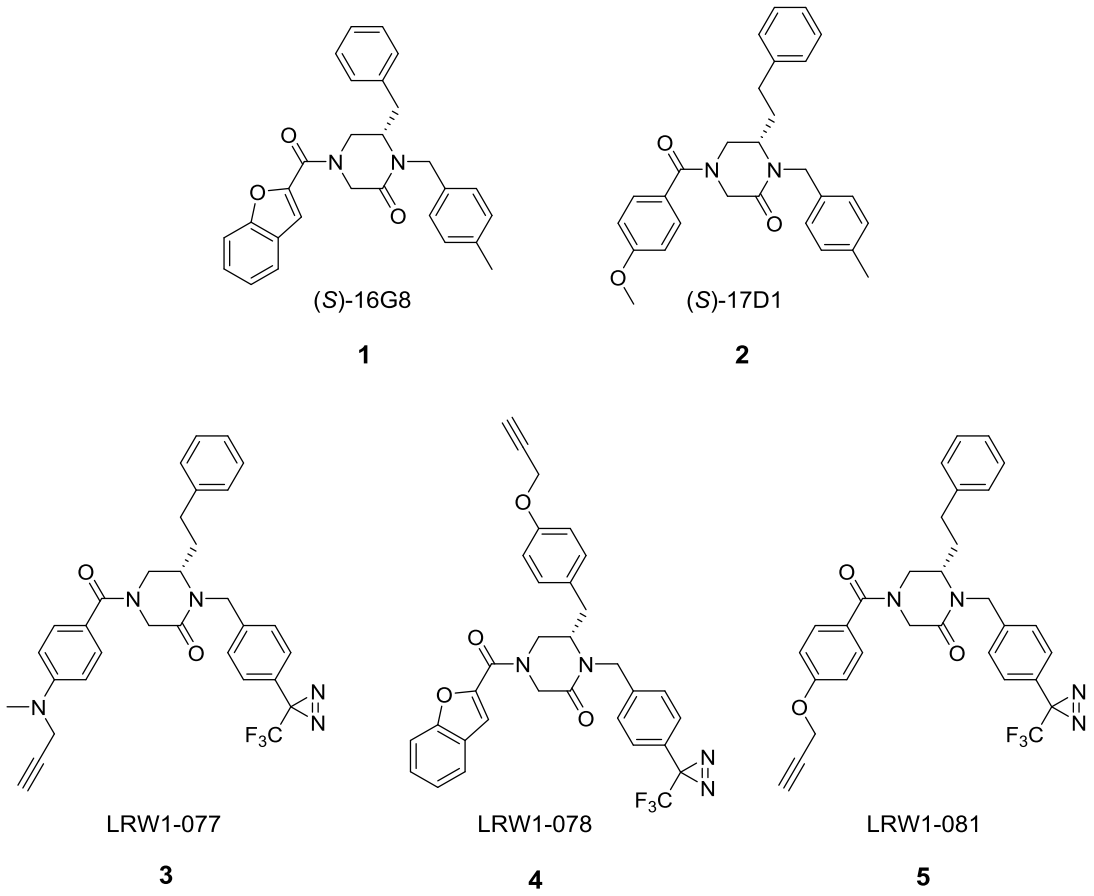

Figure 3-2: Chemical structures of fusion inhibitors and photoaffinity derivatives. (S)-16G8 (Lassamycin-1; compound **1)** [40] and (S)-17D1 (compound **2**) [39] provide the respective starting scaffolds for LRW1-078 (**4)** and for LRW1-077 (**3**) and LRW1-081 (**5**). These photoaffinity probes include a photolabile trifluoromethyldiazirine moiety as well as a pendant alkyne for copper-catalyzed click chemistry addition of a TAMRA fluorophore.

Photoaffinity derivatives inhibit LASV GPC-mediated cell-cell fusion. The inhibitory potencies of compounds **3** to **5** were determined by inhibition of pH-induced cell-cell fusion using Vero cells expressing LASV GPC in a β-galactosidase reporter assay [39, 54, 55]. The respective IC_{50} values for **3**, **4** and **5** were 70 nM, 80 nM and 165 nM, relative to 30 nM for 17D1 in this assay. Thus, and as predicted from known structure-activity relationships, the photoaffinity derivatives maintained good potency compared to unmodified 17D1 parent compound (Fig. 3-3).

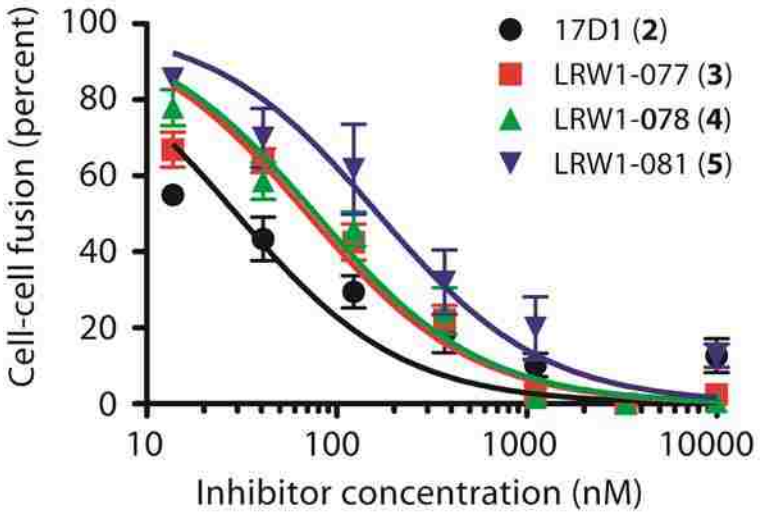

Figure 3-3: Photoaffinity derivatives 3 – 5 potently inhibit LASV GPC-mediated cell-cell fusion. pH-induced syncytium formation was quantitated using a vaccinia virus-based β-galactosidase fusion reporter assay. Co-cultures of GPC-expressing and target cells were incubated with serial dilutions of the fusion inhibitors prior to exposure to acidic medium (pH = 5.0), and reporter activity was quantitated by chemiluminescence. Inhibition curves were fit to single-slope dose-response curves using GraphPad Prism software. Symbols: 17D1 (**2**), ●; LRW1-077 (**3**), ■; LRW1-078 (**4**), ▲; and LRW1-081 (**5**), ▼.

Characterization of recombinant LASV GPC expressed in insect cells. LASV GPC from the Josiah isolate was produced in insect cells and used as substrate for photoaffinity labeling. We have previously described the purification and characterization of full-length trimeric JUNV GPC expressed in insect cells [53] and similar methods were used to generate the LASV protein. In contrast to JUNV GPC, which appeared to be refractory to cleavage by the insect S1P/SKI-1 protease [70], the purified LASV GPC contained significant amounts of the mature GP1 and GP2 subunits (Fig. 4, insert). The enhanced susceptibility of LASV GPC to cleavage may reflect the presence of a preferred aromatic residue at position P7 in the S1P/SKI-1 recognition motif [128]. Size-exclusion chromatography demonstrated that LASV GPC formed a relatively homogeneous trimer in solution (Fig. 3-4), as reported for JUNV GPC [53] and consistent with the trimeric assembly of Class I fusion proteins.

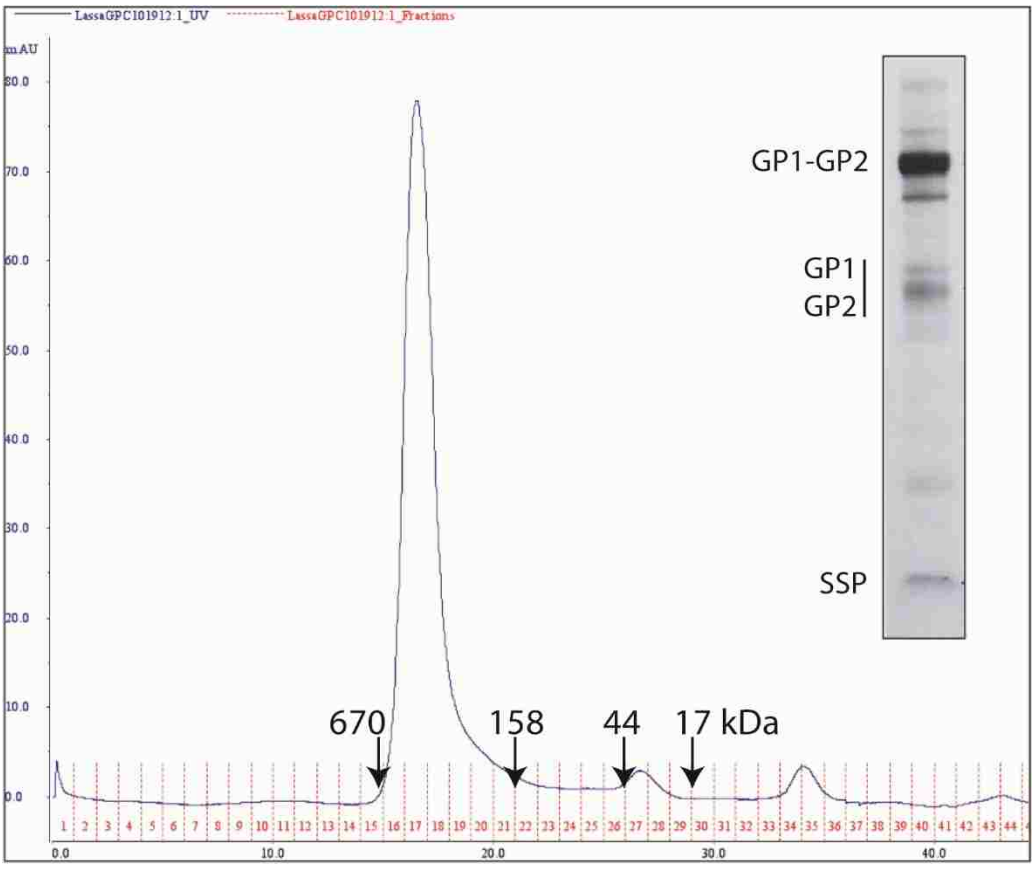

Figure 3-4: Characterization of purified LASV GPC from insect cells. LASV GPC was solubilized from insect-cell membranes and purified by affinity chromatography using the C-terminal FLAG tag. Size-exclusion chromatography reveals a relatively homogeneous peak consistent with a GPC trimer. Molecular size markers (in kilodaltons) are indicated by arrows. Insert: The affinity-purified protein was resolved by SDS-PAGE and stained using Sypro Red. The heavily glycosylated GP1 subunit is heterodispense and co-migrates with GP2 in this analysis.

Photoaffinity labeling of LASV GPC. We have previously reported that membrane reconstitution of purified JUNV GPC greatly enhances the affinity of inhibitor binding relative to the solubilized protein [53]. Thus, we chose to incubate the photolabile inhibitor derivatives with LASV GPC in purified insect-cell membranes. An initial titration of LRW1-077 revealed maximal photoaddition at 3 μM compound (not shown) and subsequent studies were performed using 10 μM of the inhibitors. At this concentration, we were unable to detect any photolabeling of solubilized LASV GPC (not shown).

A standard workflow was adopted for photoaffinity labeling of LASV GPC is described in Materials and Methods. In brief, insect-cell membranes containing LASV GPC were incubated with the photoreactive inhibitor and subjected to long wavelength UV light (~366 nm) to activate the photolabile trifluoromethyldiazirine group. The resultant short-lived and highly reactive carbene is able to insert across proximal bonds to covalently link the inhibitor to the protein. LASV GPC was then solubilized in DDM-containing buffer and bound to immobilized anti-FLAG MAb on agarose beads. Coupling of the pendant alkyne on the inhibitor adduct to an azide-containing linker bearing a fluorescent TAMRA moiety was accomplished using copper-catalyzed click chemistry. GPC was then eluted from the FLAG beads, and the fluorescently tagged subunits were identified by SDS-PAGE analysis.

By using this procedure, we could detect photoaddition by each of the modified inhibitors to SSP and either the GP1 or GP2 subunit; the last two subunits are difficult to resolve in SDS-PAGE analysis (Fig. 3-5A). PNGase F digestion enables clear differentiation of the GP1 and GP2 polypeptides and revealed that only GP2 was labeled (Fig. 3-5B). The labeling efficiency by the three compounds was comparable, and in all cases SSP was preferentially labeled relative to GP2. Although each inhibitor reacts with both SSP and GP2, multiple lines

of evidence support a single inhibitor-binding site on GPC [41, 53, 70]. Therefore, we conclude that photoaddition of these probes can occur stochastically with either SSP or GP2. This result provides direct confirmation for inhibitor binding at the SSP-GP2 interface. Notably, the GP1-GP2 precursor that constitutes ~90% of the total protein (Fig. 3-4, insert) is not labeled.

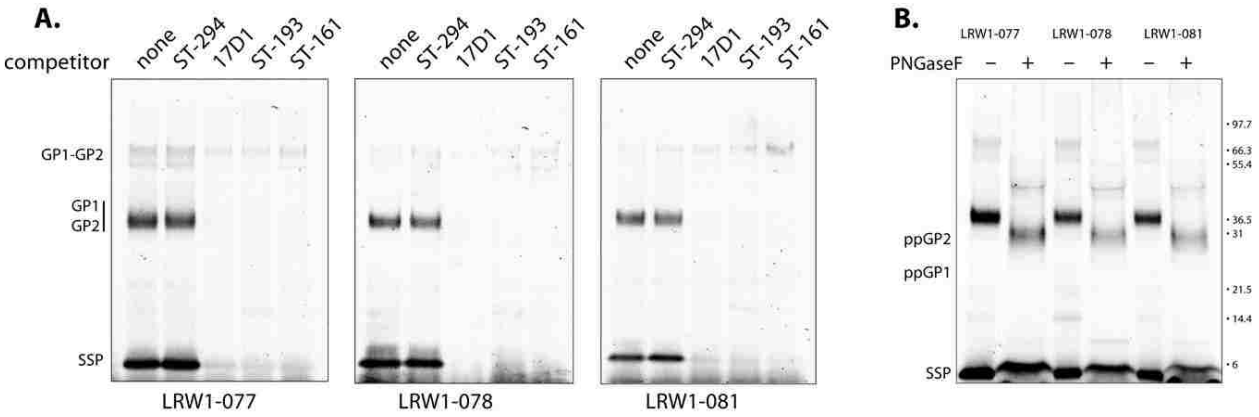

Figure 3-5: Photoaffinity labeling of LASV GPC. LASV GPC in purified insect-cell membranes was subjected to photoaffinity labeling, and the covalently linked inhibitors were subsequently modifed with TAMRA using click chemistry. Subunits were resolved by SDS-PAGE analysis and TAMRA was detected by fluorescence imaging. **A**. GPC was incubated with the indicated photoreactive inhibitors alone (none) or together with an excess of non-photoreactive competitor. ST-294 [37] is specific to NW arenaviruses, while 17D1 [40] and ST-193 [38] are broadly active against both NW and OW arenaviruses. ST-161 [119] is specific to OW arenaviruses. **B**. PNGase F was used to deglycosylate GPC to demonstrate that the FLAG-tagged GP2 polypeptide (ppGP2; calculated molecular weight 28 kDa), and not GP1 (ppGP1; calculated molecular weight 22.7 kDa), is photoaffinity labeled.

Photoaffinity labeling of SSP and GP2 is competed by OW-active, but not NW-active, inhibitors. The specificity of photoaddition was demonstrated by competition using 17D1 (compound **2**), the parent inhibitor from which LRW1-077 and -081 were derived. By using a 5-fold molar excess of 17D1, labeling of both the SSP and GP2 subunits by each of the three photoreactive compounds was completely blocked (Fig. 5A). The effectiveness of competition is likely enhanced by the higher binding affinity of the parental inhibitor (Fig. 3-3). Furthermore, photoaddition was also blocked by the addition of excess ST-161 and ST-193, two independently identified SIGA compounds that are respectively selective for LASV [119] or broadly active against NW and OW arenaviruses [38] (Fig. 3-5A). The NW-specific inhibitor ST-294 [37] failed to block photoaddition (Fig. 3-5A), in keeping with the converse result that OW-specific inhibitors fail to bind JUNV GPC [53]. Together, these results validate the specificity of the photoaddition reaction and the notion that these chemically distinct fusion inhibitors share a common binding site on GPC [37, 38, 41, 53]. The coordinate loss of SSP and GP2 labeling provides further support for a single binding site at the SSP-GP2 interface.

Neither SSP nor GP1-GP2 is labeled in the GPC precursor complex. Despite its predominance in purified LASV GPC protein, the GP1-GP2 precursor is not labeled (Fig. 3-5A). To determine whether SSP associated with the (unlabeled) GP1-GP2 precursor is still susceptible to photoaddition, we generated a cleavage-defective (cd) form of LASV GPC in which the S1P/SKI-1 cleavage motif (RRLL) was mutated to AALL. As illustrated in Fig. 3-6A, cd-GPC is expressed well in insect cells, with no evidence of proteolytic cleavage. Photoaddition studies revealed only background labeling of SSP and the GP1-GP2 precursor in cd-GPC, none of which was competed by an excess of 17D1 or ST-193 (Fig. 3-6B). These

results indicate that SSP in GPC containing the uncleaved GP1-GP2 precursor is not susceptible to photoaffinity labeling by these inhibitors. This result is in apparent contrast with previous surface plasmon resonance studies that demonstrated binding of NW-active inhibitors to the uncleaved JUNV GPC precursor [53, 70]. It is possible that the inhibitors differ in their ability to bind their respective GPC precursors. However, the failure to label does not necessarily exclude inhibitor binding to the precursor complex. Protein bonds that are potential targets for insertion by the reactive carbene may be displaced in the LASV GPC precursor and no longer accessible for reaction. In either case, the absence of labeling indicates that the environment at the inhibitor-binding site differs in precursor and mature LASV GPC and suggests that proteolytic cleavage is associated with conformational changes that alter the SSP-GP2 interface, perhaps to establish the pH-sensitive state of mature GPC complex.

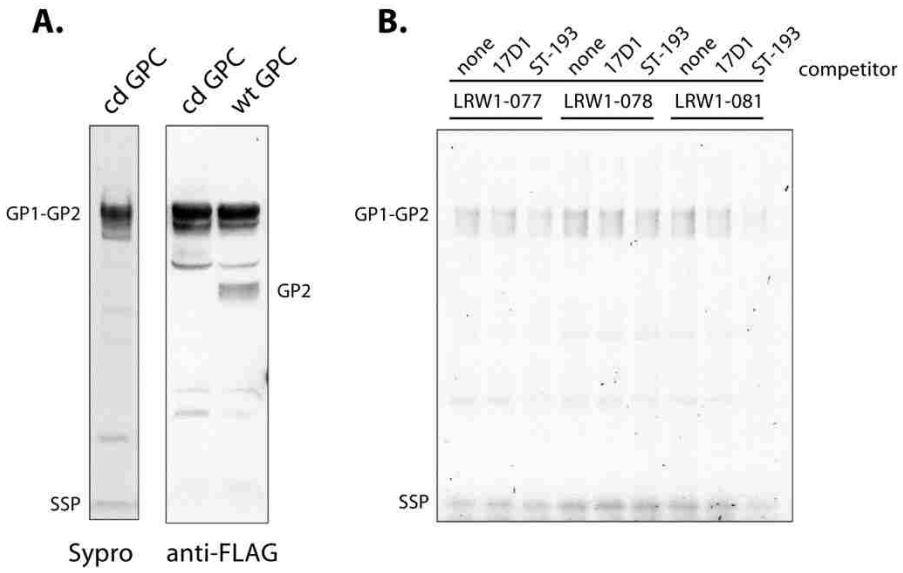

Figure 3-6: Cleavage-defective LASV GPC is not susceptible to photoaffinity labeling. The SKI-1/S1P cleavage site in LASV GPC was mutated (RRLL to AALL) to prevent proteolytic maturation. **A**. SDS-PAGE analysis confirms the absence of mature GP1 and GP2 subunits in cd GPC by Sypro Red staining (left) and western blot analysis for the C-terminal FLAG tag (right). Wild-type (wt) LASV GPC is shown for comparison. **B**. Photoaffinity labeling studies using the indicated photoreactive inhibitors show that neither GP2 nor SSP is significantly labeled in the precursor GPC complex. A low level of background labeling is not competed by 17D1 or ST-193.

pH-induced fusion activation of GPC prevents labeling. Small-molecule arenavirus fusion inhibitors target the prefusion form of GPC to block pH-induced fusion activation [37, 41, 70]. By virtue of controlling the fusion activation of GPC, it is also likely that the SSP-GP2 interface undergoes structural reorganization during the fusion process. To investigate whether the inhibitor-binding site is retained in the postfusion complex, we pretreated insect-cell membranes bearing the wild-type LASV GPC with buffer adjusted to pH 5.0, a pH that efficiently and irreversibly triggers LASV GPC-mediated cell-cell fusion. Following return to neutral pH and incubation with LRW1-077, we were unable to detect photolabeling of the postfusion GPC complex (Fig. 3-7). We conclude that the inhibitor-binding site at the SSP-GP2 interface is disrupted upon exposure to acidic pH, consistent with the notion that this intersubunit interaction maintains the prefusion GPC complex at neutral pH and responds to acidic pH to trigger the conformational changes leading to membrane fusion.

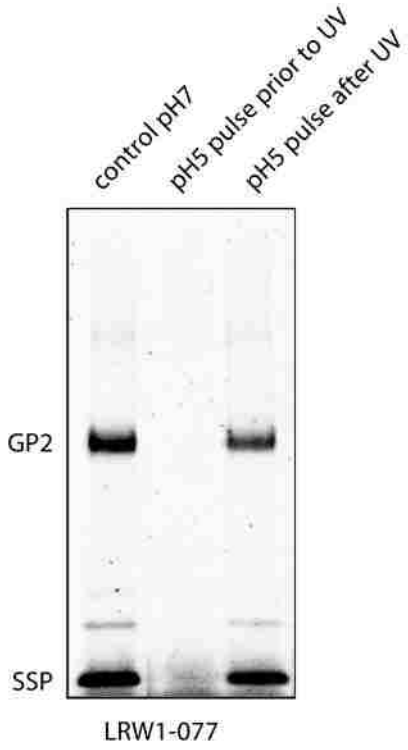

Figure 3-7: pH-triggered fusion activation abrogates photoaffinity labeling. Insect-cell membranes bearing wild-type LASV GPC were incubated with LRW1-077 (**3**) and exposed to long wavelength ultraviolet light at neutral pH as per the standard workflow (control pH 7) or following a 10 min pulse in buffer adjusted to pH 5.0 and subsequent neutralization (pH 5 pulse prior to UV). In order to exclude any adverse effects of the acidic buffer, the control pH 7.0 membranes were subsequently pulsed with pH 5.0 buffer prior to SDS-PAGE analysis (pH 5 pulse after UV).

Identification of photolabeled protein using mass spectrometry. To identify the modified amino acids in SSP and GP2 subunits, samples were photolabeled as described in the materials and methods section. The FLAG-purified protein samples were delipidated using SDS clean-up kit (GE healthcare). The pellets were solubilized in buffer containing 8 M urea and 0.1% Rapigest (Waters), reduced and alkylated. Samples were then sequentially digested with LysC protease and either trypsin (18hrs) or chymotrypsin (a time series of 2, 6 and 18 hr) as described [129, 130]. We were able to achieve nearly complete sequence coverage for unmodified LASV GPC, including the membrane-proximal and transmembrane regions of SSP and GP2 (Fig. 3-8). However, we were unable to find any photo-adducts. This perhaps is due to the physical property of the hydrophobic photo-adduct and its difficulty to form fragmented ions. Protease digestion and mass spectrometry analysis was carried out by Dr. Ziwei W. Chen in Dr. Alex S. Evers's laboratory at Washington University School of Medicine, St. Louis. MO.

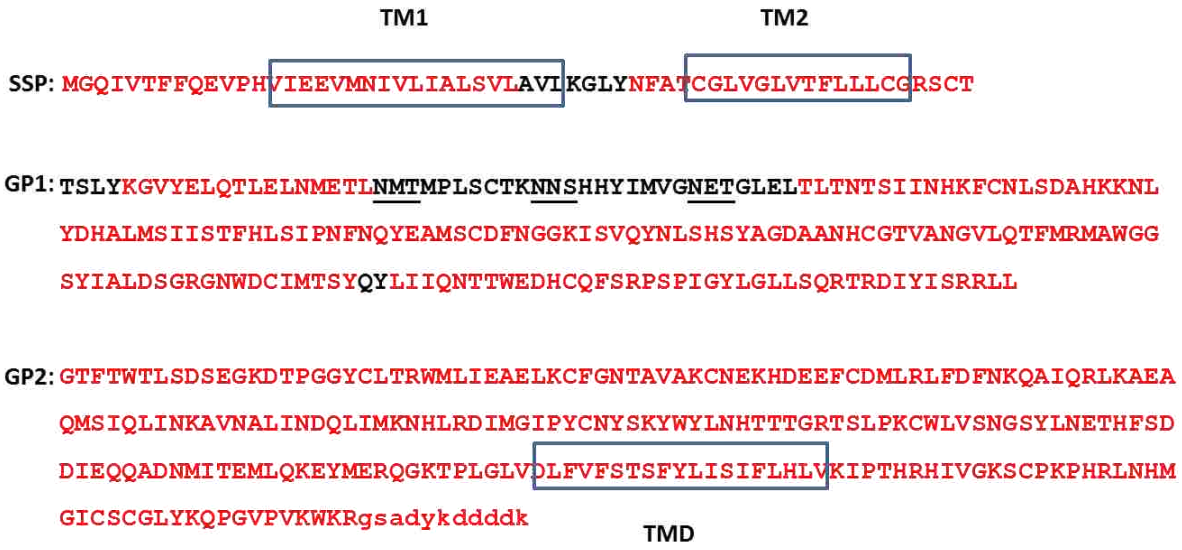

Figure 3-8: Sequence coverage map of unmodified LASV GPC. Amino acid residues show in red represent sequence coverage obtained from LC-MS/MS. Proposed transmembrane region 1 (TM1) and TM2 is represented in blue box for SSP. Transmembrane domain (TMD) of GP2 is also highlighted in blue box.

Enrichment of photolabeled protein and identification of photolabeled peptide-adduct using mass spectrometry. Based on the relatively small amount of cleaved GPC subunits (~10% of total protein) and the typically low efficiency of photoaddition (~5%), we wanted to enrich for the photolabeled protein. We performed enrichment using different click-linkers (biotin azide or Tamra-biotin azide). Briefly, photoaffinity labeled GPC was bound to immobilized anti-FLAG M2 antibody and an on-bead click reaction was performed using click-linker. Protein was eluted using 3xFLAG peptide and bound to magnetic streptavidin beads (pierce). The streptavidin beads were washed using stringent 2% SDS wash at 60^0C to remove any non-specific binding. The bound photo-adduct was eluted from streptavidin beads using SDS-biotin elution buffer [125]. The eluted samples were run on a SDS-PAGE and analyzed for TAMRA signal or by western blot using anti-FLAG antibody. GP2 and SSP subunits were selectively enriched relative to untagged GP1-GP2 precursor on streptavidin beads (Fig. 3-9).

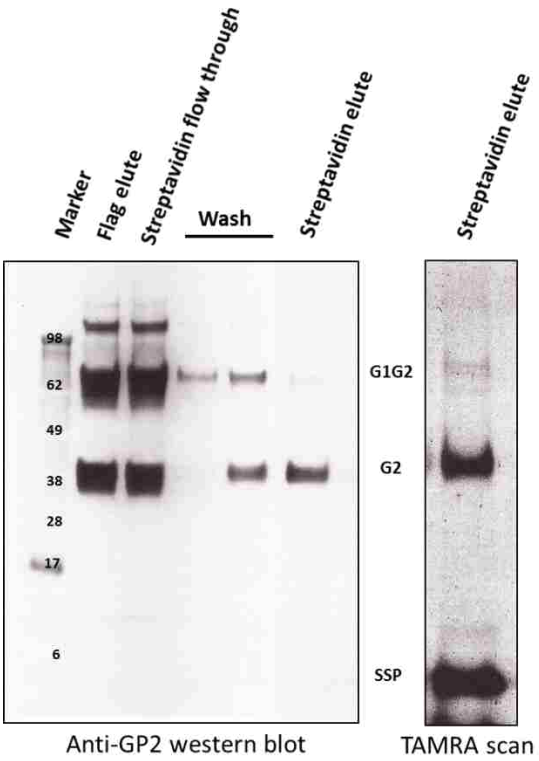

Figure 3-9: Streptavidin enriched LASV GPC photo-adduct. (*Left*) Western blot with anti-FLAG antibody showing specific enrichment of GP2 subunit relative to untagged GP1-GP2 precursor in the streptavidin elution. (*Right*) SDS-PAGE gel scanned for TAMRA fluorescence showing specific enrichment of GP2 and SSP subunits of GPC.

To demonstrate enrichment of the photo-adduct peptides, initially enrichment was performed using a TAMRA based trivalent linker (TAMRA-azide-biotin) from click chemistry tools. LASV GPC was photo-labeled in its native membrane environment using LRW1-077, and then solubilized in nonionic detergent and purified using immobilized anti-FLAG M2 antibody. To enrich for labeled peptides, we added a biotin purification tag (TAMRA-azide-Biotin) to the covalently bound inhibitor using click chemistry. Following this the protein was eluted from the FLAG –agarose column. The FLAG eluted protein was then subsequently reduced, alkylated and treated with chymotrypsin overnight at 37^0C. The digested peptides were further enriched on streptavidin beads and eluted with SDS-biotin elution buffer [125]. Post elution the photo-adduct peptides were subjected to either precipitation by SDS clean-up kit (GE healthcare) or by Folch extraction [126]. Most of the peptides were lost during precipitation using SDS clean-up kit. Due to the hydrophobic nature of the photo-adduct, they were selectively partitioned into the organic phase during Folch extraction. The organic phase was dried and the peptides were solubilized in 0.1% TFA and 30% acetonitrile. The solubilized peptides were separated on a Superdex peptide 3.2/300 size-exclusion column (GE healthcare) and monitored for the TAMRA absorbance at 550 nm (Fig. 3-10). The eluted fractions were analyzed for TAMRA signal using a dot blot assay and by MALDI-TOF (Fig. 3-11). The results of dot blot assay shows fractions with TAMRA signal, indicating that these fractions may contain chymotrypsin digested peptide-adducts. MALDI trace with low and high intensity peaks did not correspond to any possible peptide-adduct from a chymotrypsin digest, suggesting that it could be background peaks. To confirm this we subjected these samples to LC-MS/MS analysis. A positive ID on any of the

peaks observed in the MALDI could not be ascertained by *de novo* sequencing because of lower signal-to-noise ratio in the MS spectra.

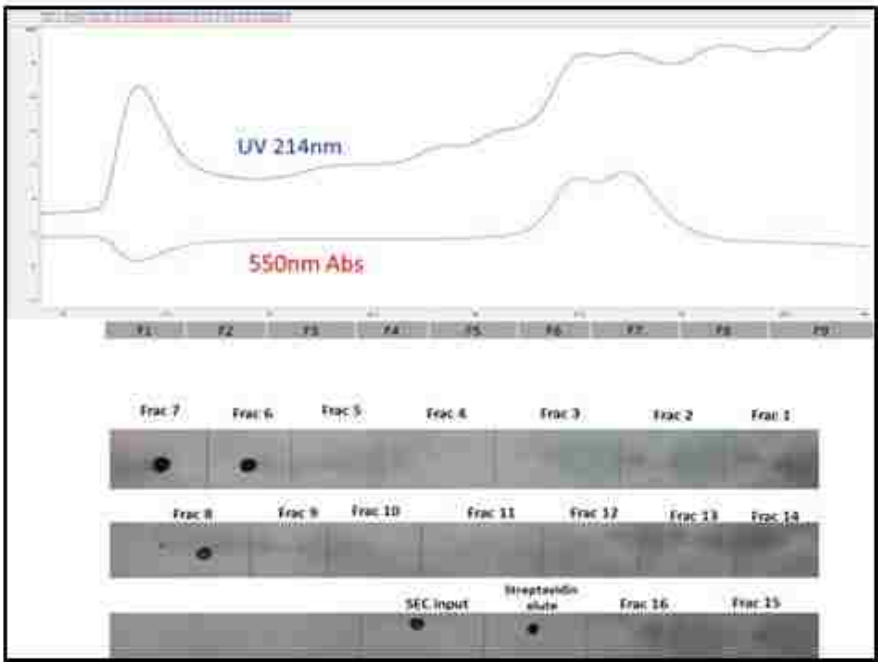

Figure 3-10. Size-exclusion chromatography profile of peptide-adducts after clean-up. SEC profile of Folch extracted peptides (top) on a Superdex peptide 3.2/300 column showing traces of 214 nm (peptide) and 550 nm (TAMRA) absorbance, and dot blot assay of SEC fractions scanned for TAMRA signal (Bottom).

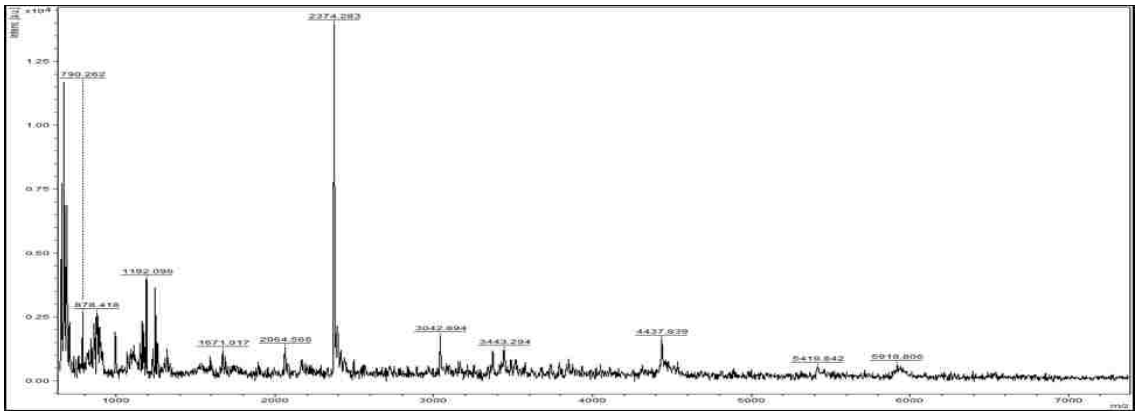

Figure 3-11. MALDI-TOF analysis of pooled size-exclusion chromatography fractions (6-8) of Folch extracted sample.

D. Discussion

Our studies demonstrate specific photoaffinity labeling of both the SSP and GP2 subunits of LASV GPC using the novel photoreactive fusion inhibitors **3**-**5**. The coordinate labeling of both subunits provides direct evidence for inhibitor binding at the SSP-GP2 interface. This result is consistent with previous genetic studies identifying determinants of inhibitor sensitivity in both these subunits [37, 38, 41, 55]. In considering the role of SSP-GP2 interactions in modulating pH-induced activation of GPC membrane fusion [54, 112], these new findings support the notion that these fusion inhibitors bind at the SSP-GP2 interface to stabilize the prefusion GPC complex against acidic pH, thereby preventing fusion activation and virus entry [41, 70]. In addition, the failure to photochemically label either subunit in the uncleaved GPC precursor reveals that proteolytic maturation of GPC is accompanied by conformational changes at the SSP-GP2 interface, changes that may be critical in establishing the pH-sensitive metastable state of the prefusion GPC complex. Similarly, the inability to label GPC after exposure to acidic pH highlights specific fusion-associated conformational changes at the SSP-GP2 interface, consistent with its role in triggering the fusogenic cascade.

Interestingly, a number of chemically diverse small-molecule fusion inhibitors of influenza virus hemagglutinin, another Class I fusion protein, have been shown to act through an analogous mechanism, albeit by targeting a different intersubunit interface [131-134]. Thus, stabilization of the prefusion state through the fortuitous binding of small-molecule compounds may prove to be a general mechanism for effective fusion inhibition. Indeed, a newly described inhibitor of the OW lymphocytic choriomeningitis virus GPC may act in this manner [135].

In the absence of atomic-level structural information on the tripartite GPC complex, our photoaffinity labeling studies provide an important perspective from which to better understand the structure and function of this unique viral fusion protein. Identification of SSP and GP2 residues modified by these inhibitors has been quite a challenge. Due to the hydrophobic nature of the membrane proximal and transmembrane regions of SSP and GP2, *de novo* sequencing to identify modified residues using tandem mass spectrometry has been an uphill task. Different enrichment strategies and use of different click-linkers will help increase our chances of identifying modified residues. Identifying photo-adducts and using inhibitors bearing photoreactive groups at other positions in the molecule, will help us triangulate inhibitor interactions with GPC and provide insights to guide the development of potent therapeutic agents to treat Lassa hemorrhagic fever.

SUPPLEMENTAL MATERIALS

Shankar et al. Small-molecule fusion inhibitors bind the pH-sensing SSP-GP2 subunit interface of the Lassa virus envelope glycoprotein,

Synthesis of photoaffinity probes were carried out by Dr. Landon R. Whitby at The Scripps Research Institute.

Fig. S1: Synthesis of photoaffinity probes.

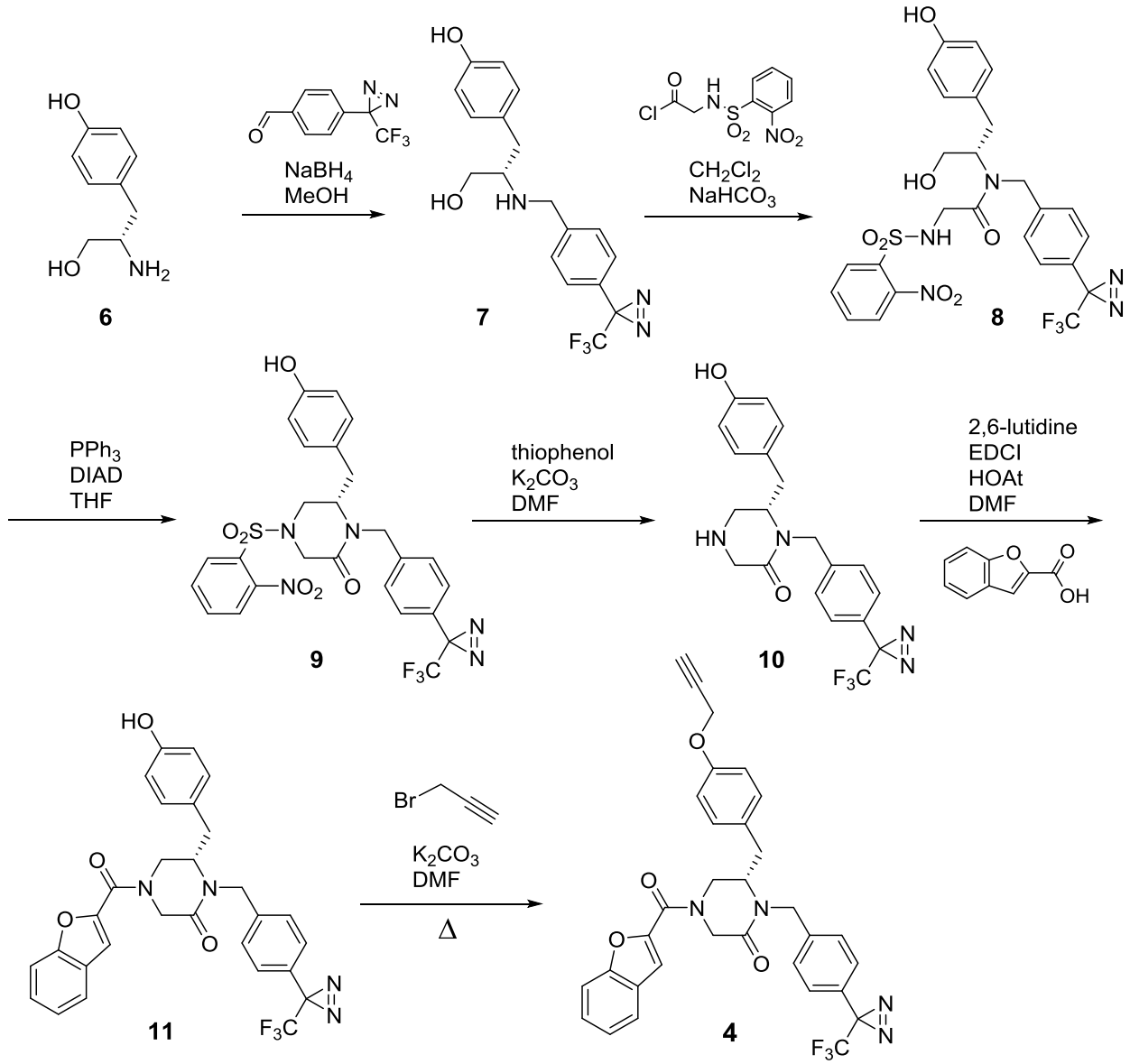

Panel A: Synthesis of probe 4. Briefly, L-tyrosinol (**6**) was reductively alkylated using 4-[3-(trifluoromethyl)-3H-diazirin-3-yl]benzaldehyde [127] and sodium borohydride ($NaBH_4$) in MeOH to provide **7**. The secondary amine **7** was chemoselectively acylated using slow addition of the acyl chloride of N-[(2-nitrophenyl)sulfonyl]glycine to provide **8**. Intramolecular Mitsonobu alkylation was then employed using triphenylphosphine (PPh_3) and diisopropyl azodicarboxylate (DIAD) in THF to yield piperazinone **9**. The cleavage of the (2-nitrophenyl)sulfonyl group was accomplished using thiophenol and K_2CO_3 in DMF to provide secondary amine **10**, which was then acylated using benzofuran-2-carboxylic acid and 1-Ethyl-3-(3-dimethylaminopropyl)carbodiimide (EDCI) in DMF to yield **11**. The synthesis was then completed by alkylation of the phenol using propargyl bromide and K_2CO_3 in DMF to provide (S)-4-(benzofuran-2-carbonyl)-6-(4-(prop-2-yn-1-yloxy)benzyl)-1-(4-(3-(trifluoromethyl)-3H-diazirin-3-yl)benzyl)piperazin-2-one (**4**).

^{1}H NMR (600 MHz, DMSO-d_6) δ 7.68 (d, J = 7.8 Hz, 1H), 7.63 – 7.37 (m, 3H), 7.31 (dd, J = 8.5, 1.9 Hz, 3H), 7.18 (d, J = 8.1 Hz, 2H), 7.05 – 6.45 (m, 3H), 5.41 (d, J = 15.2 Hz, 1H), 5.04 (s, 1H), 4.69 (d, J = 13.6 Hz, 1H), 4.66 – 4.28 (m, 3H), 3.88 (d, J = 15.1 Hz, 1H), 3.57 – 3.36 (m, 1H), 3.14 – 2.57 (m, 3H), 2.46 (s, 1H). High-resolution mass spectrometry (HRMS) for $[C_{32}H_{26}F_3N_4O_4]^+$ calculated 587.1901; observed 587.1901.

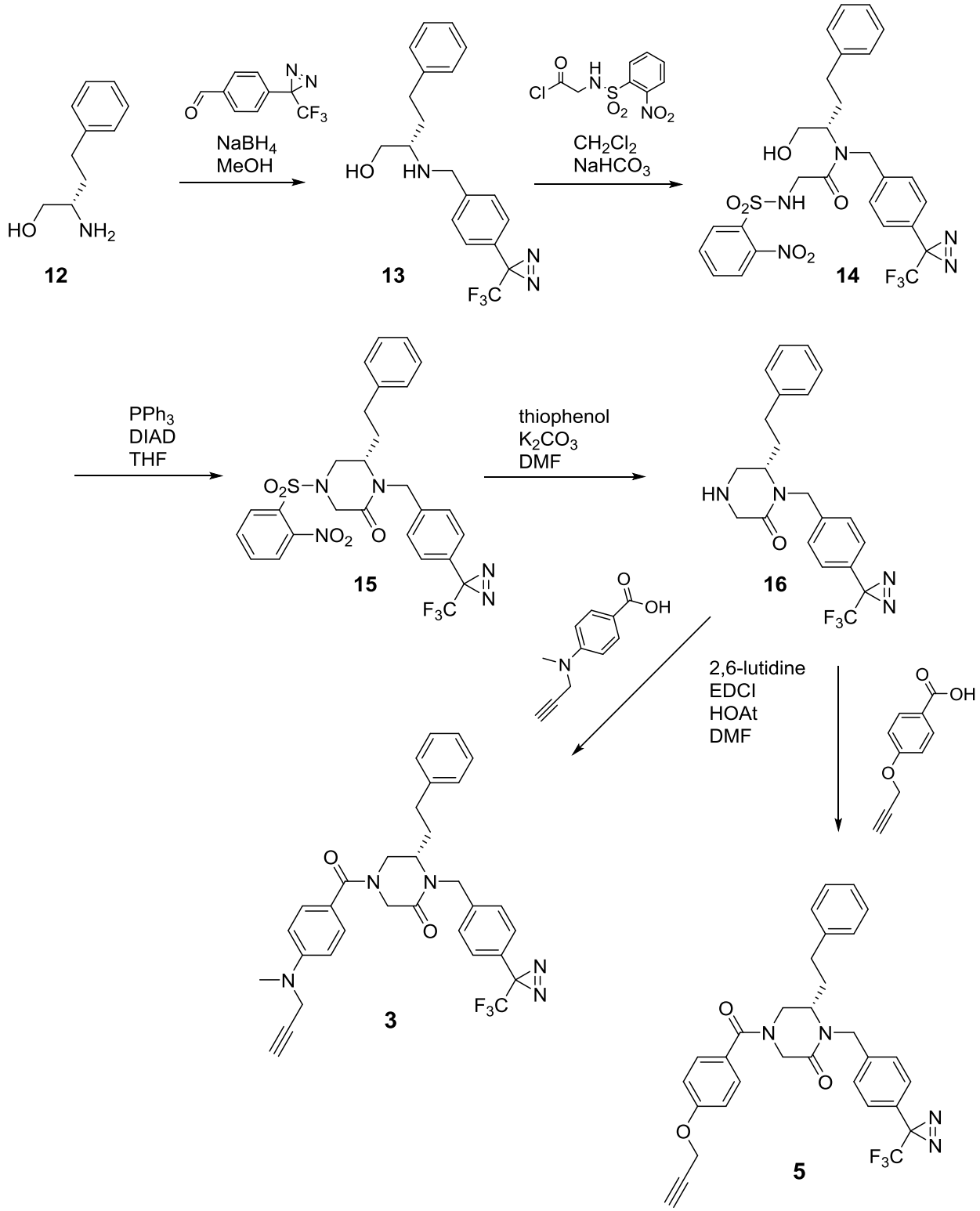

Panel B: Synthesis of probes 3 and 5. The synthesis was accomplished using primarily the same synthetic route as probe **4.** Briefly, L-homophenylalaninol was reductively alkylated

using 4-[3-(trifluoromethyl)-3H-diazirin-3-yl]benzaldehyde to yield aminoalcohol **13**, which was then chemoselectively acylated with the acyl chloride of N-[(2-nitrophenyl)sulfonyl]glycine to provide intermediate **14**. Intramolecular Mitsonobu alkylation of the sulfonamide provided **15** and the subsequent cleavage of the (2-nitrophenyl)sulfonyl group yielded **16**. The secondary amine **16** was then acylated using 4-(methyl-2-propyn-1-ylamino) benzoic acid to provide probe **3** or 4-(2-propynyloxy)benzoic acid to provide probe **5**.

(S)-4-(4-(methyl(prop-2-yn-1-yl)amino)benzoyl)-6-phenethyl-1-(4-(3-(trifluoromethyl)-3H-diazirin-3-yl)benzyl)piperazin-2-one (**3**). ^{1}H NMR (400 MHz, Chloroform-*d*) δ 7.40 (d, *J* = 8.8 Hz, 2H), 7.32 – 7.20 (m, 4H), 7.15 – 7.01 (m, 5H), 6.81 (d, *J* = 8.8 Hz, 2H), 5.22 (d, *J* = 14.8 Hz, 1H), 4.60 (s, 2H), 4.20 – 3.99 (m, 3H), 3.76 (d, *J* = 14.9 Hz, 1H), 3.16 (d, *J* = 24.7 Hz, 2H), 3.04 (s, 3H), 2.93 – 2.62 (m, 1H), 2.52 – 2.28 (m, 1H), 2.19 (t, *J* = 2.3 Hz, 1H), 1.88 (td, *J* = 8.6, 5.1 Hz, 2H). HRMS for $[C_{32}H_{31}F_3N_5O_2]^+$ calculated 574.2424; observed 574.2422.

(S)-6-phenethyl-4-(4-(prop-2-yn-1-yloxy)benzoyl)-1-(4-(3-(trifluoromethyl)-3H-diazirin-3-yl)benzyl)piperazin-2-one (**5**). ^{1}H NMR (400 MHz, Chloroform-*d*) δ 7.42 (d, *J* = 8.6 Hz, 2H), 7.37 – 7.19 (m, 5H), 7.15 – 6.95 (m, 6H), 5.23 (d, *J* = 14.8 Hz, 1H), 4.74 (d, *J* = 2.4 Hz, 2H), 4.40 (br s, 1H), 4.12 (d, *J* = 17.7 Hz, 1H), 3.75 (d, *J* = 14.8 Hz, 1H), 3.14 (s, 2H), 2.87 (br s, 1H), 2.62 (s, 1H), 2.54 (d, *J* = 2.5 Hz, 1H), 1.88 (d, *J* = 7.4 Hz, 2H). HRMS for $[C_{31}H_{28}F_3N_4O_3]^+$ calculated 561.2108; observed 561.2107.

Chapter 4

Characterization of pH-dependent membrane fusion of Old World Lassa virus GPC

A. Introduction

Among class I fusion proteins including those of retroviruses, filoviruses, coronaviruses, orthomyxo- and paramyxoviruses, arenavirus envelope glycoprotein (GPC) is unique in retaining its signal peptide (SSP) that is noncovalently associated with the complex. In our previous studies, we have shown that New World (NW) Junín virus (JUNV) GPC is able to mediate cell-cell fusion in a pH-dependent manner and that the fusion activity of GPC is inhibited by recently identified small-molecule inhibitors. These inhibitors stabilize the prefusion complex by binding to a common site at the pH-sensitive SSP-GP2 interface, thereby depressing the pH of fusion [41, 53]. Interaction between GP2 and transmembrane domain 1 (TM1) of SSP is crucial for GPC-mediated membrane fusion in SSP chimeras containing JUNV and Old World (OW) Lassa fever virus (LASV) sequences [55].

Although JUNV and LASV GPC have only ~ 41% sequence identity at amino acid level, they share many structural features. Based on genetic analysis carried out on JUNV GPC, we identified a charged residue in SSP (lysine 33) that is specifically required for pH-dependent fusion activity of the GPC complex [54]. K33 is located in the short ectodomain loop of SSP and mutating K33 to alanine (A) completely abolishes GPC-mediated fusion. Substitutions in K33 to positively charged (arginine, R; histidine, H) or polar neutral (glutamine, Q) residues lower the pH threshold at which cell-cell fusion is triggered [54]. Although membrane fusion activity of JUNV GPC is inhibited by NW-active inhibitors, one of the mutants (K33H) now

showed *de novo* sensitivity to OW (LASV) - specific inhibitor (ST-161), suggesting that these compounds bind to same site in JUNV and LASV [41]. This led us to hypothesize that despite the difference in sequences, the underlying mechanism of pH-induced activation and its inhibition is conserved between OW and NW viruses. In this chapter we propose to identify residues that are important for pH-induced activation and sensitivity of inhibitors in LASV GPC to compare the underlying mechanisms.

B. Materials and methods:

LASV GPC mutants. Mutations in SSP of LASV GPC *(strain Mouse/Sierra Leone/Josiah/1976)* were generated in a pcDNA 3.1(+) vector using QuikChange mutagenesis kit (Agilent technologies) and all constructs were verified by DNA sequencing.

Vaccinia-based cell to cell fusion assay. WT LASV GPC and mutants were expressed in Vero cells and β-galactosidase fusion reporter assay was carried out as previously described [54, 87, 122]. In brief, Vero 76 cells infected with a recombinant vaccinia virus encoding the bacteriophage T7 RNA polymerase (vTF7-3) at a MOI of 2.0 in Dulbecco's minimal essential medium containing 2% fetal bovine serum (FBS) and 10 μM cytosine arabinoside (araC) [136]. Cells were then washed and transfected with LASV GPC expressing plasmids using Lipofectamine 2000 (Invitrogen). Previously, we have shown that co-expression of SSP in *trans* with GP1-GP2 precursor containing human CD4 signal peptide allows SSP association and maturation of GPC complex [48, 49]. GP1-GP2 were co-expressed with WT and SSP mutants in a 3:1 ratio. vTF7-3 infected cells expressing LASV GPC from the minimal T7 promoter in the pcDNA3.1 vector are mixed with target cells infected with vCB21R-lacZ, a recombinant vaccinia virus capable of expressing β-galactosidase under the control of the T7 promoter [54, 122]. GPC-mediated cell-cell fusion is induced upon

exposure to acidic medium (pH 5.0) and drives expression of the β-galactosidase reporter, which is quantitated using the chemiluminescent GalactoLite Plus β-Galactosidase Reporter Gene Assay System (Applied Biosystems) in a SpectraMax L microplate luminometer (Molecular Devices).

For studies of resistance, cells were incubated with IC_{90} concentrations of the compounds from SIGA Technologies (ST161-10nM, ST193-10nM and ST294>1μM) and The Scripps Research Institute (TSRI) (17D1-1μM) for LASV GPC. The cells were treated with acidic medium and incubated in neutral pH medium for 5 hours, followed by quantitation of expression of β-galactosidase reporter. Three replicate wells were used for each and an equivalent amount of DMSO solvent served as no drug control for 100% fusion activity.

C. Results

Role of K33 in promoting membrane fusion. Previous studies on JUNV GPC showed that the conserved residue at position 33 of SSP is important for fusion activity of GPC. Presence of a positive charge at this position plays a crucial role in pH of fusion-activation [54]. In order to test if lysine 33 of SSP in LASV GPC play a similar role in pH-induced fusion activity of GPC, we generated mutants of LASV SSP, by substituting K33 with positively charged residues (arginine and histidine), a polar but neutral residue (glutamine) or a small slightly hydrophobic residue (alanine) using Quikchange® mutagenesis kit. All the SSP mutants (K33H, K33Q, K33R and K33A) were co-expressed with LASV GP1-GP2, bearing a human CD4 signal sequence, in Vero cells and pH-dependent syncytium formation was determined using a recombinant vaccinia-based β-galactosidase-reporter assay. Mutation K33A was dead and changing the K33 residue to histidine or glutamine, respectively, reduced the fusion activity to ~20% or 10% of WT-level (Figure 4-1). In contrast to JUNV,

pH-dependent fusion was abrogated with mutant bearing arginine residue at position 33. Arginine mutant perhaps might be sterically incompatible with other LASV residues at the interface. These results suggest that mutation at lysine 33 in LASV GPC behave similar to JUNV GPC with respect to fusion activity at pH 5.0, except for mutant bearing arginine residue at position 33.

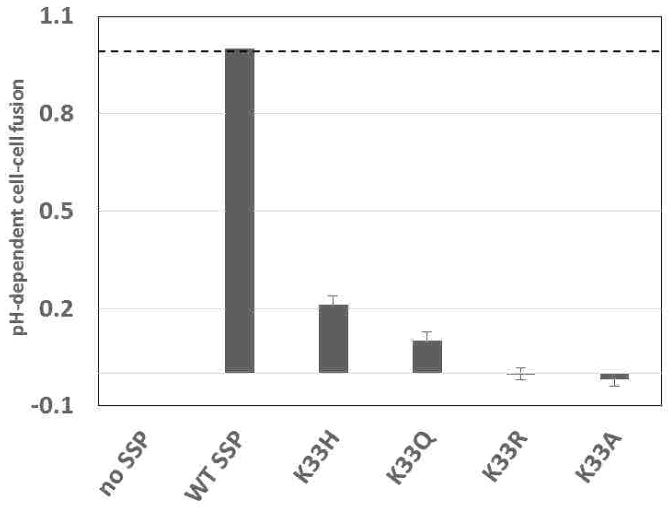

Figure 4-1: Membrane fusion activity of LASV SSP K33 mutants. pH-dependent syncytium formation was detected by using the recombinant vaccinia virus-based β-galactosidase-reporter assay as previously described [54]. The SSP mutants were coexpressed with GP1-GP2 containing human CD4 signal peptide. Cocultures of Vero cells infected with vTF7-3 expressing GPC and those infected with the reporter vaccinia virus vCB21R-LacZ were pulsed for 20 min in medium adjusted to pH 5.0 and subsequently returned to neutral pH for 5 h to allow for syncytium formation and LacZ expression. β-Galactosidase activity was quantitated by using the chemiluminescent substrate GalactoLite Plus (Applied Biosystems). pH-dependent fusion measurements with activity of WT SSP in *trans* are shown equals 1.0 after subtraction of background levels from neutral-pH cultures. The error bars show estimated standard deviation (typically 2 to 4%).

K33 mutants do not lower the pH threshold of fusion. Genetic analysis carried out on JUNV GPC show that reducing the positive charge at the lysine 33 of SSP systematically lowers the pH of fusion [112]. In case of LASV GPC, we examined if the change in charge affects the pH-threshold of fusion by varying the pH of acidic medium in the recombinant vaccinia based cell-cell fusion assay. Earlier studies have shown that LASV GPC fuse at an unusually low pH [137]. Unexpectedly, none of the mutants showed any change in pH of fusion (Figure 4-2). On the contrary, in our assay WT, K33H and K33Q GPC showed maximum fusion at pH 5.0 and lowering the pH did not affect fusion. However, this result could be specific to the assay or to a particular clone of LASV. Based on these results, we can posit that interaction in LASV GPC at the titratable GP2 interface results from the side-chain interactions that is different from the one observed in JUNV K33 mutants. Recent work carried out on LASV suggests a role of secondary intracellular LAMP1 receptor to be required for LASV entry in the late endosome [27]. Interestingly the GPC binding to the LAMP1 receptor occur at low pH [27, 138]. In our cell-cell fusion assay, we are looking at fusion by expressing GPC on the cell-surface. Absence of LAMP1 on the cell-surface of most cells and perhaps conformational changes associated upon LAMP1 binding is probably required to set up the pH-sensitive interface. The role of LAMP1 could also be prior to fusion activation and can be tested by expressing LAMP1 on cell-surface [139] and carrying out cell-cell fusion assay at different pH.

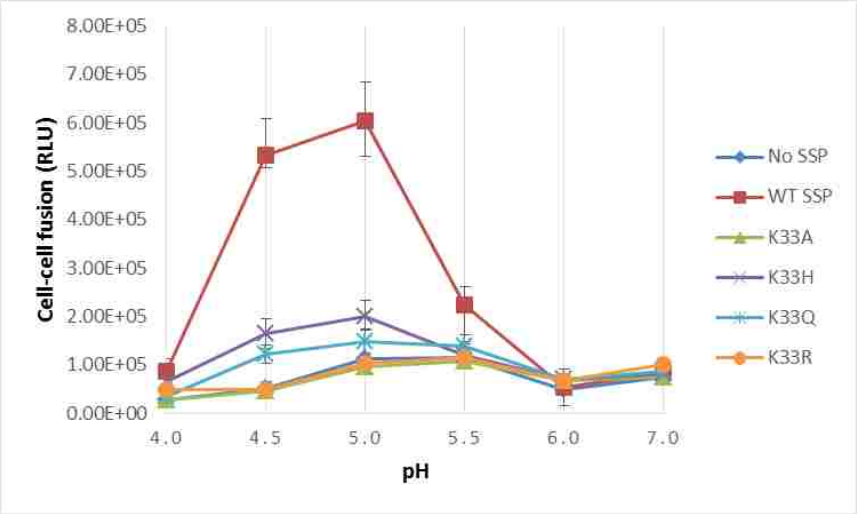

Figure 4-2: pH-threshold of cell-cell fusion. vTF7-3 infected Vero cells expressing GP1-GP2 and SSP in trans and LacZ expressing cells were cocultured. The cells were pulsed for 20 min with media adjusted to indicated pH (pH 4.0 through 7.0) and returned to neutral pH for syncytium formation and β–galactosidase expression. pH-dependent relative absorbance units (RLU) measurements are shown.

K33Q mutant in SSP confers resistance to inhibition by OW-active ST-193 and 17D1. The SSP K33 mutants of JUNV GPC engender resistance to inhibition by NW-specific ST-294 [112]. In addition, mutation at the conserved lysine 33 residue can enhance sensitivity towards OW-specific inhibitor (ST-161). We tested the SSP K33 mutants of LASV GPC using cell-cell fusion assay for resistance to inhibition by ST-161, ST-193 (broadly active inhibitor from SIGA Technologies) [38], 17D1 (LASV active TSRI inhibitor) [40] and ST-294. The cells were incubated with different concentrations of inhibitors, equivalent to IC90 values with respect to WT LASV GPC. The results show that K33Q mutant, but not K33H, confer resistance to inhibition by both 17D1 and ST-193 (Figure 4-3). None of the mutants showed sensitivity to NW-specific ST-294 (Figure 4-3). Despite the similarities in sensitivity of K33 mutants to inhibition in LASV and JUNV, the side-chain interaction with GP2, similar to the pH studies, can also produce different results.

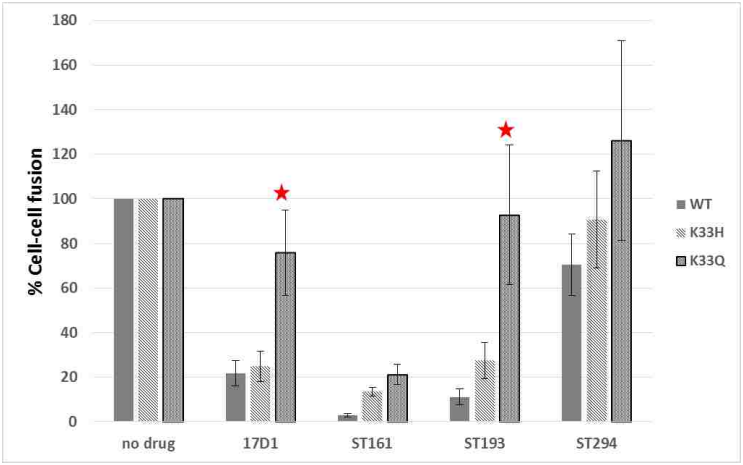

Figure 4-3: K33Q mutant resistant to inhibition by 17D1 and ST-193. Cells expressing trans- complemented LASV GPC were treated with 17D1 (1uM), ST-161(10nM), ST-193 (10nM) and ST-294(1uM) prior to pulsing with acid pH medium. Percentage fusion was normalized to no drug control. K33Q mutant of SSP show resistance to inhibition by 17D1 and ST-193 marked as red star.

D. Discussion

Among OW and NW species of arenaviruses, there are several residues that are highly conserved. Studies carried out in JUNV GPC show that mutations at charged residues in SSP do not affect the biogenesis and transport of the mature GPC to the cell membrane. However, mutation at conserved lysine 33 of SSP has a significant impact on its fusion activity [54]. This suggests that the presence of charge at lysine 33 is crucial for pH-dependent fusion of virus to the endosomal membrane and subsequent release of virion into the cell. To determine the role of lysine 33 of LASV SSP in fusion, we carried out studies on LASV GPC using vaccinia-based cell-cell fusion assay. Mutating K33 in some cases reduced the fusion activity of GPC (K33H and K33Q) and in the other cases abolished fusion (K33R and K33A). Lowering the pH did not change the threshold of fusion between WT and mutants. This is different from what is observed in JUNV GPC, the difference seen could be due to interacting residues or due to the steric conflict. Recent work supports a requirement of secondary intracellular receptor (LAMP1) in the endosome for LASV entry [27]. A conformational difference in LASV GPC at low pH has also been reported that facilitates its interaction with LAMP1 [138]. Our data also suggest that K33 in LASV remains important for interaction of GPC with small-molecule inhibitors, as K33Q mutant showed resistance to inhibition to OW-active ST-193 and 17D1. Overall, LASV and JUNV GPC share similar mechanism of activation, albeit the differences observed can be attributed to the atomic level side-chain interactions that can be species specific. Also, the unique requirement of LAMP1 by LASV for entry can add to the complexity of fusion mechanism. Further studies needs to be carried out in exploring the details of differences or similarities in mechanism involved in fusion activation and inhibition of LASV GPC to that of JUNV GPC.

Chapter 5

Role of envelope glycoprotein complex (GPC) in arenavirus assembly and egress

A. Introduction:

During the final stages of the lifecycle, viruses assemble and leave the cell to form mature infectious virus particles. Viruses have developed various strategies to exit the cell either by lysing the cell or through a budding process. Assembly is an important aspect of viral life cycle and understanding the mechanism involved will shed more light towards developing better therapies. During assembly and budding events, some enveloped viruses utilize membrane microdomains of the host cell membrane, to which the envelope glycoproteins are targeted, and recruit matrix protein and other viral components to the site of budding. In New World (NW) arenavirus, JUNV, the envelope glycoprotein complex (GPC) is targeted to membrane microdomains that are non-raft associated [66]. The matrix Z protein, a 11 kDa RING zinc-finger protein, drives the assembly and budding of arenaviruses. The N-terminal glycine residue (G2) of arenavirus Z protein is co-translationally modified by covalent attachment of myristate and is required for membrane association [61, 140]. Centrally located in the Z is the zinc-finger RING domain that is important for incorporation of NP in Z containing VLPs [141]. The RING domain also consists of a late domain motif, YxxL, which is thought to mediate protein-protein interactions with components of endosomal sorting complexes for transport (ESCRT) during assembly and budding [142]. The RING domain is highly conserved in arenaviruses, whereas the late domains in the C-terminus differ among NW and Old World (OW) species [25]. The late domains PT/SAP and PPPY are conspicuous in OW viruses, with the exception of Lujo virus which only has the PT/SAP domain [9, 143].

The Z protein of NW arenaviruses contains only the PT/SAP domain with the exception of Tacaribe virus (TCRV), which has a non-canonical ASAP domain. The main force driving budding activity is the interaction of the late domains of Z with the host machinery, like ESCRT-system, which has been co-opted by the viruses for their own budding. The viral PT/SAP and PPPY domains interact with host Tsg101 (ESCRT I) and Nedd4-like ubiquitin ligase respectively [60, 140]. Apart from its role in virus assembly and budding, Z protein also inhibits viral transcription and replication by interacting with RNA-dependent RNA polymerase [144].

During budding, Z is localized to the inner surface of the plasma membrane and is reported to interact with GPC and nucleoprotein protein (NP) [62, 141]. The RING or the late domains of Z does not play a role in its association with GPC [62]. Z is suggested to directly interact with stable signal peptide (SSP) in the absence of other components of GPC [62]. In case of JUNV, co-immunoprecipitation studies with VLPs show that GPC and NP either independently or in combination are incorporated into VLPs produced by Z [145]. Although studies in JUNV using dual-immunogold staining electron microscopy did not show clear co-localization of GPC with Z on the plasma membrane, it is conceivable that the interaction between GPC and Z may be transient and/ or may require additional viral components [66]. In case of TCRV, another NW virus, efficient budding of VLPs by matrix protein Z requires coexpression of NP [145]. Another point of control of assembly is reflected in the exclusion of GPC precursor from virions [46, 145]. Taken together, it is likely that the assembly process is regulated and may be different among arenaviruses. To better understand the steps involved in assembly of JUNV, we are interested in dissecting the interaction between GPC and Z and also to identify the factors that might affect association of GPC with Z.

A variety of approaches can be used to study protein-protein interactions (PPIs), including genetic, biochemical, biophysical and microscopic methods. Biochemical methods include chemical crosslinking, coimmunoprecipitation and comigration of protein complex in a size exclusion chromatography. Among the genetic methods, yeast two hybrid (Y2H) systems is the classical and most widely used method [146]. Microscopic techniques have furthered the understanding of PPIs qualitatively and also aided in assessing the intracellular localization of interactions. Widely used microscopy techniques for studying colocalization include electron microscopy (EM), confocal and super resolution fluorescent microscopy. Biophysical techniques like analytical ultracentrifugation and Förster resonance energy transfer (FRET) have helped to investigate interaction under physiological condition and in living cells, respectively [147]. In recent years, advances in imaging and software technologies as well as novel fluorescent probes have improved the ability to visualize PPIs. Fluorescent protein-based biosensors are widely being used to report on biochemical events showing PPIs in live cells [148, 149]. We chose one such biosensor, dimerization-dependent red fluorescent protein (ddRFP), to study the interaction between GPC and matrix Z protein. Dimerization-dependent red fluorescent protein is designed in such a way that one of the monomers (ddRFP-copy A) contains a fluorophore that is non-fluorescent in its monomeric state. The second monomer (ddFP-copy B) does not form a fluorophore and acts only to substantially increase the fluorescence of copy A upon formation of the AB heterodimer [149] (Figure. 5-1). My work in this chapter focuses on using these dimerization-dependent fluorescent proteins as a tool to study the interaction between GPC and Z.

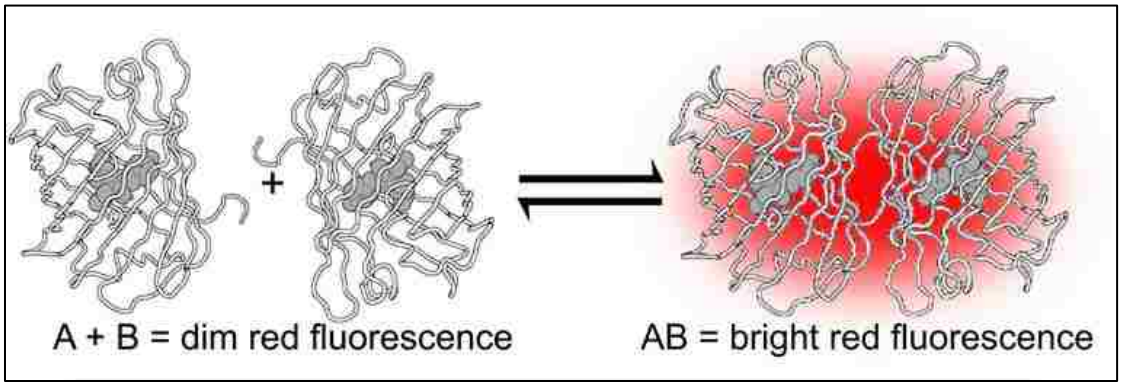

Figure 5-1: Graphical representation of dimerization-dependent fluorescent proteins. Monomers ddRFP-A and ddFP-B alone show less or no red fluorescence (left). The red fluorescence is increased upon formation of AB heterodimers (right). [Adapted from [148]]

B. Materials and methods:

Cloning. JUNV GPC-ddRFP, JUNV Z-ddFP-Spep, human CD4-ddRFP and human CD4-ddFP constructs were created using In-Fusion cloning Kit (Clontech laboratories Inc). Initially PCR products containing ddRFP or ddFP were generated from ddRFP-CaM and M13-ddFP plasmids (kindly provided by Dr. Thomas E. Hughes, Montana State University). The primers (Table. 5-1) designed to generate the PCR products had 15mer flanking regions that were complementary to the pcDNA3.1 (+) vector with JUNV GPC P3, Z-Spep and Human CD4 plasmids. Two 14 amino acid sequences, SGAGTASSGGSTGS and GHGTGSTGSGSSGT, were used as linkers for GPC-ddRFP, human CD4-ddRFP and Z-ddFP-Spep, human CD4-ddFP respectively. Linearized plasmid DNA were made by inverse PCR using primers (Table. 5-2) for JUNV GPC P3, Z-Spep and Human CD4 in such a way that the ends had matching 15mers of the PCR product. In-fusion reaction was carried out based on manufacturer's recommendation. GPC is poorly expressed in pcDNA vector, in the absence of vaccinia T7 virus infection. Also, performing PCR on pCAGGS vector is difficult due to its high GC content. For better expression, GPC-ddRFP was later cloned into pCAGGS vector using SacI and XhoI restriction enzymes. As a negative control, JUNV G2A Z mutant was created wherein glycine 2 residue of Z was changed to alanine using the primers GC-ZG2A and Z-G2A (Table. 5-3), using Z-ddFP-Spep plasmid as a template in the QuikChange II XL Site-Directed Mutagenesis (Agilent technologies).

Bimolecular fluorescent complementation-based system (BIFC) was also used as an alternative technique to detect PPI between GPC and Z. In this system, split fluorescent protein, N- and C-terminal halves of Venus fluorescent protein (VN and VC), was fused to the C-terminal end of GPC and Z using In-Fusion cloning Kit. In-Fusion reaction was carried

out based on manufacturer's recommendation. Briefly, PCR products containing VN and VC were generated from pBG262-VN and pBG265-VC plasmids (kindly provided by Dr. Brian J. Geiss, Colorado State University). The primers (Table. 5-4) designed to generate the PCR products had 15mer flanking regions that were complementary to the pcDNA3.1 (+) vector with JUNV GPC P3, Z-Spep and Human CD4 plasmids. The 14mer linkers used for attachment of VN and VC were same as previously mentioned above for GPC, CD4 and Z. PCR products were fused to their respective linearized vector by In-fusion reaction.

Confocal Microscopy. Transiently transfected Vero cells were re-seeded at 80,000 cells per chamber concentration, into poly-D-lysine treated 4-chamber glass bottom dishes (Greiner 627870) at 24 hr post-transfection. After 48 hr post transfection, cells were washed with 1X PBS and treated with Hoechst stain at 37^0C for 15 min. The cells were then visualized directly using an Olympus Fluoview 1000 laser scanning confocal microscope.

In some instances cells were fixed with freshly prepared 4% Paraformaldehyde (PFA) for 20 min at 4^0C. Cells were treated with 50mM Tris for 10 min followed by either directly blocking and staining for surface or by permeabilizing with 0.2% TX-100 in PBS for 20 min. Cells were blocked for 20 min and then probed for 60 min with primary antibody (Z-ddFP-Spep specific α-spep at 1:250, or α-GP1 MAB BE08 or BF11 at 1:500, or NP specific AG12 at 1:500) in block solution (5% FBS with or without 0.1% Triton X-100). Chambers were washed 3 times with block solution and then cells were incubated with the secondary, GAM-488 at a 1:800 dilution for 60 min. After washing 3 times, cells were treated with SlowFade Gold with DAPI (Invitrogen S36938) and examined using an Olympus Fluoview 1000 laser scanning confocal microscope

Syncytium formation assay. Vero cells were transiently transfected with GPC-ddRFP in a pCAGGS vector. Cells were harvested 24 hr post transfection and reseeded in a 96 well plate. After 48 hr post transfection, cells were treated for 20 min with media adjusted to pH 5.0. The cells were further treated with neutral pH medium and fixed with methanol: acetone (50:50) after 3 hours. The Syncytium formation was monitored by immunohistochemically staining the fixed cells with GP1-specific antibody (BE-08).

Table 5-1: Primers for generating PCR product/mega primers for In-fusion reaction

Name	Sequence 5'-3'
Fwd dRFP-GPC	TGGCGCAGAGGACACAGCGGCGCCGGCACCGCCAGCAGCGGCGGTAGCACCGGCAGCGTG AGCAAGAGCGAGGAG
rev dRFP-GPC	CTTCGGGAGGTCTTACAGGTGGTGGCGGCCCT
Fwd ddFP-Z	ACAGCACCACCACCAGGGCATGGCACCGGCA
Rev ddFP-Z	AGCGGTCTCCTTGCTCTTGTACCGCTCGTCCATG
Fwd ddFP-CD4	ACATGTAGCCCCATTGGGCATGGCACCGGCA
rev ddFP-CD4	TGGCCTCGTGCCTCACTTGTACCGCTCGTCCATG
Fwd dRFP-CD4	ACATGTAGCCCCATTAGCGGCGCCGGCACCGCCAGCAGCGGCGGTAGCACCGGCAGCGTGA GCAAGAGCGAGGAGGTC
rev dRFP-CD4	TGGCCTCGTGCCTCACAGGTGGTGGCGGCCCTC

Table 5-2: Primers for generating linear plasmid for In-fusion reaction

Name	Sequence 5'-3'
Inv to fwd JGPCP3	GTGTCCTCTGCGCCAAACTG
Inv to rev JGPCP3	TAAGACCTCCCGAAGGTCCCCAC
Inv to fwd Z-Spep	TGGTGGTGGTGCTGTTGGCTC
Inv to rev Z-Spep	AGCAAGGAGACCGCTGCTGC
Inv to fwd CD4	AATGGGGCTACATGTCTTCTG
Inv to rev CD4	TGAGGCACGAGGCCAGGCA

Table 5-3: Primers for generating G2A mutant using Quikchange mutagenesis

Name	Sequence 5'-3'
Z-G2A	GCTTGGTACCACCATGGCCAACTGCAACGGGGCATCC
Z-G2A complement	GGATGCCCCGTTGCAGTTGGCCATGGTGGTACCAAGC

Table 5-4: Primers used for generating BiFC constructs using In-Fusion reaction

Name		Sequence 5'-3'
Fwd JGPC/CD4-VN-mp	Primers for generation of PCR product/ mega primers for In-Fusion reaction	GGTAGCACCGGCAGCGTGAGCAAGGGCGAGGAGCT
Rev JGPC-VN-mp		CTTCGGGAGGTCTTACTCGATGTTGTGGCGGATCTTG
Fwd Z-VN-mp		GGCAGCTCCGGTACCGTGAGCAAGGGCGAGGAGCT
Rev Z-VN-mp		GGTCTCCTTGCTCTCGATGTTGTGGCGGATCTTG
Fwd JGPC/CD4-VN-mp		GGTAGCACCGGCAGCGTGAGCAAGGGCGAGGAGCT
Rev CD4-VN-mp		TGGCCTCGTGCCTCACTCGATGTTGTGGCGGATCTTG
Fwd JGPC/CD4-VC-mp		GGTAGCACCGGCAGCGACAAGCAGAAGAACGGCATCAAG
Rev JGPC-VC-mp		CTTCGGGAGGTCTTACTTGTACAGCTCGTCCATGC
Fwd Z-VC-mp		GGCAGCTCCGGTACCGACAAGCAGAAGAACGGCATCAAG
Rev Z-VC-mp		AGCGGTCTCCTTGCTCTTGTACAGCTCGTCCATGC
Fwd JGPC/CD4-VC-mp		GGTAGCACCGGCAGCGACAAGCAGAAGAACGGCATCAAG
Rev CD4-VC-mp		TGGCCTCGTGCCTCACTTGTACAGCTCGTCCATGC
Inv to fwd JGPC/CD4-dRFP	Primers for generating linearized plasmid for In-Fusion reaction	GCTGCCGGTGCTACCGCCGCT
Inv to rev JGPCP3		TAAGACCTCCCGAAGGTCCCCAC
Inv to Fwd Z-ddFP-Spep		GGTACCGGAGCTGCCGCT
Inv to rev Z-Spep		AGCAAGGAGACCGCTGCTGC
Inv to fwd JGPC/CD4-dRFP		GCTGCCGGTGCTACCGCCGCT
Inv to rev CD4		TGAGGCACGAGGCCAGGCA

C. Results

GPC and Z fusion-proteins are expressed at the cell-surface and are functional. Nascent JUNV GPC is co-translationally transported to ER via its signal peptide SSP and undergoes maturation in the Golgi apparatus by the action of S1P/SKI-1 [46, 47]. It is further transported to the cell-surface, which is the site of virus budding. Previous studies carried out in our lab have shown that attaching a C-terminal tag does not alter the expression or function of GPC [54, 70]. We made GPC-ddRFP construct by attaching ddRFP-copy A to the C-terminal end of GP2 via a 14 amino acid long linker. In order to test efficient folding and expression of the GPC-fusion protein, GPC-ddRFP was transiently transfected in Vero cells and confocal microscopy was used to assess the cell-surface expression of GPC. The results of the confocal experiment reveal efficient cell-surface expression of GPC shown by Vero cell-surface stained using GP1-specific antibodies (Figure 5-2A). The membrane fusion activity of GPC was also tested by performing a syncytium formation assay. Syncytium formation was monitored by immunohistochemically staining the cells with GP1-specific antibody. The results show that GPC-ddRFP is able to mediate cell-cell fusion, similar to WT GPC, in a pH-dependent manner (Figure 5-2C).

Matrix Z protein is expressed in the cytoplasm and associates with the plasma membrane upon myristoylation. Previous studies have shown that attaching a tag to the C-terminus of Z does not perturb its biogenesis and function [150]. Z-ddFP-Spep construct was made by attaching the ddFP-copy B to the C-terminus of Z. A Spep-tag was also attached to the C-terminal end of ddFP subunit to enable immunochemical detection of the fusion protein. Protein expression and cellular localization of Z was confirmed by confocal microscopy. Vero cells transfected with Z-ddFP-Spep and were stained with anti-Spep antibodies after

permeabilizing the cell membrane, 48 hr post transfection. Z protein was concentrated mostly at the plasma membrane and also diffused through the cytoplasm as previously observed (Figure. 5-2B) [62, 141].

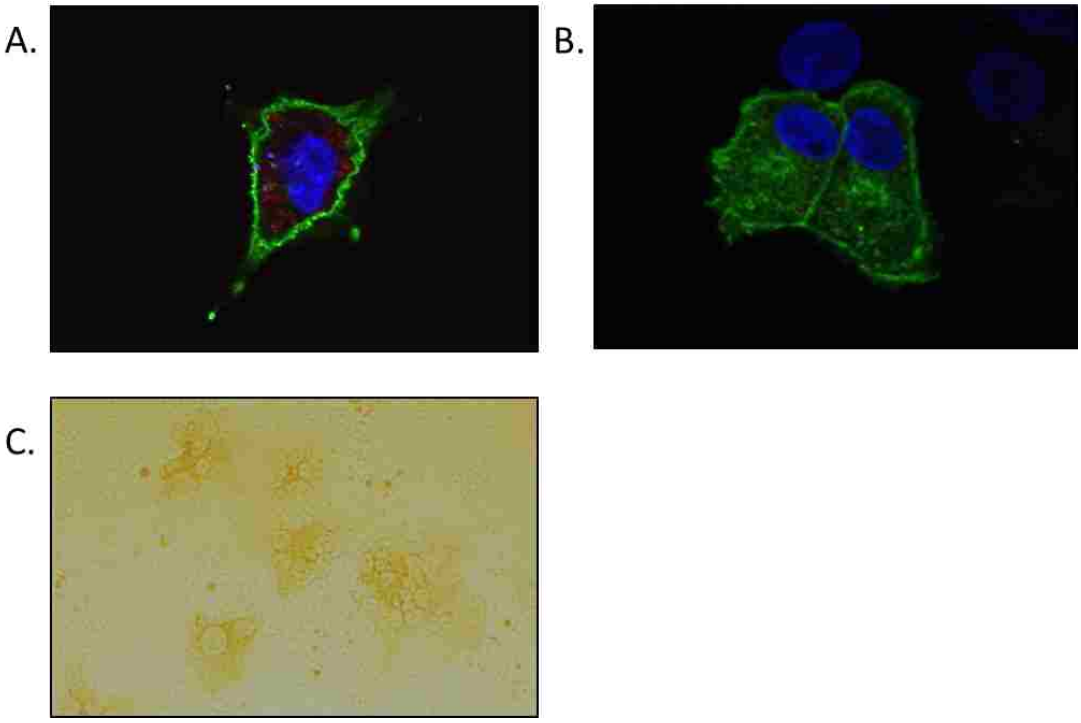

Figure 5-2. Analysis of GPC and Z expression. (A-B) Confocal microscopy**:** Vero cells expressing either **(A)** JUNV GPC-ddRFP only or **(B)** JUNV Z-ddFP-Spep only, were stained with GP1-specific MAb BE08 or anti-Spep MAb, respectively. Cells were then incubated with GAM-488 MAb, washed and treated with SlowFade Gold with DAPI (nucleus-blue). Cells expressing GPC were fixed and surface stained and Z expressing cells were fixed, permeabilized and then stained. **(C) Syncytium formation.** Vero cells expressing GPC-ddRFP were treated with acidic pH medium for 20 min at 37^0C followed by incubation with neutral pH medium. Cells were fixed and stained with GP1-specific MAb BF11.

GPC interacts with matrix Z protein. To test for the interaction between GPC and Z protein during virus assembly and budding, dimerization-dependent red fluorescent protein monomers were attached as tags to the respective C-termini. GPC-ddRFP and Z-ddFP-Spep constructs were co-transfected in Vero cells in a 6 cm dish. At 24 hr post transfection, cells were reseeded onto confocal dish and incubated at 37^0C overnight. Cells were washed with 1X PBS and treated with Hoechst stain to visualize nucleus. Live cells were directly visualized under confocal microscope for red fluorescence, indicative of interaction. When expressed alone GPC-ddRFP and Z-ddFP-Spep did not show fluorescence (Figure 5-3 (A & B)), consistent with less or no fluorescence in its monomeric state. Upon co-expression, a clear red fluorescent signal was observed at the cell-surface (Figure 5-3 C), suggesting interaction between GPC and Z.

Myristoylation at the conserved G2 residue on Z is essential for membrane insertion and budding [62]. G2A mutant of Z does not associate with the membrane and hence may not interact with GPC [61]. To test for association of G2A mutant of Z with GPC, we generated G2A Z-ddFP-Spep construct and co-expressed with GPC-ddRFP. Consistent with previous findings, the results show no red fluorescent signal, confirming that the G2A mutant of Z does not associate with GPC at the plasma membrane. (Figure 5-4 B).

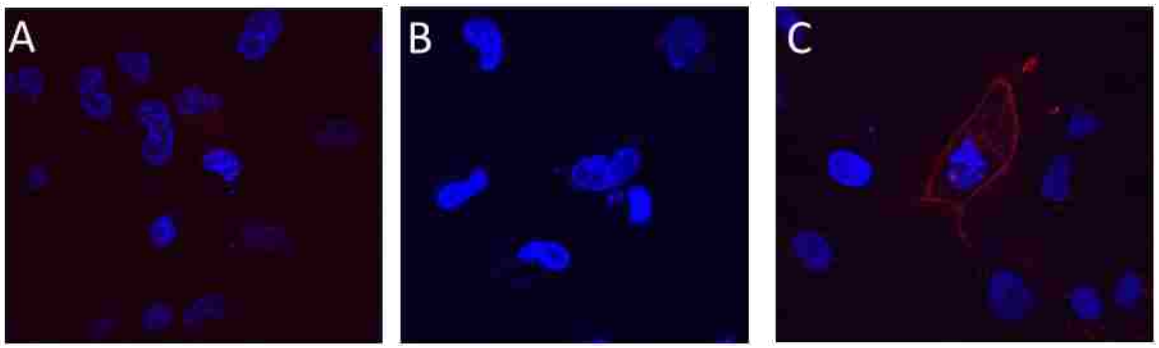

Figure 5-3. GPC interacts with Z. (A-C) Confocal microscopy: Vero cells expressing (A) GPC-ddRFP only, or (B) Z-ddFP-Spep only, or (C) GPC-ddRFP and Z-ddFP-Spep, were washed and stained with Hoechst stain (nucleus–blue) at 37^0C for 15 min and visualized under confocal microscope. (C) Illustrates positive red fluorescent signal for GPC and Z interaction.

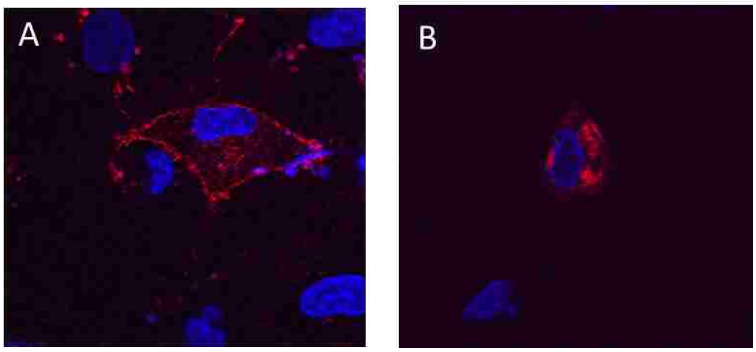

Figure 5-4. Z G2A mutant do not associate with GPC. Vero cells expressing (A) GPC-ddRFP and Z-ddFP-Spep or (B) GPC-ddRFP and G2A Z-ddFP-Spep were washed and stained with Hoechst stain (nucleus-blue) at 37^0C for 15 min and visualized under confocal microscope. G2A Z-ddFP-Spep mutant coexpressed with GPC-ddRFP do not show surface red fluorescence and the staining observed is mostly intracellular, likely due to aggregation.

Association of dimerization-dependent fluorescent protein subunits when co-expressed with unrelated membrane protein. To investigate the specificity of the association, we carried out studies with an irrelevant membrane protein, human CD4, which is not known to associate with GPC or matrix Z protein. We coexpressed human CD4-ddRFP or human CD4-ddFP with Z-ddFP-Spep or GPC-ddRFP, respectively. Results with human CD4 show that low affinity of the two monomeric subunits (A and B) was sufficient to drive fluorescent protein-mediated association, when concentrated onto two-dimensional plasma membrane (Figure 5-5). Despite our initial observation of dimerization-dependent fluorescence using GPC-ddRFP and Z-ddFP-Spep, the control studies with CD4 constructs reveals that this interaction could be as a result of fluorescent protein's monomer association. Thus, carrying out studies on two membrane-associated proteins using this technique can be misleading.

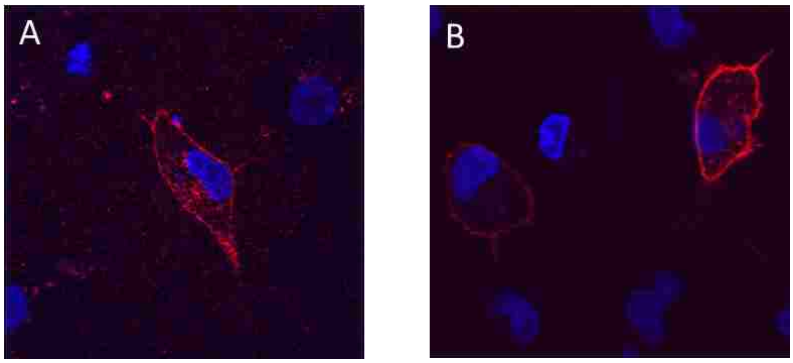

Figure 5-5: Z associates with human CD4 (control) protein. (A-B) Vero cells showing surface red fluorescence signal. Cells were expressed with (A) GPC-ddRFP and human CD4-ddFP or (B) Human CD4-ddRFP and Z-ddFP-Spep, washed and fixed with Hoechst stain (nucleus-blue) at 37^0C for 15 min and visualized under confocal microscope.

D. Discussion

During assembly of enveloped viruses, the viral components have to come together at the virus budding site. There are many interesting questions that remain to be addressed in virus assembly. One of the main challenges remains to be the difficulty in studying the interactions at the plasma membrane. In the case of arenaviruses, the matrix Z protein plays a crucial role in assembly and budding of the virus particle. Although co-immunoprecipitation studies and confocal microscopy show association of GPC with Z [62], immunogold-electron microscopy fail to show evidence of colocalization [66]. To address this kind of discrepancies, we chose a recently developed approach using dimerization-dependent fluorescent proteins, which is modified in such a way to reduce the affinity between the subunits of a red fluorescent protein dimer, as a tool to study this interaction. Although our initial observation of dimerization-dependent fluorescence is consistent with association of GPC and Z protein, we are unable to exclude that the association may be based on weak monomer-monomer association at the membrane. In addition, studies using a different system (BiFC) to study association of GPC and Z also showed similar results (data not shown). Studying two membrane-associated proteins using these techniques can be misinterpreted, as concentrating the proteins on plasma membrane allows monomers or fragments of fluorescent proteins to be at a closer distance such that the fluorescent proteins interact irrespective of PPIs of their fused partners.

Chapter 6

Conclusion

Arenaviruses, causative agents of hemorrhagic fevers, spread infection in humans through zoonotic transmission of virus from their respective rodent host. Due to the severity of the disease and lack of suitable treatment, arenaviruses continue to be a significant threat to public health [32]. There is a dire need to develop better therapies, as the current treatment options are limiting and no FDA-approved vaccines are available. My dissertation research has employed the use of recombinant proteins and genetic tools to understand the mechanism involved in envelope glycoprotein complex (GPC)-mediated virus entry of arenaviruses. My research was focused on two areas: to understand the role of the GPC of arenaviruses in viral and endosomal membrane fusion and its inhibition by small-molecule fusion inhibitors, and to explore events that take place during arenavirus assembly. We also explored the mechanism of inhibition by small-molecule fusion inhibitors that antagonize pH-induced activation and identified the inhibitor interactions with GPC. We compared the structure-function relationships that promote fusion activation in LASV and JUNV GPC. In addition, my work also explored a new technique for investigating virus assembly by studying the interaction of GPC and Z at the plasma membrane.

Upon activation by acidic pH in the late endosome, arenavirus GPC undergoes a large-scale structural reorganization leading to membrane fusion. GPC, a class I fusion protein, exists in a kinetically trapped metastable state, primed to undergo conformational changes to a highly stable post-fusion state, thereby driving membrane fusion. My work in chapter 2 summarizes the studies carried out to understand the mechanism of fusion activation and its inhibition by small-molecule fusion inhibitors. In the absence of atomic-level structural

information of GPC, our study using recombinant GPC has shown that GPC expressed in insect cells can be used to study the fusion mechanism. Our characterization of recombinant GPC shows that it exists as a trimer in size-exclusion chromatography, consistent with a class I fusion protein [70]. The structural integrity of the purified recombinant GPC may be because of the interaction among the nine transmembrane domains in GPC trimer, in comparison to the three transmembrane domain of classical type I fusion protein trimer, and the intersubunit zinc-finger structures. An early event of GPC-mediated fusion is characterized by shedding of GP1 subunit upon pH-induced conformational change. Using surface plasmon resonance (BIACORE), we demonstrated shedding of GP1 subunit upon pH activation. Importantly, we showed successful reconstitution of membrane-fusion activity of GPC using a liposome-based fusion assay. This GPC-mediated liposomal fusion was sensitive to inhibition by NW-specific small-molecule inhibitor (ST-294) and not by an OW-specific inhibitor (ST-161) [70]. Taken together, we have developed an *in vitro* system to carry out biochemical and biophysical analysis of GPC-mediated membrane fusion and its inhibition. Future work, using this *in vitro* system, will allow us to study the effects of mutation in GPC, thus providing detailed mechanistic understanding of mechanism of fusion and inhibition.

In the absence of effective antivirals, recently identified small-molecule fusion inhibitors have opened up new avenues in developing better therapy. Development of potent inhibitors requires a good knowledge of inhibitor interactions with GPC at atomic-level. In the absence of structural information, my work in chapter 3 using photoaffinity inhibitors has created new opportunities to study inhibitor interactions with arenavirus GPC. Our findings from earlier genetic analysis suggest that these inhibitors target the interactions between SSP and GP2

subunits [41]. Studies with recombinant proteins confirm inhibitor binding to the same region on GPC [53], suggesting that all the inhibitors target the SSP-GP2 interface. Our studies now provide direct physical evidence for this binding. We demonstrated specific photoaffinity-labeling of SSP and GP2 of LASV GPC using photoreactive inhibitors provided by our collaborators at TSRI, confirming inhibitor binding to interface [151]. Our study also suggests a conformational change at SSP-GP2 interface associated with proteolytic cleavage. We also showed specificity of labeling by competing with non-photoreactive inhibitors active against OW-viruses and not by NW-specific inhibitors [151]. Identifying the amino acids labeled in the photo-adduct will provide an important perspective to understand GPC-inhibitor interactions. Our study provides an approach that can be used for mapping adducts of these and other inhibitors, and facilitate triangulation of inhibitor interactions with GPC. This work will guide development of novel therapeutic agents against arenavirus infection.

Species specificity of these small-molecule inhibitors is determined by the amino acid difference between OW and NW arenaviruses. Specifically, the short ectodomain loop of SSP harbors lysine (K33) and substituting this residue with histidine makes JUNV GPC sensitive to inhibition by an OW-specific inhibitor [41]. In chapter 4 we explored the mechanism of pH-activation and membrane fusion of OW-LASV GPC and compared it to NW-JUNV GPC that has same structural features. We showed that residue K33 in LASV SSP, like in JUNV, is important for its pH-activation and fusion function. Mutating K33 also affects the sensitivity of LASV GPC to both a LASV-specific inhibitor and broadly-active inhibitor. This work has led us to propose that although the mechanism of pH-activation in LASV GPC is similar to that in JUNV GPC, differences observed in LASV can be related to the side-chain interactions of amino acids in the SSP-GP2 interface. A recent finding

suggests requirement of secondary LAMP 1 receptor for Lassa virus entry [27]. Based on this observation and cryo-EM work on LASV GPC, *Li, S., et al* have proposed a hypothetical entry model, which suggests that GP1 subunit exposes a binding site for LAMP1in the low pH of endosome. Further lowering of pH in the lysosomal compartment allows GP1 detachment and primes the GP2 subunit to promote membrane fusion [138]. Future work using LAMP1 receptor in studying mechanism of fusion and inhibitor binding to LASV GPC will allow us to examine inhibitor interaction that may prevent LAMP1 binding or not allow the later pH change.

An important step in the life cycle of enveloped viruses is the recruitment and assembly of the viral structural proteins in membrane-compartments at the site of virus budding. During the assembly and budding of arenaviruses, the interaction between GPC and Z at the site of virus budding is less clear. My work in chapter 5 explored a new technique to examine the assembly events by studying the association of GPC and Z at the plasma membrane. We chose dimerization-dependent fluorescent protein [148, 149] and split yellow fluorescent protein (YFP) [152] to study the interaction between GPC and Z. Interaction of GPC and Z at plasma membrane by confocal microscopy was studied using their fused partners that fluoresce when brought into close proximity. Although, association of GPC with Z was evident, we also observed association of GPC and Z with an irrelevant membrane protein, raising a possibility of non-specific association of fluorescent protein due to concentration along the membrane. Therefore, we cannot exclude that the interaction between GPC and Z assessed by this method could be misleading. Importantly, studying interaction of two membrane-associated proteins with this technique may be difficult to

unequivocally interpret. Future studies using FRET, which is between two non-associating reporters, may be beneficial in studying interactions at the plasma membrane.

The work I present here has furthered the understanding of GPC and the role it plays in arenavirus life cycle. In the absence of atomic-level structural details, it has brought us a step closer to unraveling the mechanism involved in low-pH induced activation and membrane fusion of GPC. By laying initial steps towards understanding the interaction of inhibitors with GPC, future photoaffinity labeling studies will help support the design and development of newer drugs for therapeutic intervention. By studying mechanism of activation of pH-dependent fusion between the OW and NW species, we will advance our knowledge in understanding the evolution of arenavirus entry mechanism and also the molecular basis for specificity of these inhibitors. This comparative study will be beneficial in designing potent broadly-active inhibitors.

References

1. Clegg, J.C.S., *Molecular phylogeny of the arenaviruses.* Curr Top Microbiol Immunol, 2002. **262**: p. 1-24.

2. Salazar-Bravo, J., L.A. Ruedas, and T.L. Yates, *Mammalian reservoirs of arenaviruses.* Curr Top Microbiol Immunol, 2002. **262**: p. 25-63.

3. Charrel, R.N. and X. de Lamballerie, *Zoonotic aspects of arenavirus infections.* Vet Microbiol, 2010. **140**: p. 213-20.

4. Briese, T., et al., *Genetic detection and characterization of Lujo virus, a new hemorrhagic fever-associated arenavirus from southern Africa.* PLoS Pathog, 2009. **5**: p. e1000455.

5. Palacios, G., et al., *Genomic and phylogenetic characterization of Merino Walk virus, a novel arenavirus isolated in South Africa.* J Gen Virol, 2010. **91**: p. 1315-24.

6. Stenglein, M.D., et al., *Identification, characterization, and in vitro culture of highly divergent arenaviruses from boa constrictors and annulated tree boas: candidate etiological agents for snake inclusion body disease.* MBio, 2012. **3**(4): p. e00180-12.

7. Hetzel, U., et al., *Isolation, identification, and characterization of novel arenaviruses, the etiological agents of boid inclusion body disease.* J Virol, 2013. **87**(20): p. 10918-35.

8. Charrel, R.N., X. de Lamballerie, and S. Emonet, *Phylogeny of the genus Arenavirus.* Curr Opin Microbiol, 2008. **11**: p. 362-8.

9. Wolff, S., H. Ebihara, and A. Groseth, *Arenavirus budding: a common pathway with mechanistic differences.* Viruses, 2013. **5**(2): p. 528-49.

10. Günther, S., et al., *Application of real-time PCR for testing antiviral compounds against Lassa virus, SARS coronavirus and Ebola virus in vitro.* Antiviral Res, 2004. **63**: p. 209-15.

11. Charrel, R.N., et al., *Phylogeny of New World arenaviruses based on the complete coding sequences of the small genomic segment identified an evolutionary lineage produced by intrasegmental recombination.* Biochem Biophys Res Commun, 2002. **296**: p. 1118-24.

12. Peters, C.J., *Human infection with arenaviruses in the Americas.* Curr Top Microbiol Immunol, 2002. **262**: p. 65-74.

13. Delgado, S., et al., *Chapare virus, a newly discovered arenavirus isolated from a fatal hemorrhagic fever case in Bolivia.* PLoS Pathog., 2008. **4**: p. e1000047.

14. McCormick, J.B., et al., *A prospective study of the epidemiology and ecology of Lassa fever.* J Infect Dis, 1987. **155**: p. 437-44.

15. McCormick, J.B. and S.P. Fisher-Hoch, *Lassa fever.* Curr Top Microbiol Immunol, 2002. **262**: p. 75-109.

16. Ogbu, O., E. Ajuluchukwu, and C.J. Uneke, *Lassa fever in West African sub-region: an overview.* J Vector Borne Dis, 2007. **44**(1): p. 1-11.

17. Richmond, J.K. and D.J. Baglole, *Lassa fever: epidemiology, clinical features, and social consequences.* BMJ, 2003. **327**(7426): p. 1271-5.

18. Moraz, M.L. and S. Kunz, *Pathogenesis of arenavirus hemorrhagic fevers.* Expert Rev Anti Infect Ther, 2011. **9**(1): p. 49-59.

19. Centers for Disease Control and Prevention. *Lassa Fever in Nigeria*. 2016; Available from: http://wwwnc.cdc.gov/travel/notices/watch/lassa-fever-nigeria.

20. Parodi, A.S., et al., *[Concerning the epidemic outbreak in Junin]*. Dia Med, 1958. **30**(62): p. 2300-1.

21. McKee, K.T., Jr., et al., *Virus-specific factors in experimental Argentine hemorrhagic fever in rhesus macaques.* J Med Virol, 1987. **22**(2): p. 99-111.

22. Gonzalez, P.H., et al., *Lymphatic tissue in Argentine hemorrhagic fever. Pathologic features.* Arch Pathol Lab Med, 1980. **104**(5): p. 250-4.

23. Radoshitzky, S.R., et al., *Transferrin receptor 1 is a cellular receptor for New World haemorrhagic fever arenaviruses.* Nature, 2007. **446**: p. 92-6.

24. Radoshitzky, S.R., et al., *Receptor determinants of zoonotic transmission of New World hemorrhagic fever arenaviruses.* Proc Natl Acad Sci U S A, 2008. **105**: p. 2664-9.

25. Fehling, S.K., F. Lennartz, and T. Strecker, *Multifunctional nature of the arenavirus RING finger protein Z.* Viruses, 2012. **4**(11): p. 2973-3011.

26. Buchmeier, M.J., J.C. de la Torre, and C.J. Peters, *Arenaviridae: The Viruses and Their Replication*, in *Fields Virology*, D.M. Knipe and P.M. Howley, Editors. 2007, Lippincott Williams & Wilkins: Philadelphia, PA. p. 1791-1828.

27. Jae, L.T., et al., *Virus entry. Lassa virus entry requires a trigger-induced receptor switch.* Science, 2014. **344**(6191): p. 1506-10.

28. Martinez, M.G., S.M. Cordo, and N.A. Candurra, *Characterization of Junin arenavirus cell entry.* J Gen Virol, 2007. **88**(Pt 6): p. 1776-84.

29. Kunz, S., *Receptor binding and cell entry of Old World arenaviruses reveal novel aspects of virus-host interaction.* Virology, 2009. **387**(2): p. 245-9.

30. Rojek, J.M. and S. Kunz, *Cell entry by human pathogenic arenaviruses.* Cell Microbiol, 2008. **10**: p. 828-35.

31. Baird, N.L., J. York, and J.H. Nunberg, *Arenavirus infection induces discrete cytosolic structures for RNA replication.* J Virol, 2012. **86**: p. 11301-10.

32. Kerber, R., et al., *Research efforts to control highly pathogenic arenaviruses: a summary of the progress and gaps.* J Clin Virol, 2015. **64**: p. 120-7.

33. NIAID. *NIAID Category A, B, and C Priority Pathogens*. 2009; Available from: http://www.niaid.nih.gov/topics/BiodefenseRelated/Biodefense/research/Pages/CatA.aspx.

34. Gunther, S. and O. Lenz, *Lassa virus.* Crit Rev Clin Lab Sci, 2004. **41**: p. 339-90.

35. Graci, J.D. and C.E. Cameron, *Mechanisms of action of ribavirin against distinct viruses.* Rev Med Virol, 2006. **16**(1): p. 37-48.

36. Mendenhall, M., et al., *T-705 (favipiravir) inhibition of arenavirus replication in cell culture.* Antimicrob Agents Chemother, 2011. **55**(2): p. 782-7.

37. Bolken, T.C., et al., *Identification and characterization of potent small molecule inhibitor of hemorrhagic fever New World arenaviruses.* Antiviral Res, 2006. **69**: p. 86-9.

38. Larson, R.A., et al., *Identification of a broad-spectrum arenavirus entry inhibitor.* J Virol., 2008. **82**: p. 10768-75.

39. Lee, A.M., et al., *Unique small molecule entry inhibitors of hemorrhagic fever arenaviruses.* J. Biol Chem, 2008. **283**: p. 18734-42.

40. Whitby, L.R., et al., *Characterization of Lassa virus cell entry inhibitors: determination of the active enantiomer by asymmetric synthesis.* Bioorg Med Chem Lett, 2009. **19**: p. 3771-4.

41. York, J., et al., *pH-induced activation of arenavirus membrane fusion is antagonized by small-molecule inhibitors.* J Virol, 2008. **82**: p. 10932-9.

42. Cashman, K.A., et al., *Evaluation of Lassa antiviral compound ST-193 in a guinea pig model.* Antiviral Res, 2011. **90**: p. 70-9.

43. Blobel, G., et al., *Translocation of proteins across membranes: the signal hypothesis and beyond.* Symp Soc Exp Biol, 1979. **33**: p. 9-36.

44. Martoglio, B. and B. Dobberstein, *Signal sequences: more than just greasy peptides.* Trends in Cell Biology, 1998. **8**: p. 410-415.

45. Briknarova, K., et al., *Structure of a zinc-binding domain in the Junin virus envelope glycoprotein.* J. Biol. Chem, 2011. **286**: p. 1528-36.

46. Kunz, S., et al., *Mechanisms for lymphocytic choriomeningitis virus glycoprotein cleavage, transport, and incorporation into virions.* Virology, 2003. **314**: p. 168-78.

47. Lenz, O., et al., *The Lassa virus glycoprotein precursor GP-C is proteolytically processed by subtilase SKI-1/S1P.* Proc Natl Acad Sci U S A, 2001. **98**: p. 12701-5.

48. Eichler, R., et al., *Identification of Lassa virus glycoprotein signal peptide as a trans-acting maturation factor.* EMBO Rep, 2003. **4**: p. 1084-8.

49. Agnihothram, S.S., J. York, and J.H. Nunberg, *Role of the stable signal peptide and cytoplasmic domain of G2 in regulating intracellular transport of the Junin virus envelope glycoprotein complex.* J Virol, 2006. **80**: p. 5189-98.

50. Harrison, S.C., *Viral membrane fusion.* Nat Struct Mol Biol, 2008. **15**: p. 690-8.

51. White, J.M., et al., *Structures and mechanisms of viral membrane fusion proteins: multiple variations on a common theme.* Crit Rev Biochem Mol Biol, 2008. **43**: p. 189-219.

52. Bullough, P.A., et al., *Structure of influenza haemagglutinin at the pH of membrane fusion.* Nature, 1994. **371**: p. 37-43.

53. Thomas, C.J., et al., *A specific interaction of small-molecule entry inhibitors with the envelope glycoprotein complex of the Junín hemorrhagic fever arenavirus.* J Biol Chem, 2011. **286**: p. 6192-200.

54. York, J. and J.H. Nunberg, *Role of the stable signal peptide of the Junín arenavirus envelope glycoprotein in pH-dependent membrane fusion.* J Virol, 2006. **80**: p. 7775-80.

55. Messina, E.L., J. York, and J.H. Nunberg, *Dissection of the role of the stable signal peptide of the arenavirus envelope glycoprotein in membrane fusion.* J Virol, 2012. **86**: p. 6138-45.

56. Welsch, S., B. Müller, and H.G. Kräusslich, *More than one door - Budding of enveloped viruses through cellular membranes.* FEBS Lett, 2007. **581**: p. 2089-97.

57. Griffiths, G. and P. Rottier, *Cell biology of viruses that assemble along the biosynthetic pathway.* Semin Cell Biol, 1992. **3**(5): p. 367-81.

58. Lyles, D.S., *Assembly and budding of negative-strand RNA viruses.* Adv Virus Res, 2013. **85**: p. 57-90.

59. Jose, J., J.E. Snyder, and R.J. Kuhn, *A structural and functional perspective of alphavirus replication and assembly.* Future Microbiol, 2009. **4**(7): p. 837-56.

60. Strecker, T., et al., *Lassa virus Z protein is a matrix protein and sufficient for the release of virus-like particle.* J Virol, 2003. **77**: p. 10700-5.

61. Strecker, T., et al., *The role of myristoylation in the membrane association of the Lassa virus matrix protein Z.* Virol J, 2006. **3**: p. e93.

62. Capul, A.A., et al., *Arenavirus Z-GP association requires Z myristoylation but not functional RING or L domains.* J Virol, 2007. **81**: p. 9451-60.

63. Chen, B.J., et al., *Influenza virus hemagglutinin and neuraminidase, but not the matrix protein, are required for assembly and budding of plasmid-derived virus-like particles.* J Virol, 2007. **81**: p. 7111-23.

64. Scheiffele, P., et al., *Influenza viruses select ordered lipid domains during budding from the plasma membrane.* J Biol Chem, 1999. **274**: p. 2038-44.

65. Brown, E.L. and D.S. Lyles, *A novel method for analysis of membrane microdomains: vesicular stomatitis virus glycoprotein microdomains change in size during infection, and those outside of budding sites resemble sites of virus budding.* Virology, 2003. **310**: p. 343-58.

66. Agnihothram, S.S., et al., *Assembly of arenavirus envelope glycoprotein GPC in detergent-soluble membrane microdomains.* J Virol, 2009. **83**: p. 9890-900.

67. Amorosa, V., et al., *Imported Lassa fever, Pennsylvania, USA, 2010.* Emerg Infect Dis, 2010. **16**: p. 1598-600.

68. Haas, W.H., et al., *Imported Lassa fever in Germany: surveillance and management of contact persons.* Clin Infect Dis, 2003. **36**: p. 1254-8.

69. Di Simone, C. and M.J. Buchmeier, *Kinetics and pH dependence of acid-induced structural changes in the lymphocytic choriomeningitis virus glycoprotein complex.* Virology, 1995. **209**: p. 3-9.

70. Thomas, C., et al., *Biochemical reconstitution of arenavirus envelope glycoprotein-mediated membrane fusion.* PLOS One, 2012. **7**: p. e51114.

71. Burton, D.R., et al., *HIV vaccine design and the neutralizing antibody problem.* Nat Immunol, 2004. **5**: p. 233-6.

72. Health and Human Services, *Implementation Plan for Chemical, Biological, Radiological and Nuclear Threats*. 2007.

73. Beyer, W.R., et al., *Endoproteolytic processing of the lymphocytic choriomeningitis virus glycoprotein by the subtilase SKI-1/S1P*. J Virol, 2003. **77**: p. 2866-72.

74. Cao, W., et al., *Identification of alpha-dystroglycan as a receptor for lymphocytic choriomeningitis virus and Lassa fever virus.* Science, 1998. **282**: p. 2079-81.

75. Di Simone, C., M.A. Zandonatti, and M.J. Buchmeier, *Acidic pH triggers LCMV membrane fusion activity and conformational change in the glycoprotein spike.* Virology, 1994. **198**: p. 455-65.

76. Eschli, B., et al., *Identification of an N-terminal trimeric coiled-coil core within arenavirus glycoprotein 2 permits assignment to class I viral fusion proteins.* J Virol, 2006. **80**: p. 5897-907.

77. York, J., et al., *An antibody directed against the fusion peptide of Junin virus envelope glycoprotein GPC inhibits pH-induced membrane fusion.* J Virol. , 2010. **84**: p. 6119-6129.

78. Igonet, S., et al., *X-ray structure of the arenavirus glycoprotein GP2 in its postfusion hairpin conformation.* Proc Natl Acad Sci U S A, 2011. **108**.

79. York, J., et al., *The signal peptide of the Junín arenavirus envelope glycoprotein is myristoylated and forms an essential subunit of the mature G1-G2 complex.* J Virol, 2004. **78**: p. 10783-92.

80. Agnihothram, S.S., et al., *Bitopic membrane topology of the stable signal peptide in the tripartite Junín virus GP-C envelope glycoprotein complex.* J Virology, 2007. **81**: p. 4331-7.

81. York, J. and J.H. Nunberg, *A novel zinc-binding domain is essential for formation of the functional Junín virus envelope glycoprotein complex.* J Virol, 2007. **81**: p. 13385-91.

82. Sanchez, A., et al., *Junin virus monoclonal antibodies: characterization and cross-reactivity with other arenaviruses.* J Gen Virol, 1989. **70**: p. 1125-32.

83. Gawlik, K., et al., *Autocatalytic activation of the furin zymogen requires removal of the emerging enzyme's N-terminus from the active site.* PLoS One, 2009. **4**: p. e5031.

84. Bravo, D.A., et al., *Accurate and efficient cleavage of the human insulin proreceptor by the human proprotein-processing protease furin. Characterization and kinetic parameters using the purified, secreted soluble protease expressed by a recombinant baculovirus.* J Biol Chem, 1994. **269**: p. 25830-7.

85. Touré, B.B., et al., *Biosynthesis and enzymatic characterization of human SKI-1/S1P and the processing of its inhibitory prosegment.* J Biol Chem, 2000. **275**: p. 2349-58.

86. Stenlund, P., et al., *Capture and reconstitution of G protein-coupled receptors on a biosensor surface.* Anal Biochem, 2003. **316**: p. 243-50.

87. Fuerst, T.R., et al., *Eukaryotic transient-expression system based on recombinant vaccinia virus that synthesizes bacteriophage T7 RNA polymerase.* Proc Natl Acad Sci U S A, 1986. **83**: p. 8122-6.

88. Rawson, R.B., *The SREBP pathway--insights from Insigs and insects.* Nat Rev Mol Cell Biol, 2003. **4**: p. 631-40.

89. Albariño, C.G., et al., *Efficient reverse genetics generation of infectious Junin viruses differing in glycoprotein processing.* J Virol, 2009. **83**: p. 5606-14.

90. Rojek, J.M., et al., *Targeting the proteolytic processing of the viral glycoprotein precursor is a promising novel antiviral strategy against arenaviruses.* J Virol, 2010. **84**: p. 573-84.

91. Cano-Monrealn, G.L., J.C. Williams, and H.W. Heidner, *An arthropod enzyme, Dfurin1, and a vertebrate furin homolog display distinct cleavage site sequence preferences for a shared viral proprotein substrate.* J Insect Sci, 2010. **10**: p. 29.

92. Binley, J.M., et al., *Enhancing the proteolytic maturation of human immunodeficiency virus type 1 envelope glycoproteins.* J Virol, 2000. **76**: p. 2606-16.

93. Moore, J.P., et al., *Dissociation of gp120 from HIV-1 virions induced by soluble CD4.* Science, 1990. **250**: p. 1139-1142.

94. Hoekstra, D., et al., *Fluorescence method for measuring the kinetics of fusion between biological membranes.* Biochemistry, 1984. **23**: p. 5675-81.

95. Armstrong, R.T., A.S. Kushnir, and J.M. White, *The transmembrane domain of influenza hemagglutinin exhibits a stringent length requirement to support the hemifusion to fusion transition.* J Cell Biol, 2000. **151**: p. 425-37.

96. Kemble, G.W., T. Danieli, and J.M. White, *Lipid-anchored influenza hemagglutinin promotes hemifusion, not complete fusion.* Cell, 1994. **76**: p. 383-91.

97. Melikyan, G.B., J.M. White, and F.S. Cohen, *GPI-anchored influenza hemagglutinin induces hemifusion to both red blood cell and planar bilayer membranes.* J Cell Biol, 1995. **131**: p. 679-91.

98. Weiss, C.D. and J.M. White, *Characterization of stable Chinese hamster ovary cells expressing wild-type, secreted, and glycosylphosphatidylinositol-anchored human immunodeficiency virus type 1 envelope glycoprotein.* J Virol, 1993. **67**: p. 7060-6.

99. Hernandez, J.M., et al., *Membrane fusion intermediates via directional and full assembly of the SNARE complex.* Science, 2012. **336**: p. 1581-4.

100. Earl, P., R.W. Doms, and B. Moss, *Oligomeric structure of the human immunodeficiency virus type 1 envelope glycoprotein.* Proceedings of the National Academy of Sciences USA, 1990. **87**: p. 648-652.

101. Yin, H.S., et al., *Structure of the uncleaved ectodomain of the paramyxovirus (hPIV3) fusion protein.* Proc Natl Acad Sci U S A, 2005. **102**: p. 9288-93.

102. Yin, H.S., et al., *Structure of the parainfluenza virus 5 F protein in its metastable, prefusion conformation.* Nature, 2006. **439**: p. 38-44.

103. Pantophlet, R. and D.R. Burton, *GP120: target for neutralizing HIV-1 antibodies.* Annu Rev Immunol, 2006. **24**: p. 739-69.

104. Skehel, J.J. and D.C. Wiley, *Receptor binding and membrane fusion in virus entry: the influenza hemagglutinin.* Annu Rev Biochem, 2000. **69**: p. 531-569.

105. Chen, J., et al., *Structure of the hemagglutinin precursor cleavage site, a determinant of influenza pathogenicity and the origin of the labile conformation.* Cell, 1998. **95**: p. 409-417.

106. Wilson, I.A., J.J. Skehel, and D.C. Wiley, *Structure of the haemagglutinin membrane glycoprotein of influenza virus at 3 Å resolution.* Nature, 1981. **289**: p. 366-375.

107. Carr, C.M., C. Chaudhry, and P.S. Kim, *Influenza hemagglutinin is spring-loaded by a metastable native conformation.* Proceedings of the National Academy of Sciences USA, 1997. **94**: p. 14306-14313.

108. Buzon, V., et al., *Crystal structure of HIV-1 gp41 including both fusion peptide and membrane proximal external regions.* PLoS Pathog, 2010. **6**: p. e1000880.

109. Scherer, E.M., et al., *Aromatic residues at the edge of the antibody combining site facilitate viral glycoprotein recognition through membrane interactions.* Proc Natl Acad Sci U S A, 2010. **107**: p. 1529-34.

110. Jiang, J. and C. Aiken, *Maturation-dependent human immunodeficiency virus type 1 particle fusion requires a carboxyl-terminal region of the gp41 cytoplasmic tail.* J Virol, 2007. **81**: p. 9999-10008.

111. Zokarkar, A. and R.A. Lamb, *The paramyxovirus fusion protein C-terminal region: mutagenesis indicates an indivisible protein unit.* J Virol, 2012. **86**: p. 2600-9.

112. York, J. and J.H. Nunberg, *Intersubunit interactions modulate pH-induced activation of membrane fusion by the Junin virus envelope glycoprotein GPC.* J Virol, 2009. **83**: p. 4121-6.

113. Albariño, C.G., et al., *The major determinant of attenuation in mice of the candid1 vaccine for argentine hemorrhagic Fever is located in the g2 glycoprotein transmembrane domain.* J Virol, 2011. **85**: p. 10404-8.

114. Droniou-Bonzom, M.E., et al., *Substitutions in the glycoprotein (GP) of the Candid#1 vaccine strain of Junin virus increase dependence on human transferrin receptor 1 for entry and destabilize the metastable conformation of GP*. J Virol, 2011. **85**: p. 13457-62.

115. Centers for Disease Control and Prevention. *Lassa Fever Reported in U.S. Traveler Returning from West Africa*. 2014 [cited 2014; Available from: http://www.cdc.gov/media/releases/2014/p0404-lassa-fever.html.

116. York, J. and J.H. Nunberg, *Role of hydrophobic residues in the central ectodomain of gp41 in maintaining the association between HIV-1 envelope glycoprotein subunits gp120 and gp41*. J Virol, 2004. **78**: p. 4921-26.

117. Parsy, M.L., et al., *Crystal structure of Venezuelan hemorrhagic fever virus fusion glycoprotein reveals a class 1 postfusion architecture with extensive glycosylation.* J Virol, 2013. **87**(23): p. 13070-5.

118. York, J., et al., *Genetic analysis of heptad-repeat regions in the G2 fusion subunit of the Junin arenavirus envelope glycoprotein.* Virology, 2005. **343**: p. 267-79.

119. Burgeson, J.R., et al., *Lead optimization of an acylhydrazone scaffold possessing antiviral activity against Lassa virus.* Bioorg Med Chem Lett, 2013. **23**(21): p. 5840-3.

120. Froeschke, M., et al., *Long-lived signal peptide of lymphocytic choriomeningitis virus glycoprotein pGP-C.* J Biol Chem, 2003. **278**: p. 41914-20.

121. York, J. and J.H. Nunberg, *Distinct requirements for signal peptidase processing and function of the stable signal peptide (SSP) subunit in the Junin virus envelope glycoprotein.* Virology, 2007. **359**: p. 72-81.

122. Nussbaum, O., C.C. Broder, and E.A. Berger, *Fusogenic mechanisms of enveloped–virus glycoproteins analyzed by a novel recombinant vaccinia virus-based assay quantitating cell fusion–dependent reporter gene activation.* J Virol, 1994. **68**: p. 5411-22.

123. Rostovtsev, V.V., et al., *A stepwise huisgen cycloaddition process: copper(I)-catalyzed regioselective "ligation" of azides and terminal alkynes.* Angew Chem Int Ed Engl, 2002. **41**(14): p. 2596-9.

124. Tornoe, C.W., C. Christensen, and M. Meldal, *Peptidotriazoles on solid phase: [1,2,3]-triazoles by regiospecific copper(i)-catalyzed 1,3-dipolar cycloadditions of terminal alkynes to azides.* J Org Chem, 2002. **67**(9): p. 3057-64.

125. Austin, R.J., et al., *Proteomic analysis of the androgen receptor via MS-compatible purification of biotinylated protein on streptavidin resin.* Proteomics, 2012. **12**(1): p. 43-53.

126. Folch, J., M. Lees, and G.H. Sloane Stanley, *A simple method for the isolation and purification of total lipides from animal tissues.* J Biol Chem, 1957. **226**(1): p. 497-509.

127. Odell, L., et al., *Azido and diazarinyl analogues of bis-tyrphostin as asymmetrical inhibitors of dynamin GTPase.* ChemMedChem, 2009. **4**: p. 1182–1188.

128. Burri, D.J., et al., *Differential recognition of Old World and New World arenavirus envelope glycoproteins by subtilisin kexin isozyme 1 (SKI-1)/site 1 protease (S1P).* J Virol, 2013. **87**(11): p. 6406-14.

129. Chen, Z.W., et al., *Neurosteroid analog photolabeling of a site in the third transmembrane domain of the beta3 subunit of the GABA(A) receptor.* Mol Pharmacol, 2012. **82**(3): p. 408-19.

130. Yip, G.M., et al., *A propofol binding site on mammalian GABAA receptors identified by photolabeling.* Nat Chem Biol, 2013. **9**(11): p. 715-20.

131. Bodian, D.L., et al., *Inhibition of the fusion-inducing conformational change of influenza hemagglutinin by benzoquinones and hydroquinones.* Biochemistry, 1993. **32**: p. 2967-78.

132. Luo, G., et al., *Molecular mechanism underlying the action of a novel fusion inhibitor of influenza A virus.* J Virol, 1997. **71**: p. 4062-70.

133. Russell, R.J., et al., *Structure of influenza hemagglutinin in complex with an inhibitor of membrane fusion.* Proc Natl Acad Sci U S A, 2008. **105**: p. 17736-41.

134. Vanderlinden, E., et al., *Novel inhibitors of influenza virus fusion: structure-activity relationship and interaction with the viral hemagglutinin.* J Virol, 2010. **84**: p. 4277-88.

135. Ngo, N., et al., *Identification and Mechanism of Action of a Novel Small-Molecule Inhibitor of Arenavirus Multiplication.* J Virol, 2015. **89**(21): p. 10924-33.

136. Hruby, D.E., D.L. Lynn, and J.R. Kates, *Identification of a virus-specified protein in the nucleus of vaccinia virus-infected cells.* J Gen Virol, 1980. **47**: p. 293-9.

137. Klewitz, C., H.D. Klenk, and J. ter Meulen, *Amino acids from both N-terminal hydrophobic regions of the Lassa virus envelope glycoprotein GP-2 are critical for pH-dependent membrane fusion and infectivity.* J Gen Virol, 2007. **88**: p. 2320-8.

138. Li, S., et al., *Acidic pH-Induced Conformations and LAMP1 Binding of the Lassa Virus Glycoprotein Spike.* PLoS Pathog, 2016. **12**(2): p. e1005418.

139. Kima, P.E., B. Burleigh, and N.W. Andrews, *Surface-targeted lysosomal membrane glycoprotein-1 (Lamp-1) enhances lysosome exocytosis and cell invasion by Trypanosoma cruzi.* Cell Microbiol, 2000. **2**(6): p. 477-86.

140. Urata, S., et al., *Cellular factors required for Lassa virus budding.* J Virol, 2006. **80**: p. 4191-5.

141. Casabona, J.C., et al., *The RING domain and the L79 residue of Z protein are involved in both the rescue of nucleocapsids and the incorporation of glycoproteins into infectious chimeric arenavirus-like particles.* J Virol, 2009. **83**: p. 7029-39.

142. Shtanko, O., et al., *ALIX/AIP1 is required for NP incorporation into Mopeia virus Z-induced virus-like particles.* J Virol, 2011. **85**: p. 3631-41.

143. Urata, S. and J.C. de la Torre, *Arenavirus budding.* Adv Virol, 2011. **2011**: p. 180326.

144. Cornu, T.I. and J.C. de la Torre, *RING finger Z protein of lymphocytic choriomeningitis virus (LCMV) inhibits transcription and RNA replication of an LCMV S-segment minigenome.* J Virol, 2001. **75**: p. 9415-26.

145. Groseth, A., et al., *Efficient budding of the Tacaribe virus matrix protein Z requires the nucleoprotein.* J Virol, 2010. **84**: p. [Epub ahead of print].

146. Rual, J.F., et al., *Towards a proteome-scale map of the human protein-protein interaction network.* Nature, 2005. **437**(7062): p. 1173-8.

147. Ngounou Wetie, A.G., et al., *Investigation of stable and transient protein-protein interactions: Past, present, and future.* Proteomics, 2013. **13**(3-4): p. 538-57.

148. Alford, S.C., et al., *A fluorogenic red fluorescent protein heterodimer.* Chem Biol, 2012. **19**(3): p. 353-60.

149. Ding, Y., et al., *Ratiometric biosensors based on dimerization-dependent fluorescent protein exchange.* Nat Methods, 2015. **12**(3): p. 195-8.

150. Perez, M., R.C. Craven, and J.C. de la Torre, *The small RING finger protein Z drives arenavirus budding: implications for antiviral strategies.* Proc Natl Acad Sci U S A, 2003. **100**: p. 12978-83.

151. Shankar, S., et al., *Small-molecule fusion inhibitors bind the pH-sensing SSP-GP2 subunit interface of the Lassa virus envelope glycoprotein.* J Virol, 2016.

152. Steel, J.J. and B.J. Geiss, *A novel system for visualizing alphavirus assembly.* J Virol Methods, 2015. **222**: p. 158-63.